Title
In Situ Regeneration of the Nucleus Pulposus

Author
Kim, Anne Jungjoo

Publication Date
2009

Peer reviewed|Thesis/dissertation

In Situ Regeneration of the Nucleus Pulposus

by

Anne Jungjoo Kim

DISSERTATION

Submitted in partial satisfaction of the requirements for the degree of

DOCTOR OF PHILOSOPHY

in

Bioengineering

in the

GRADUATE DIVISION

of the

UNIVERSITY OF CALIFORNIA, SAN FRANCISCO

AND

UNIVERSITY OF CALIFORNIA, BERKELEY

Acknowledgements

Although I wouldn't quite say writing a dissertation is a near-death experience, there *is* something about staring the last seven years of work in the face that makes you contemplate your place in the universe. And while that is something I'm still trying to figure out, there are some people who need to be thanked, for helping me be right here today…

To Jeffrey Lotz, our fearless leader – thank you for being the kind of mentor who helps students develop into independent scientists.

Thanks to my dissertation committee members Serena Hu and Alfred Kuo – I truly appreciate the time you took to provide me with valuable feedback.

To all past and present members of the Lotz, Alliston, and Schneider labs, particularly Andy Walsh, Jill Ulrich McCoy, Kirk Pedersen, Jane Liu, Ellen Liebenberg, Kevin Cheng, Azucena Rodriguez, Tamara Alliston, Emily Chin, Dan Nguyen, Christian Solem, and Andrew Jheon – thank you for all the ways you have made my life as a grad student easier and better.

Thanks to Evelyn Cheng, Craig Hashi, Arnold Kim, Kyle Kurpinski, Gary Lee, Ray Schmidt, and Jon Tang – your encouraging words, helpful suggestions, offers to proofread, and ability to make me laugh have helped the last month fly by.

To Gary Stevens – thank you for trusting me with your anatomy class, and giving me the opportunity to realize what it means to be a teacher.

To Zorica Buser – I can't even begin to say how happy I am you joined the Lotz lab. Thank you for all of your help, and for becoming one of my dearest friends. And thanks to you and Chris and Hannah for always looking out for me.

To Olivia Billett, Odile Joly, and Gwynna Norman – I feel extremely lucky to have had you in my life over the last eleven years. Thank you for being part of my family, and for being the people I can count on to lift me up and make me smile.

To Christopher Kim – thank you for your trust and love, all while keeping me on my toes. I want to be like you when I grow up, little brother.

And most importantly, to my amazing parents, Myoung Hwan and Hye Sook Kim – everything you've done, you've done for us. I can't believe I survived the last seven years, but I know it is all because of you. I'm not sure it is even possible to let you know how much I love you, or how grateful I am for the many ways you make my life better. Thank you for your love and support.

Abstract

In Situ Regeneration of the Nucleus Pulposus

By

Anne Jungjoo Kim

Doctor of Philosophy in Bioengineering

University of California, San Francisco

And

University of California, Berkeley

Professor Jeffrey C. Lotz, Chair

Intervertebral disc degeneration is a contributing cause for many spine-related disabilities, and is a significant health concern in the United States. Currently available treatments aim to gain symptomatic relief, and do not treat the underlying biological problem. Cell therapy aims to target the cause of disc degeneration by repopulating the disc with cells capable of synthesizing appropriate matrix, restoring its biomechanical properties. The goal of this research was to investigate the use of mesenchymal stem cells (MSCs) for nucleus pulposus regeneration.

An *in vivo* injection model was used to characterize the regeneration potential of undifferentiated MSCs, juvenile chondrocytes, and fibrin carrier in rat coccygeal discs. Juvenile chondrocyte-injected discs displayed significantly improved MRI index over fibrin-injected discs, and histology indicated that injecting a more mature cell type resulted in maintenance of normal disc morphology.

To advance our understanding of the phenotypic changes that might arise in MSCs after transplantation to the disc environment, a novel bioreactor system was

developed that mimics they hypoxia and hydrostatic pressure found in the intervertebral disc. Culturing MSCs in this system demonstrated that the physiochemical environment of the disc is sufficient to induce differentiation of MSCs, as evidenced by GAG production and increase in chondrogenic genes such as aggrecan, Sox9, and collagen II.

Pre-treatment of MSCs with TGF-β3 prior to bioreactor culture indicated that differentiated cells may function more effectively in disc-mimetic conditions, as evidenced by increased cell viability, GAG production, and persistence of TGF-β3-induced gene expression. More importantly, environment-dependent differences in gene expression highlighted the necessity of mimicking several aspects of the disc environment in concert when evaluating the fate of cells post-implantation. To better mimic the degenerated disc environment, inflammation was incorporated into the bioreactor. Expression levels of aggrecan, collagen II, and collagen X suggest that when MSCs are appropriately pre-differentiated and evaluated in a disc-mimetic environment, inflammation may not be as detrimental as seen in previous *in vitro* experiments.

This research highlights the importance of representing the salient features of the anticipated environment when evaluating cells for *in situ* disc regeneration, and demonstrates that MSCs may be optimized for nucleus pulposus regeneration.

Table of Contents

List of Tables

List of Figures

Chapter 1: Introduction

1.1 The Healthy Human Intervertebral Disc

The intervertebral disc lies between two adjacent vertebral bodies, acting as a joint and conferring flexibility to the spine. The disc has three specific components: the annulus fibrosus, the nucleus pulposus, and the cartilage endplates. The annulus is a ring of fibrocartilage layers enclosing the gelatinous nucleus, and together, this structure is sandwiched between the cartilage endplates [1].

The annulus contains up to 25 rings composed of mostly type I collagen fibers [2]. The fibers are attached to the adjacent vertebrae so that they lie 60 degrees to the spine's axis, alternating direction in each adjacent layer. The alternating arrangement of collagen fibers within the rings allows the disc to resist forces generated during normal movement such as bending or twisting [3]. As the rings grow closer to the disc center, an increasing amount of type II collagen fibers can be found [4].

The disc nucleus is not as structured, containing a network of type II collagen and elastin fibers embedded in a proteoglycan-rich extracellular matrix [5]. The most abundant proteoglycan, aggrecan, contains negatively charged glycosaminoglycans that attract water, causing the nucleus to swell [6]. This swelling is bounded by the annulus and endplates; the resulting hydrostatic pressure helps the nucleus and disc resist compressive loads [3].

The disc cells function to balance synthesis of extracellular matrix (ECM) molecules and proteases [7, 8]. Cells found in the annulus are elongated, fibroblastic, and produce primarily type I collagen matrix, while nucleus pulposus cells are phenotypically

similar to articular chondrocytes and secrete type II collagen and proteoglycan [5, 9-11]. Both the annulus and nucleus have a relatively low concentration of cells – 9,000 cells/mm^3 and 4,000 cells/mm^3, respectively [12]. The low cell density makes it difficult for the disc to maintain the extracellular matrix.

The disc is largely avascular, with a few capillaries penetrating the outer layers of the annulus fibrosus. However, disc cells, especially those in the nucleus pulposus, can be up to 8 mm away from the blood vessels that penetrate the cartilage endplates or the annulus [7, 12], and undergo anaerobic metabolism due to the lack of oxygen in the environment. The lactic acid byproducts contribute to the increased acidity of the disc [13].

The cartilage endplate is a thin layer of hyaline cartilage between the disc and vertebral body, and is less than 1 mm thick. It is composed of proteoglycans reinforced by collagen - similar to, but less hydrated than, articular cartilage [14]. Disc cells must rely on diffusion for nutrient, oxygen, and waste exchange [4], and the endplates serve as a selectively permeable barrier to solutes. Small, uncharged solutes such as oxygen and water can diffuse across the endplate easily, but loss of hydration or calcification of the endplate can significantly hinder nutrient transport [13]. Nerve fibers have been identified in the endplates, as well the outer portion of the annulus, but are not found in the inner annulus or nucleus of healthy discs [15-18].

1.2 Intervertebral Disc Degeneration

Disc degeneration can have several different causes, and is the result of a number of factors acting individually or collectively. Classically, disc degeneration is interpreted as the result of age-related changes. However, it is more accurate to observe that the disc morphology and biochemical changes that are seen with degeneration also increase with age. The question of why these changes occur is still not fully explained.

Aging, Nutrition, and Morphological Changes

Major changes in the intervertebral disc that occur due to aging can be seen by the end of the first decade, with matrix degeneration in the cartilage endplate and nucleus pulposus (NP) cell death occurring as early as two years of age [19]. Some of these changes coincide with (and perhaps are a result of) a dramatic regression of blood vessels in the endplate, a phenomenon seen between 6 and 30 months of age [20]. In an autopsy study, 97% of individuals studied who were 50 years or older showed signs of disc degeneration [21].

Natural changes that occur during aging are also seen in disc degeneration: changes in ECM molecules and water content, cell senescence and death, impaired metabolite transport, neurovascular ingrowth, and structural failure [22]. Disc cells rely on diffusion of glucose and oxygen from capillaries near the endplates. With aging, endplate cartilage calcifies and cell density is reduced [23], limiting the diffusion of nutrients and waste products to and from disc cells. When disc cells are cultured *in vitro*, they are highly sensitive to changes in oxygen levels; a reduction in oxygen tension results in lower levels

of proteoglycan production, correlating with an increase in lactic acid production [24]. The resulting accumulation of lactic acid waste can alter the production of matrix components by the disc cells [19], but also lead to cell death; cell viability in elderly discs can be as low as 20% [22]. Disc cell necrosis and resulting matrix changes can lead to structural changes, including annular lamellae disorganization, damage to collagen crosslinks [25], and formation of annular tears [26]. Breakage of collagen fibers weakens the connection between the annulus and vertebral body [27], and the normally clear distinction between the nucleus and annulus is blurred as the disorganized annular layers bulge into the increasingly fibrotic nucleus [19, 26].

Biomechanical and Biochemical Changes

With morphological changes come alterations in disc biomechanics. Depressurization of the nucleus (either by loss of proteoglycans and therefore water, or by structural changes in the annulus) hinders its ability to transmit loads between the vertebrae, increasing loading of the collagen network. This abnormal loading regime can result in changes to the mechanical function of the disc. Modifications to collagen, proteoglycan, and elastin can result in loss of elasticity and strength in disc tissue. Degenerative discs lose regularity of elastic modulus [28] and have less range of motion than healthy discs [29]. Stiffness decreases during early degeneration, but increases as degeneration advances [28, 30].

Abnormalities in load can also trigger changes to the biochemical environment of the disc. The lumbar intervertebral disc structure enables it to sustain beneficial compression loads, and load can act as a stimulus for normal matrix turnover [31-33]. In

order to prepare the disc matrix for new synthesis, loading can stimulate expression of matrix metalloproteinases (MMPs) [31, 33, 34] and nitric oxide [35]. However, when load is abnormal due to structural changes of the disc, harmful changes can occur, such as decreased aggrecan formation, reduction of anabolic protein gene expression, and increased expression of MMPs [33]. Resulting changes in the extracellular matrix leave the disc cells more vulnerable to mechanical loads [36].

In addition to increased production of MMPs, the degenerated disc environment can be inflammatory due to presence of cytokines, which can modulate connective tissue anabolism and catabolism [37, 38]. Pro-inflammatory cytokines are found in higher concentrations in painful degenerated discs than health discs [39]. Cytokines that have been identified in degenerated human disc tissue include interleukin 1 (IL-1), tumor necrosis factor alpha (TNF-α), interleukin 6 (IL-6), and interleukin 8 (IL-8) [38, 40-44]. These same cytokines are produced by disc cells when cultured *in vitro,* as well as prostaglandin E_2 (PGE_2) and nitric oxide (NO) [41, 43, 45-48]. Along with matrix degeneration, pro-inflammatory cytokines can generate pain through nerve contact [49]. It is difficult to determine the precise action and contribution of each cytokine to the overall degeneration process, due to the high degree of redundancy and cross-talk among the induction pathways [50].

The cartilage endplate is highly vulnerable to abnormal compression, and can fracture due to a sudden, severe load, or as a result of fatigue failure [36, 51]. A fractured endplate can result in biochemical changes such as altered activity of ECM molecules, induction of inflammatory response, and altered pH. Endplate damage can also interfere with disc nutrition or result in changes in annular structure resulting from

depressurization of the nucleus [36, 52-57]. Experimental injury of the endplate leads to degenerative changes, such as decreased proteoglycan and water content, depressurization of the nucleus, and the resulting delamination of the inner annulus [58, 59].

Discogenic Pain

The relationship between disc pain and disc degeneration remains unclear. Painful degenerative discs can be morphologically similar to asymptomatic degenerative discs, and patients suffering from back pain may have discs that appear normal on lumbar disc radiographs or MRI [60-63].

Discogenic pain can result from herniation of disc material into the vertebral foramen, where it impinges upon the spinal cord, or by a combination of factors that can be aggravated by degenerative changes. Normally the disc is avascular and innervated at the outer margins [64], but nociceptors (unmyelinated fibers containing substance P) may be present, though typically unresponsive [16, 65, 66]. During degeneration, decreases in disc pressure and proteoglycan content facilitate nerve and vessel ingrowth [67]. Inflammatory cytokines can sensitize nociceptors, diminishing their activation threshold [65, 68], and are found in significantly greater amounts in disc tissue excised from painful discs compared to asymptomatic discs [69]. Cytokines can be secreted either by inflammatory cells in the case of disc herniation [70, 71], or by the degenerated disc cells themselves [69]. Abnormal loading may compress nerves found in the outer annulus and cartilage endplate, causing pain [7]. These same nerve fibers may be sensitized by bulging or ruptured annulus [64, 72, 73], and can be irritated by enzymes and

inflammatory cytokines that can travel from the nucleus through fissures or tears in the annulus [74]. In addition, the loss of disc height can put abnormal stress on the facet joints and ligaments adjacent to discs; these structures are also innervated, leading to pain [7]. Considering all these factors, back pain could possibly be alleviated or prevented by restoring normal disc structure and function.

1.3 Cell-Based Therapies for Intervertebral Disc Regeneration

Motivation

Low back pain (LBP) is a condition that almost 84% of the population will experience at some point in their lifetime [75], making it one of the most common musculoskeletal disorders and also one of the most expensive healthcare problems in the United States [76, 77]. Patients who suffer an acute attack of LBP may recover without major intervention, or with conservative therapies [78]. Conservative therapies are also used for patients with chronic LBP, and include short-term pain relief, physical therapy, massage, acupuncture, and transcutaenous electrical nerve stimulators. In addition, epidural, facet joint, or corticosteroid injections may be administered, although the long-term benefits are unclear [79].

For patients who do not respond to conservative therapy, surgical intervention may be necessary. The most common procedure is spinal fusion, but the efficacy of this treatment is controversial, with little agreement on whether or not surgery results in a positive outcome. In 2001, a Swedish study showed that patients who underwent spinal fusion fared better at 2 years than patients who were treated conservatively [80] but a 2005 UK study demonstrated there was no significant improvement in patients who

underwent fusion compared to nonsurgical patients [81]. There is also evidence that lumbar fusion may accelerate degenerative changes in adjacent disc levels [82].

Alternatively, replacement devices such as total disc replacement (TDR) can preserve mobility of the spinal motion segment. The most widely implanted TDR device is the CHARITÉ® Artificial Disc (DePuy Spine, Johnson & Johnson, Raynham, MA), which has been FDA-approved since 2004. Early studies show that these devices, and others such as the ProDisc Lumbar TDR (Synthes Spine Inc., West Chester, PA), provide significant pain reduction at 24-month follow-up [83, 84]. However, it is still too early to establish long-term effectiveness or whether there is less adjacent segment degeneration, and there are also cases of migration, prolapse, and failure of these devices [85].

Potential for Biological Repair

A major problem with conservative therapies or surgical interventions is that the treatments do not repair the intervertebral disc tissue. In each case, the overall goal is to remove the painful symptoms and to, with the exception of spinal fusion, increase mobility. Therefore, it is logical that researchers are investigating a less invasive regenerative approach for disc repair.

As described previously, the biochemical changes that occur with disc degeneration occur largely in the nucleus pulposus (NP), where type II collagen and proteoglycan synthesis decrease. The nucleus has thus become a target for researchers for regeneration of the disc, whether it is by using growth factors to stimulate disc cells to proliferate and increase proteoglycan synthesis, or by introducing cells capable of proliferating within the disc tissue and repopulating the native extracellular matrix.

The ability of cells or tissue to survive upon implantation to the nucleus has been widely documented in several animal models. Autologous disc-derived cells reimplanted into the dogs from which they were derived integrated into the disc tissue and produced cartilaginous ECM [86]. Other studies in rats and rabbits [87-90] demonstrate that reinsertion of NP cells or chondrocytes results in decreased disc "degeneration" and maintenance of cell viability. However, one of the greatest challenges for cell-based therapies is finding an appropriate source of cells. Obtaining cells from mature or native tissues can be difficult due to problems with limited harvest sites, donor tissue disease, donor site morbidity, and limited expansion capacity of adult cells that are already fully differentiated [91]. Specifically in the disc, harvesting healthy tissue can induce disc degeneration [92], and cells from the degenerate disc have shown to be senescent with altered phenotype [93, 94]. Senescent cells show a decreased rate of matrix production and increased production of MMPs, and implantation of these cells could only worsen the degenerate condition. The use of allogenic cells would also be difficult, as degenerate discs show neovascularization and innervation, and implanted cells could suffer immune rejection.

Mesenchymal Stem Cells for Nucleus Pulposus Regeneration

As a result of these limitations, many groups are investigating the use of mesenchymal stem cells. Mesenchymal stem cells can differentiate into a wide variety of cell phenotypes and have the capacity to self-renew [95]. Stem cells that are capable of differentiating have been isolated from human bone marrow, adipose tissue, and blood [96-98] meaning they can be easily harvested from adult bone marrow or liposuction

aspirates, or by using minimally invasive techniques at areas far removed from the treatment site [99]. For effective cell-based therapies, large amounts of cells are required, and MSCs are not only capable of self-renewal, but can maintain their ability to differentiate after expansion, subculturing, and cryopreseration [100].

The fact that MSCs can differentiate along a chondrogenic lineage has many researchers investigating ways to coax the cells to express a disc cell-like phenotype. MSCs have the ability to express chondrogenic markers with TGF-β2 and -3 stimulation, inducing sequential expression of fibromodulin, cartilage oligomeric matrix protein (COMP), aggrecan, versican, type II collagen, chondradherin, and finally type X collagen [101]. Nucleus pulposus cells and articular chondrocytes share some common phenotypic markers, such as those for Sox9, aggrecan, and type II collagen [11]. Unfortunately, very little is known about the complete molecular profile of AF or NP cells, so it is difficult to say whether MSCs can truly mature into disc cells. Steck et al, suggested that MSCs can adopt a gene expression profile resembling native disc cells, but the molecular markers examined are also found in cartilage tissue [102]. Rajpurohit et al. reported that NP cells express HIF-1, MMP-2, and GLUT-1, all markers that are absent from the neighboring annulus and endplate [103], and Lee et al. found that levels of annexin A3, glypican 2, keratin 19, and pleiotrophin were significantly higher in the nucleus compared to annulus or articular cartilage samples [104]. However, both of these studies were carried out using rat disc tissue, where notochordal cells may still be present, and further studies using human samples will need to be carried out before a distinct NP cell profile can be successfully characterized.

It is also not sufficient for cells that are injected into the disc to express markers similar to chondrocytes – in order for actual repair and treatment efficacy, the matrix produced by the cells must be able to withstand the environment in the disc. For example, chondrocytes cultured *in vitro* in various scaffolds are biochemically similar to those found in native cartilage (in terms of proteoglycan and collagen production and expression) yet the mechanical properties of the constructs are several orders of magnitude lower [105, 106]. Not only should the cells be prepared to withstand the environment of the disc, it may be helpful for them to be exposed to environmental elements similar to that of the disc prior to implantation. The relevant literature for this subject will be further discussed in Chapter 3.

Immunomodulation by Mesenchymal Stem Cells

Another feature that makes MSCs attractive for intervertebral disc repair is their immunosuppressive activities. First, MSCs can evade host immune elimination, as they express major histocompatibilty complex (MHC) class I but not MHC class II molecules on their cell surface, and retain this pattern of expression after differentiation into adipocytes, osteoblasts, and chondrocytes [107]. Mesenchymal stem cells have also been shown to suppress T-cell, B-cell, and natural killer cell responses [108-110], mainly by inhibiting the proliferation of these cells [111, 112]. Of particular interest is the fact that the MSCs retain their antiproliferative ability, even after differentiation along adipogenic, chondrogenic, or osteogenic lineages [107, 111, 113].

Cytokines present in the degenerated tissue could possibly play a dual role when MSCs are concerned. Nitric oxide has been shown to play a key role as one of the factors

contributing to MSC-induced immunosuppression [114, 115]. MSCs themselves secrete cytokines and growth factors that have the potential to stimulate mitosis and the reparative potential of NP cells [116, 117].

1.4 Objectives

The overall goal of this dissertation was to investigate the use of mesenchymal stem cells for nucleus pulposus regeneration. Specifically, we focused on advancing our understanding of how to optimally prepare the cells for disc transplantation, and then investigated the fate of MSCs after they spend time in an *in vivo* disc environment or an *in vitro* disc-mimetic environment. In order to accomplish this, several specific aims were completed:

1. Utilization of a rat tail-disc injection model to examine the therapeutic effects of cell transplantation on disc degeneration.

    a. Appendix A describes the percentage of cell retention within the rat coccygeal disc when cells are delivered in a fibrin glue carrier. Appendix B describes the effects of rat bone marrow-derived mesenchymal stem cell injection into a rat animal model of disc degeneration.

    b. Chapter 2 describes the effects of human mesenchymal stem cell and human juvenile chondrocyte injection on disc morphology using a non-degenerate rat animal model.

2. Development of a novel disc-mimetic bioreactor cell culture system.

    a. The problems with using a small animal model and identifying the phenotype of the cells post-transplantation highlighted the need for an *in vitro* system that more accurately reflects the disc conditions. Chapter 3 describes the development of a bioreactor system that exposes cells to low oxygen tension and hydrostatic pressure, and describes the effect of this environment on the differentiation of mesenchymal stem cells without the use of chondrogenic growth factors.

    b. Chapter 4 investigates the effect of TGF-β3 differentiation on MSCs cultured in the disc-mimetic bioreactor system.

    c. Chapter 5 describes the effect of inflammation on MSCs in a disc-mimetic environment.

Chapter 2: *In Vivo* Effects of Human Mesenchymal Stem Cell and Human Juvenile Chondrocyte Transplantation

2.1 Introduction

Intervertebral disc degeneration is an underlying factor for a majority of spine-related disabilities leading to significant patient hardship and societal expense [76]. Patients who do not respond well to conservative therapy have few options other than fusion, which can result in considerable morbidity and variable outcomes [118]. While the focus of surgical and conservative treatments is to gain symptomatic relief, the underlying biological problem typically remains unidentified. The notion that back pain patients will benefit from less invasive procedures has led researchers to investigate several approaches of biologic disc repair.

As an avascular tissue, the disc has a limited ability to regenerate itself. The cellularity of the disc is also quite low, with cells occupying less than 1% of the total disc volume [7]. The cells produce the extracellular matrix and are responsible for maintaining the balance between matrix breakdown and synthesis. Loss of cellularity and reduced extracellular matrix production is a central feature of degenerative disc disease, and consequently a tissue-engineering based method to heal the nucleus may be an effective treatment approach. The introduction of cells capable of producing and maintaining normal extracellular matrix in a high pressure, low oxygen tension, and low pH environment is critical for successful bioengineered disc regeneration.

Several researchers have demonstrated the feasibility of injecting mesenchymal stem cells, autologous intervertebral disc cells, or autologous chondrocytes into the disc for repair [87-90, 119, 120]. Mesenchymal stem cells (MSCs) are an attractive cell type given they can be isolated from bone marrow or fat and have the potential to differentiate

into an number of musculoskeletal tissues. However, once placed in the body, MSC differentiation is influenced by a number of local environmental cues including growth factors, mechanical forces, cytokines, oxygen tension, and pH that may be beyond investigator control. Based on our investigation of MSCs in varying differentiated stages and their response to load [121, 122], we believe a more differentiated or mature cell type may be more stable relative to uncontrolled site factors and thereby respond more predictably than undifferentiated cells during the acute healing phase *in vivo*. To test this hypothesis, we injected either undifferentiated human MSCs or proliferating chondrocytes harvested from juvenile human articular cartilage (juvenile chondrocytes) into the coccygeal disc of rats using a fibrin glue carrier. The *in vivo* response was characterized by histology, MRI imaging, and PCR analysis at 2, 4 and 12 weeks after injection. Articular chondrocytes have phenotypic similarities to nucleus pulposus cells, and have been transplanted into humans to repair articular chondral defects [123]. Juvenile chondrocytes can be expanded *in vitro* and produce neocartilage under conditions where adult articular chondrocytes cannot [124]. Based on our previous efforts investigating cell injections to the degenerated disc (Appendix B), we used healthy rat discs and modified the cell injection protocol so that the needle placement would remove some of the nucleus pulposus prior to injection, making space for the injected cells.

2.2 Methods

Materials

Human juvenile chondrocytes (JCs) from a three-year-old male donor were provided by ISTO Technologies, Inc. Human MSCs were purchased from Lonza Corporation and passaged twice prior to injection.

Inbred Fisher rats (Simonsen Laboratories, Inc.) were used for the juvenile chondrocyte injections and *rnu* homozygous (National Cancer Institute) rats were used for the human MSC injections. The *rnu* homozygous rats were used to prevent any immunological response to the human stem cell injections, while Fisher rats were used for the juvenile chondrocyte injections as juvenile chondrocytes are reported to be immuno-privileged [125]. The UCSF Institutional Animal Care and Use Committee approved all experiments.

Rat Coccygeal Disc Injections

Rats were anesthetized with a mix of ketamine (90 mg/kg) and xylazine (10 mg/kg) and the injection site scrubbed with isopropyl alcohol and iodine. Buprenorphine (0.03 mg/kg) was administered for pain. Human juvenile chondrocytes were suspended into a fibrin adhesive (Tisseel VH, Baxter Bioscience Corporation) at a concentration of 10^7 cells/mL. An exact volume of 20 μL of each component (fibrinogen and thrombin) of the fibrin adhesive was injected simultaneously using two separate 29 gauge needles inserted in direct opposition to one another as visualized under fluoroscopic guidance (Figure 2.1). A total volume of 40 μL was injected into each of four consecutive discs in an inbred Fisher rat. Some of the nucleus pulposus is displaced during this injection.

Previous cell retention experiments show 55% of this volume is retained in the disc after injection (Appendix A), or 220,000 cells per disc. This cell amount is in excess of what is normally found in a rat disc nucleus pulposus [126]. Six rats were injected for each time point (2 weeks, 4 weeks and 12 weeks). Additionally, six rats for each time point were injected with fibrin alone to serve as a control. Three rats injected with JCs for the 2-week time point died shortly after injection, possibly due to pre-existing respiratory problems or poor reaction to anesthesia. These animals were not replaced. Human MSCs were similarly injected into *rnu* homozygous rats. Three rats for each time point (2 weeks and 4 weeks) were injected.

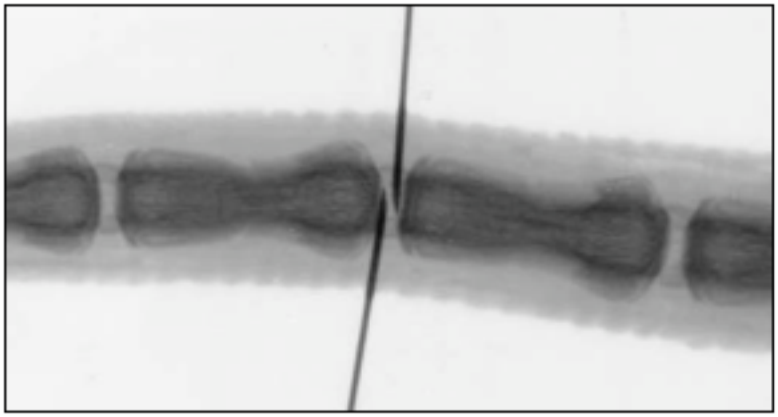

Figure 2.1 Fluoroscopic guidance was used to monitor intradiscal needle placement during delivery of thrombin (± cells) and fibrinogen. Needle placement allows fibrin components to polymerize upon contact.

MRI Disc Assessment of Juvenile Chondrocyte-injected Rats

On the day of sacrifice, each rat was anesthetized with inhaled isofluorane (5% isofluorane in 100% O_2 to induce, 1.5-25% thereafter to maintain), placed supine on a Plexiglas platform and warmed with a water-recirculated underpad. The tail was passed into a radiofrequency coil and the animal placed in a 1.5 Tesla magnet for MR imaging. The top three discs of each rat were imaged (8 consecutive 1mm slices). Nucleus size

and signal intensity were measured for each disc and a grade of 1 through 5 assigned based on these measurements (Table 2.1). A grade of 1 corresponds to healthy discs (large nucleus and high signal intensity) and a grade of 5 corresponds to degenerated discs (small or absent nucleus, very low signal intensity.) Because the grades were based on numerical measurements, they were confirmed by an unblinded grader who looked at corresponding images of each MRI slice.

Table 2.1 MRI grades according to nucleus size (pixels) and signal intensity

Grade	Nucleus Size	Signal Intensity
1	> 60 px	> 500,000
2	50-60 px	400,000-450,000
	45-50 px	450,000-500,000
3	30-45 px	> 375,000
4	20-35 px	200,000-350,000
	10-20 px	325,000-375,000
5	0-20 px	< 200,000

Disc Height Measurement

X-rays (Faxitron X-ray Corp.) were taken for each animal prior to injection, immediately post-injection, and at sacrifice. To control for animal size variability, the change in height (relative to the pre-operative value) was calculated. Measurements were made on x-ray films using SPOT image capture software (Diagnostic Instruments, Inc.) The distance between vertebrae was measured in the disc center and measurements were normalized to a fixed-length object imaged along side each tail. One-way analysis of variance was used to find statistically significant differences between groups, and a Tukey test used for pairwise comparisons.

Tissue Structure, Cell Morphology, and Cell Retention

At each time point for the JC-injected and fibrin-only groups, discs were randomized into either a histology group (n=2) or an RNA analysis group (n=2). Discs for histology were fixed in 10% neutral buffered formalin, decalcified with formic acid and embedded with paraffin. Seven μm sagittal sections were cut from the entire disc and five representative slides spanning each disc were stained with Safranin-O/fast green to observe cell phenotype and matrix architecture. RNA analysis was used to confirm the presence of the injected cells by identifying human-specific β_2 microglubulin (β_2m). Discs were harvested at sacrifice and flash frozen. RNA extraction of combined tissues (2 discs per rat) was performed using the TissueRuptor (handheld rotor-stator homogenizer) and RNeasy Fibrous Tissue Mini Kit purchased from Qiagen. All reverse transcription and PCR reagents were purchased from Invitrogen. Primers were manufactured by Integrated DNA Technologies. DNase digestion was performed prior to reverse transcription to eliminate contaminating DNA. Two microliters of cDNA were used for a 50μL PCR reaction with a primer concentration of 0.2μM. For amplification of β_2m, PCR was performed as described previously [127] with an initial denaturation for 2 min at 94ºC, followed by 35 cycles of 94ºC for 30 s, 55ºC for 30s and 72ºC for 1 min, with a final extension for 10 min at 72ºC. The primers (5'-ATA TCC ATA TCC ATA TGT CTC GCT CCG TGG CCT TAG-3' and 5'-AAC TAG GGA TCC TTA CAT GTC TCG ATC CCA C-3') amplify the entire coding sequence of human β_2m cDNA. PCR products were separated and visualized on a 1% agarose gel stained with ethidium bromide. The β_2m product size of 357bp was measured against a 100bp DNA ladder (New England BioLabs Inc.). Samples of control rat discs mixed with a range of 10,000

to 2 million human MSCs were homogenized and used for PCR to determine if low numbers of cells could be detected. Cell amounts of 50,000 cells or greater were sufficient to yield enough cDNA that was detectable by PCR and gel electrophoresis.

For the MSC-injected group, all discs were processed for histology. Five representative slides spanning each disc were stained with Safranin-O/fast green to serve cell phenotype and matrix architecture. Additionally, slides adjacent to the Safranin-O/fast green slides were stained with human-specific LAMP-1 and LAMP-2 antibodies (Developmental Studies Hybridoma Bank, University of Iowa) to visualize location of the injected cells.

2.3 Results

Change in Disc Height

At two weeks after injection disc heights in both MSC and JC-injected discs were significantly decreased compared to that of control discs (Figure 2.2, $p<0.01$). Discs injected with JCs had a significantly smaller decrease in disc height than MSC-injected discs ($p<0.01$).

At four weeks after injection, changes in disc heights were not significantly different between cell-injected and control groups. However, disc height was significantly restored at 4 and 12 weeks compared to 2 weeks ($p<0.001$) in both MSC and JC-injected discs.

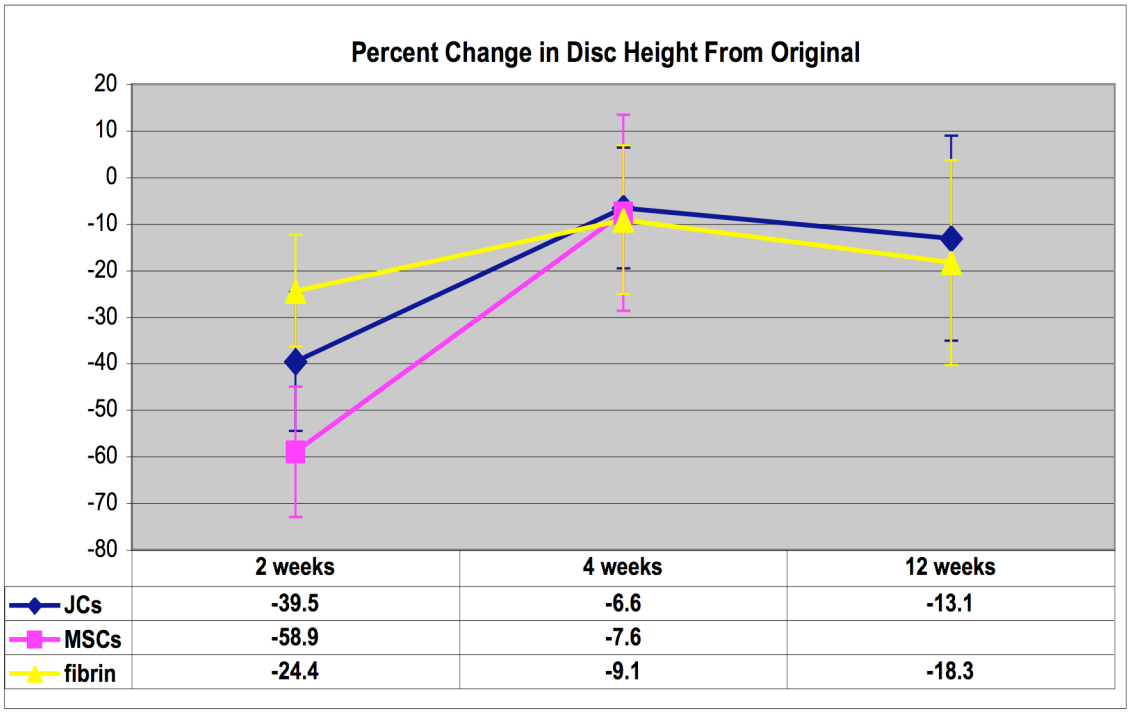

	2 weeks	4 weeks	12 weeks
JCs	-39.5	-6.6	-13.1
MSCs	-58.9	-7.6	
fibrin	-24.4	-9.1	-18.3

Figure 2.2 Disc height was significantly restored at four and twelve weeks in JC-injected discs when compared to two weeks ($p<0.001$). Discs injected with MSCs had a greater decrease in disc height at two weeks compared to JC-injected discs ($p<0.001$). Discs treated with fibrin alone showed an initial 24.4% reduction in disc height, but this transient loss of disc height appeared to be restored, in large part, by 4 and 12 weeks to levels that were nearly equivalent to JC-injected discs.

MRI Signal

At four and twelve weeks, control groups had more degenerated discs (grade four and five) than JC-injected groups, and the JC-injected groups had more healthy discs (grade 1) than control groups (Table 2.2). At four weeks, MRI grade was significantly improved in JC-injected discs (Mann-Whitney test, $p<0.02$). While more than half of the control discs degenerated over twelve weeks, all but two discs injected with JCs maintained morphology and MRI signal (results not significant, Figure 2.3).

Table 2.2 Number of discs per MRI grade at all time points

Grade	2 weeks		4 weeks		12 weeks	
	JCs	*Control*	*JCs*	*Control*	*JCs*	*Control*
1	0	0	7	1	3	0
2	3	7	3	6	6	8
3	3	7	7	5	6	3
4	1	3	1	1	1	0
5	2	1	0	5	2	7

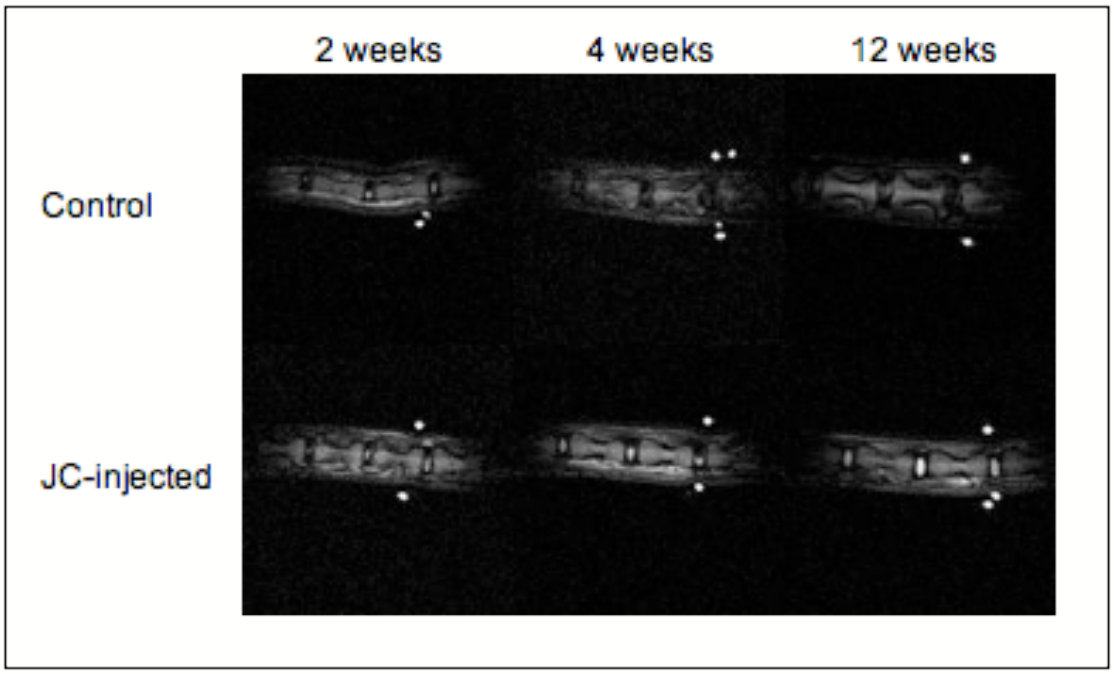

Figure 2.3 Sequential T2-weighted MRI of rat coccygeal discs demonstrated a positive healing effect with JC injection. While treatment with fibrin carrier alone resulted in a marked reduction in signal intensity (water content) between weeks 2 and 12, discs receiving JCs showed marked restoration of signal intensity. A level-identifying phantom identifies the uppermost of four treated discs; the top three discs were imaged.

Histological Analysis

At two weeks, discs in all groups show the effects of the injection with disrupted annular architecture and reduced nucleus size. In more than half of the discs, remnants of native nucleus are visible along the wound tract and pushed outside the annulus. In the MSC-injected discs, small inflammatory cells are present in the nuclear space and along

the wound tract. These are not present within the JC-injected and control discs, some inflammatory cells were observed to be present at the point of needle entry outside the annulus (Figure 2.4).

At four weeks the morphological differences between control and cell-injected discs are more apparent. Eight out of the 12 control (66.7%) discs still show remnants of nucleus outside the annulus (Figure 2.5a) and six out of the 12 (50%) discs presented with a disrupted annular architecture along the wound tract. Nine out of the 12 (75%) control discs presented with irregular nucleus shape and disrupted inner annular architecture as a result of loss of nuclear material. In contrast, JC-injected discs show evidence of regaining normal round nuclear structure. For JC-injected discs, only two out of 12 (16.7%) discs have disrupted annular architecture along the wound tract; the remaining discs show no evidence of the wound tract. Discs injected with MSCs also have no remnants of nucleus outside the annulus at four weeks, but most discs display disrupted inner annular architecture (Figure 2.5C).

At twelve weeks, six out of the 12 control (50%) discs were severely degenerated with complete absence of proteoglycan staining in the nucleus, and irregular annular structure. The remaining six control discs presented with reduced nucleus size and moderate proteoglycan staining. In contrast, only one of the 12 JC-injected (8.3%) discs was severely degenerated, but this appeared to be due to endplate damage during the initial injection. Four of the 12 (33.3%) JC-injected discs appeared to regain normal nucleus size, and six of 12 (50%) discs presented with normal nucleus size but slightly irregular shape.

Discs injected with JCs demonstrated chondrocyte-like cells proliferating at the inner annular/nuclear border (Figure 2.6b). These cells were not visible in the six control discs that were not severely degenerated.

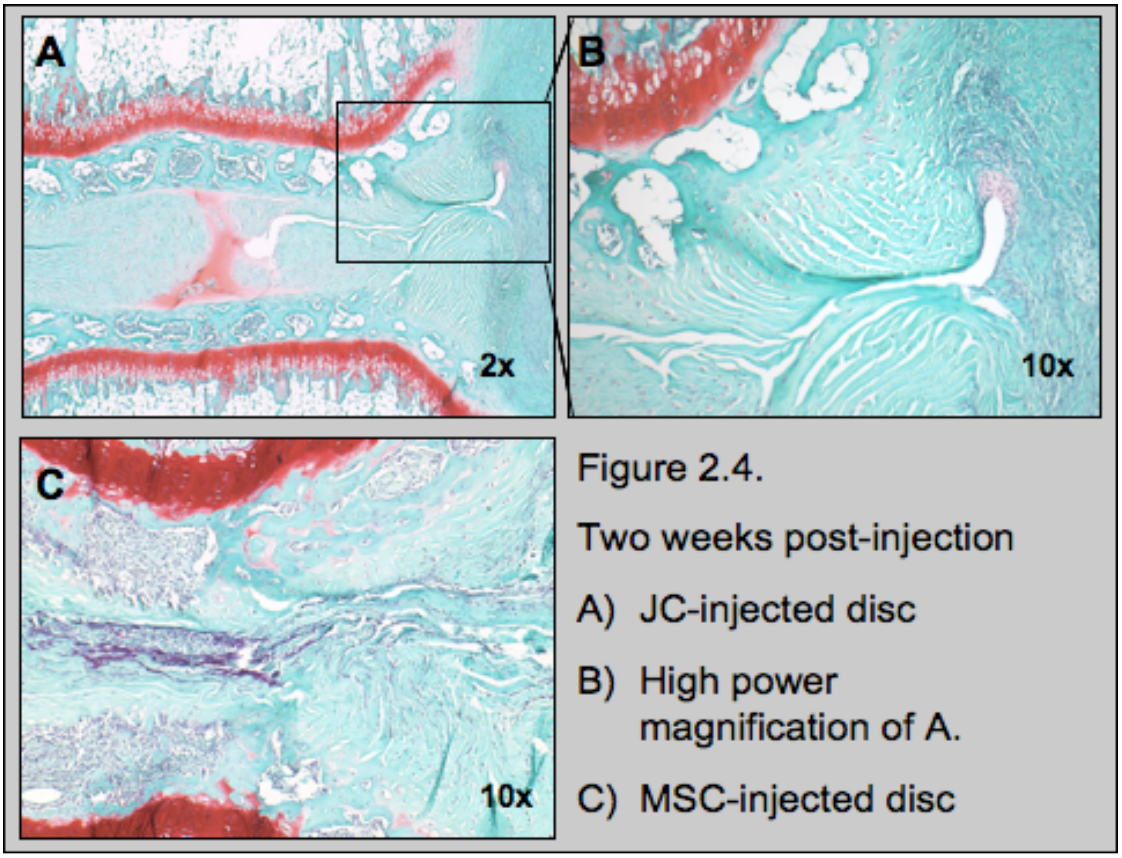

Figure 2.4 Inflammatory cells have infiltrated the wound tract and nuclear space in MSC-injected discs (C) but are absent in the JC-injected disc (A); newly synthesized hyaline matrix is typically observed in the wound tract.

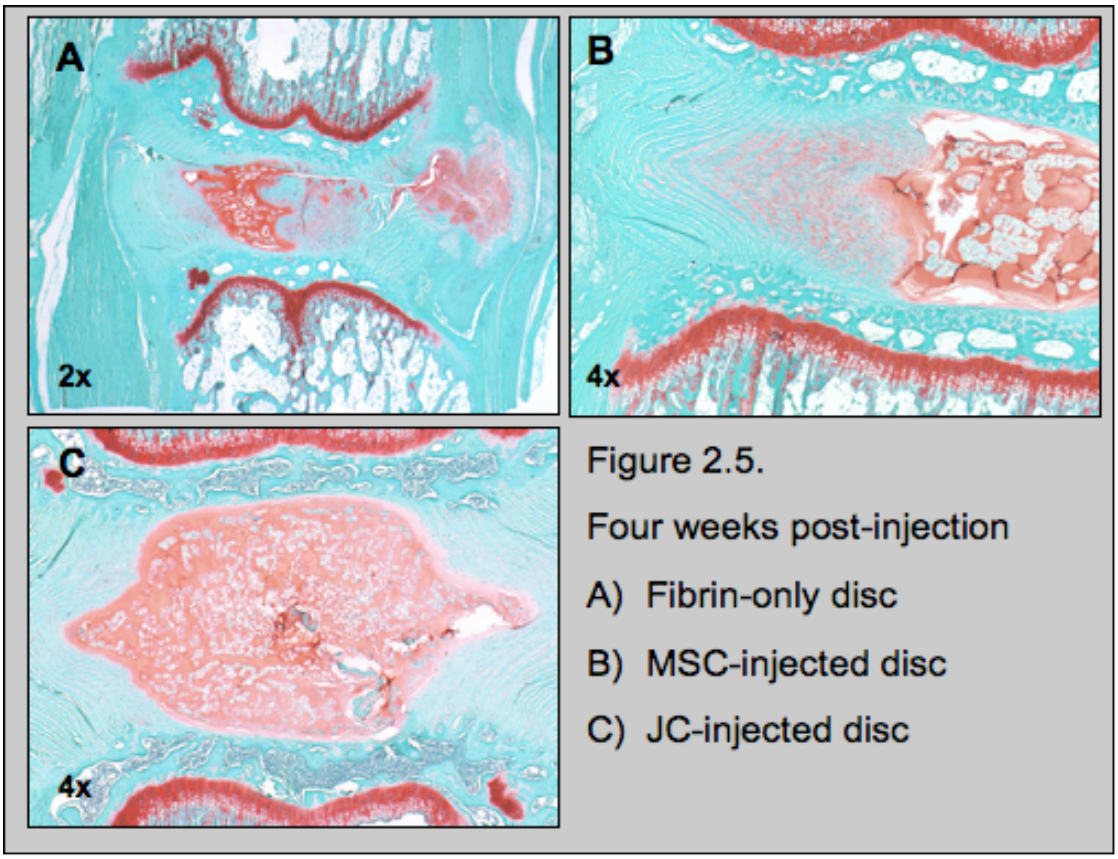

Figure 2.5 Safranin-O staining of representative discs harvested four weeks post-injection. Remnants of fibrin are found in the wound tract (A) or nuclear space (C).

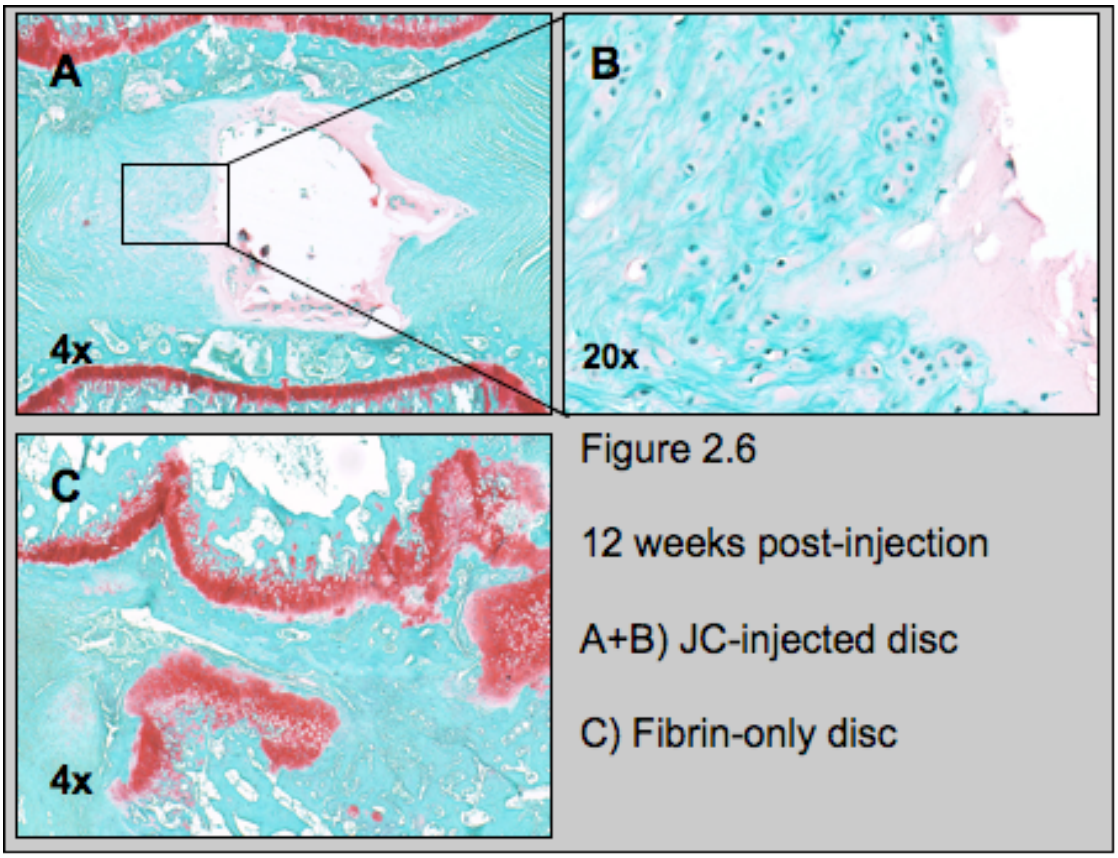

Figure 2.6 Safranin-O staining of representative discs harvested 12 weeks post-injection. Proliferating chondrocytes are observed to be present at the inner annulus border for JC-injected discs. An increase in Safranin-O staining and lamellar reorganization at the annular wound tract was observed between 2 and 12 weeks. Control discs demonstrated a marked reduction in Safranin-O content in the nucleus pulposus. Severe degeneration may be associated with disruption of the cartilage endplates. No evidence of inflammation was observed for any treatment group at 12 weeks post-injection.

Cell Retention

Injected JCs were confirmed present at all time points by PCR. Human β_2m products were not detected in any of the control rats and were detected in all three JC-injected rats at two weeks, three of the six JC-injected rats at four weeks, and five of the six JC-injected rats at twelve weeks (Figure 2.7). The absence of human β_2m products in some JC-injected rats could be due to low cell numbers that led to difficulty in detection by PCR.

For MSC-injected discs, LAMP-1 and LAMP-2 staining was not easily detected two or four weeks post-injection.

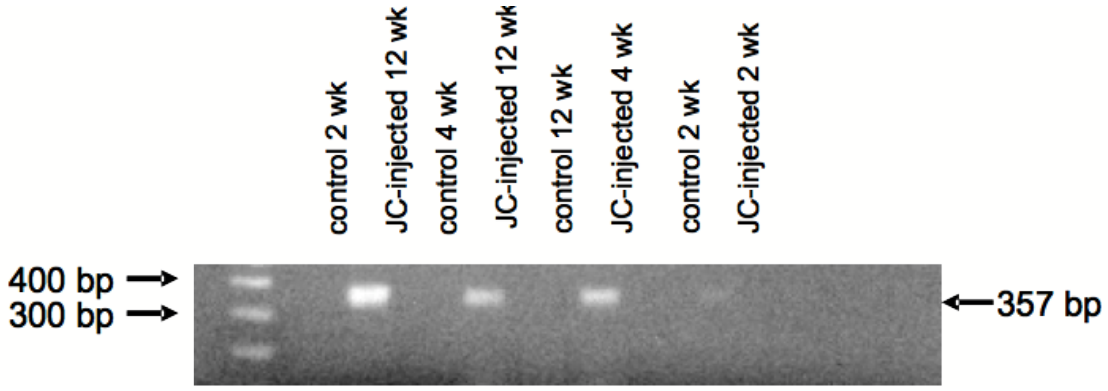

Figure 2.7 RT-PCR results confirming presence of human specific β2-microglobulin transcript (amplified fragment = 357 bp) in JC-injected discs at 2, 4 and 12 weeks post-injection.

2.4 Discussion

We hypothesized that synthetically active chondrocytes from prepubertal human donors (representative of cells differentiated along the chondrogenic lineage) would respond favorably in the disc environment. In support of this, we observed that *in vivo* transplantation of juvenile chondrocytes in a fibrin carrier results in a positive outcome relative to fibrin alone or transplantation of undifferentiated MSCs. Since juvenile chondrocytes are non-immunogenic, may be expanded in vitro [125], and respond well to *in vivo* disc conditions [128], they may provide an ideal source of cells for future human disc repair studies.

Although the disc height data suggests there is no difference between control and cell-injected discs at 4 and 12 weeks, histology reveals that discs injected with cells have normal-sized nucleus but a slightly flattened appearance, consistent with the slight

reduction in disc height. Nucleus size and signal intensity data from MRI for corresponding discs also confirm this.

Histologic data illustrates further differences between cell-injected and control discs. Discs injected with cells appear to have faster wound tract healing than control discs; fewer or no cell-injected discs display persistence of the wound tract, nuclear remnants, and disrupted annular architecture at time points where these features are still present in fibrin-only discs. Additionally, discs injected with JCs may heal faster than discs injected with MSCs. At two weeks, disc height decrease in the JC-injected discs is significantly smaller than that in MSC-injected discs (Figure 2.2). Inflammatory cells are also seen along the wound tract and in the nuclear space in MSC-injected discs but not in JC-injected discs (Figure 2.4). At four weeks post-injection, most control discs still have nuclear material in the outer annulus or outside the annulus, while most of the cell-injected discs lack this feature and are regaining normal nucleus size (Figure 2.5). This is confirmed by the significant improvement in MRI grade at four weeks in JC-injected discs. A possible explanation for this may be that JCs express bone morphogenetic proteins (BMPs) that have been implicated in accelerating cartilage repair [129], inducing chondrogenesis [130, 131], and stimulating proteoglycan and collagen synthesis by nucleus pulposus cells in vitro [132].

Limitations of this study relate to challenges of the animal models used. First, two different strains of rats were used for the experiments. Therefore, it is difficult to attribute differences in disc height changes and histology solely to the type of cell injected, as MSC experiments were performed in *rnu* homozygous rats and JC and fibrin-only experiments were performed in inbred Fisher rats. Also, it has been well established

in the literature that the intervertebral disc presents a harsh environment (high pressure, low oxygen and low pH) to newly implanted cells, and this environment can become more challenging in a degenerated disc [7, 22, 133, 134]. We used a healthy intervertebral disc model; the response of injected cells may differ in a degenerated disc environment. Thirdly, although the amount of fibrin (with or without cells) injected was constant for all discs, the amount of nucleus displaced by the injection is variable. The effects of this variability are most evident in the 12-week histological data. Although half of the control discs show complete degeneration, many also show signs of regeneration as determined by increased proteoglycan staining, suggesting that a smaller amount of nucleus was displaced during the treatment injection and the remaining nucleus cells can thereby participate in new matrix synthesis. It is important to note the differences between these "spontaneously regenerated" discs and the discs injected with JCs. The presence of proliferating chondrocytes at the border of the inner annulus and nucleus in the JC-injected discs could suggest a more active remodeling process is taking place compared to discs without cell treatment. This phenomenon has been demonstrated *in vitro* by others. Co-culture of nucleus pulposus cells with either mesenchymal stem cells or BMP-transduced articular chondrocytes resulted in increase proliferation and proteoglycan synthesis by the NP cells [116, 132]. Additionally, Le Visage et al. found that MSCs cultured in contact with annulus fibrosus cells resulted in overall enhanced proteoglycan synthesis [135]

In contrast, Richardson et al. reported that the increase in proteoglycan synthesis of MSC/NP co-culture is due to NP-mediated MSC differentiation [136]. This raises questions as to which cell types could be best suited for intervertebral disc repair. Our

findings reported here support the notion that differentiated cells are receptive to the disc milieu. This observation is consistent with prior studies that demonstrate significant differences between undifferentiated mesenchymal cells and differentiated chondrocytes in terms of their response to physical stimuli [34]. Response to compression is more pronounced in chondrocytes where the level of matrix development is more advanced [137]. Although MSCs may differentiate in the disc and ultimately secrete proteoglycan, the quality of matrix secreted may not be sufficient to regenerate the disc. For example, MSCs in three-dimensional culture have reduced potential in forming functional matrix compared to similarly cultured chondrocytes, where chondrocytes formed matrix that had two- to three-fold higher mechanical properties than that from MSCs [138]. Even when given additional culture time to allow for possible differentiation, MSC constructs never caught up to chondrocyte constructs in terms of mechanical properties and proteoglycan synthesis. MSCs in 3D culture also needed chondrogenic media to remain viable.

Other conditions of the degenerated disc such as low oxygen tension and inflammatory cytokine production may influence cell behavior and differentiation. Inflammatory cytokines such as IL-1β and TNF-α have been shown to interfere with chondrogenesis, inhibit collagen and proteoglycan synthesis, reduce TGF-beta-induced SMAD binding, or decrease Sox9 expression in chondrocytes [139-141]. Low oxygen tension can inhibit or enhance chondrogenesis in vitro depending on the cell type used [142, 143]. A combination of low oxygen tension and pressure enhanced aggrecan and collagen production in chondrocytes, but did not have the same effect on bone marrow-derived stem cells [143]. These factors affecting cell fate post-implantation should be taken into account in future in vitro experiments aiming to identify an optimal cell source

for therapeutic application in the disc, and the effects of pressure, oxygen, tension, and inflammatory cytokines should be explored in concert.

Chapter 3: Development of a Disc-Mimetic Bioreactor for Mesenchymal Stem Cell Culture

3.1 Introduction

Cell therapy aims to target the underlying cause of disc degeneration by repopulating the disc with cells capable of restoring its biomechanical properties by synthesizing appropriate matrix. Due to the difficulties associated with sourcing disc cells, such as the relative acellularity of the disc, donor site morbidity, and adjacent disc degeneration, researchers are investigating the use of mesenchymal stem cells (MSCs), which can be readily harvested, expanded, and are capable of differentiation.

Traditionally, biochemical agents such as TGF-β, BMPs, and dexamethasone are used to induce MSC chondrogenesis *in vitro* [101, 144, 145]. However, the *in vivo* disc environment plays a role in the differentiation and metabolism of disc cells, and therefore may have a significant effect on MSC chondrogenesis. The degenerated disc is a potentially hostile environment due to its altered nutritional supply and abnormal load exposure, but even the healthy disc has an environment that is not accurately represented by traditional cell culture conditions.

Oxygen concentrations in the center of the human nucleus pulposus can range from 5 mm Hg to 150 mm Hg [146], and there is no correlation with age, pathology, or degree of degeneration. Proteoglycan synthesis rates by intervertebral disc cells drop significantly when oxygen tension is reduced from 5% to 1% [24]. Low oxygen consumption rates can also be coupled with low pH levels in the disc, resulting in a decrease in the rate of matrix synthesis [134]. In contrast, hypoxia can act in a synergistic manner with chondrogenic growth factors such as TGF-β and cause increased collagen II expression and proteoglycan deposition by MSCs [147, 148]. Pilgaard et al.

demonstrated that while hypoxic pre-conditioning may not improve chondrogenic inducibility of human adipose-derived stem cells, hypoxia can upregulate factors related to cell proliferation and growth [149].

Mechanical factors can also affect disc cell behavior. As the osmotic pressure of the nucleus pulposus decreases with age, proteoglycan synthesis rates also decrease [32]. Hydrostatic pressures above or below normal physiologic levels decrease proteoglycan and collagen II synthesis and increase expression of MMPs [31, 32]. However, mechanical load is necessary to maintain matrix homeostasis in intervertebral discs [150], and can also affect MSC chondrogenesis. Exposure of MSCs to intermittent hydrostatic pressure (IHP) and TGF-β3 increases proteoglycan staining and significant increases in aggrecan, type II collagen, and sox9 mRNA expression [151, 152].

To date, there has only been one published study that attempts to differentiate mesenchymal stem cells *in vivo* [153]. Sakai et al. injected autologous MSCs into a rabbit model of disc degeneration and reported differentiation and proliferation of MSCs 48 weeks post-transplant. The degeneration procedure for this animal model resembles a partial nucleotomy, and it is difficult to say exactly how the unique microenvironment contributed to MSC differentiation. Co-culture of MSCs with NP cells can result in expression of chondrogenic genes and extracellular matrix production by MSCs [136, 154], and researchers must consider the fact that healthy NP cells may not be available to cause these effects when MSCs are transplanted into degenerated discs.

Experiments that attempt to predict the behavior of MSCs after disc transplantation suffer from either the issues faced with using small animal models (reported previously in Chapter 2 as well as in the literature), or that *in vitro* experiments

are carried out in traditional cell culture conditions. This chapter describes the development of a bioreactor culture system that mimics both the hypoxic nature of the disc and exposes cells to increased hydrostatic pressure. Our goal in this study is to determine if the physiochemical environment of the disc, absent native disc cells and chondrogenic growth factors, can induce chondrogenic differentiation of MSCs. We cultured undifferentiated MSCs in these bioreactors for up to five weeks, and then measured GAG production and expression levels of several chondrogenic genes.

3.2 Methods

Materials

Human bone marrow-derived MSCs, chondrogenic media (CM), human recombinant TGF-β3 and mesenchymal stem cell growth media (MSCGM) were purchased from Lonza Walkersville Inc. Slide-A-Lyzer dialysis cassettes (gamma-irradiated, 10,000 MWCO) were purchased from Pierce Biotechnology Inc. Fibrin glue (Tisseel VH) was purchased from Baxter Biosciences. Sodium hyaluronate powder was purchased from Genzyme. Buffer RLT, Qiashredder columns, and RNeasy kits were purchased from Qiagen. Trizol reagent and PureLink RNA Mini kits were purchased from Invitrogen. Human Col2A1 primer was purchased from SABiosciences. All other primers were supplied by the UCSF Genome Analysis Core or manufactured by Integrated DNA Technologies.

Alginate Bead Culture

Mesenchymal stem cells from different donors were expanded up to passage

seven in MSCGM. MSCs were suspended in a 1.2% alginate solution at a concentration of $4x10^6$ cells/mL. The alginate cell solution was dispensed dropwise from a syringe fitted with a 22-gauge needle into a 102mM CaCl2 bath. Beads were allowed to cure at room temperature for 15 minutes, rinsed twice with PBS and then transferred to low-attachment 6-well culture plates. Beads were then cultured in CM with 10 ng/mL TGF-β3 ("TGF-β3 beads") or MSCGM ("control beads") for one, two, three, four, or five weeks.

Bioreactor Design and Construction

A 15% hyaluronan (HA) gel was made by dissolving sodium hyaluronate powder in MSCGM. Three hundred microliters of this gel was injected through the self-sealing silicone port of a dialysis cassette and excess air was removed from the cassette. The cassette was then incubated in MSCGM for four hours to allow for gel volume expansion and osmotic pressurization (equilibration based on osmotic pressure differences between the HA gel and culture media). Undifferentiated MSCs were suspended in fibrin glue at a final concentration of 4×10^6 cells/mL and a 100 μL pellet of fibrin and cells was injected into the center of the expanded cassette. An autoclavable porous metal clip surrounds the device to permit fluid exchange but prevent membrane rupture due to internal pressurization (Figure 3.1). Cassettes were then incubated in MSCGM at 37 degrees with 5% CO_2 for one, two, three, four, or five weeks.

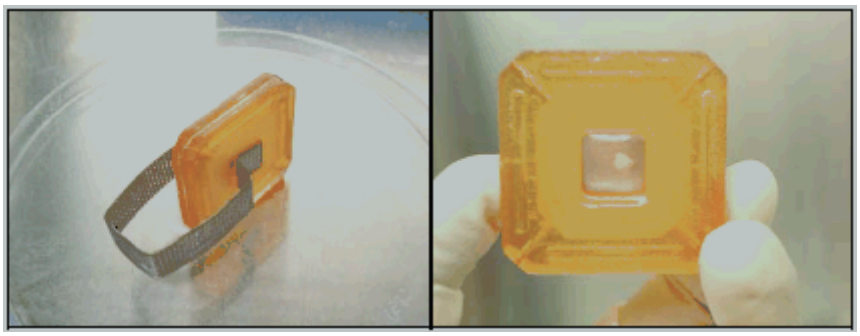

Figure 3.1 Bioreactor design (left). Cell-fibrin pellet within hyaluronan gel (right).

Bioreactor Oxygen and Pressure Measurements

Oxygen levels inside the bioreactor were measured with the assistance of Mark Rollins, M.D., Ph.D., in the UCSF Hypoxia Research Laboratory.

The LICOX MCB® Oxygen Monitoring System (GMS, Germany) and LICOX REVOXODE oxygen probe (Model C1, OD = 0.47mm) were used to determine the partial pressure of oxygen inside the bioreactor ($P_{BR}O_2$). The probe was first calibrated to room air. A 19-gauge spinal tab needle was then introduced into one of the self-sealing silicone ports of the bioreactor, and the probe was fed through the needle lumen so that the tip was placed next to the cell-fibrin pellet. The needle was pulled back so that the port was closed, leaving the probe inside the bioreactor.

Probe measurements were converted into oxygen tension using the equation: $(P_{ATM} - P_{H2O}) \times A = B\ P_{O2}$, where A = oxygen tension, and B = measurement by the oxygen probe in mmHg.

The P_{ATM} and P_{H2O} constants were determined based on the room temperature, and obtained from a physical property table in the CRC *Handbook of Chemistry and Physics*. The average oxygen tension within the bioreactor is 4.8%.

Pressure measurements were obtained using the Stryker Intra-compartmental Pressure Monitor System (Stryker Corp., U.K.). The readings were converted into MPa assuming an atmospheric pressure of 760 mmHg. Pressure readings were taken with and without the metal clip; the clip contributed roughly 0.01 MPa to the final measurement. The average pressure inside the bioreactor was 0.12 MPa, which is consistent with physiologic levels within the disc at rest.

Cell Viability and Histology

At the end of the specified time point, two bioreactors were cut open and the fibrin-cell pellet was removed. The pellet was stained with Live-Dead Assay to obtain cell viability information. Five images in different sections of each pellet were captured and the percentage of live cells calculated and averaged from each section.
The pellets were then placed in 10% buffered formalin and processed in paraffin for histology. Seven-micron sections were cut and mounted onto glass slides. Slides were deparaffinized and hydrated before staining with fast green and Safranin-O to visualize collagen and proteoglycan.

DMMB Assay for Proteoglycan Quantification

At the end of each time point, bioreactors were removed from media, and the fibrin-cell pellet was separated from the surrounding hyaluronan gel. The fibrin pellet was weighed and digested for 48 hours at 65 degrees in a papain solution (15 U/g of tissue, 100 mg/mL solution). The hyaluronan gel was digested in 5 mL of 100 U/mL hyaluronidase solution for three hours at 37 degrees. Both the digested pellet and

hyaluronan solutions were centrifuged for five minutes at 500*g* and the supernatant reserved for DMMB assay.

Standards were prepared with chondroitin sulfate A in a range of concentrations from 0 to 100 μg/mL. Pellet and hyaluronan gel samples were diluted 10-fold, and 40 μL of each sample was added to 250 μL of DMMB solution (21mg DMMB, 5mL absolute EtOH, 2g sodium formate in total volume 800mL ddH2O with pH 3.5) in a 96-well plate. Standards and samples were run in triplicate, and OD measured at 525nm.

Real-time PCR Analysis of Gene Expression

All qRT-PCR experiments were performed on at least three biological replicates. For the TGF-β3 and control bead groups, alginate beads were washed three times in PBS and digested in a 55mM sodium citrate solution to release cells from alginate matrix. Cells were homogenized in buffer RLT with Qiashredder tubes and RNA extracted using the RNeasy kit according to manufacturer's protocol.

Bioreactors were flash-frozen in liquid nitrogen and homogenized using Trizol reagent; RNA was extracted using the PureLink Mini kit according to manufacturer's protocol.

RNA quantification, reverse transcription, and real-time PCR analyses were carried out at the UCSF Genome Analysis Core. All primers (Table 3.1) were optimized by the core facility. PCR reactions were carried out in triplicate, using BioRad SybrGreen Mastermix, with no-RT and water controls. All data was analyzed using the $2^{-\Delta\Delta CT}$ method using the housekeeping gene GUS. Statistical analyses were performed on the

ΔCt values; one-way ANOVA and Student t-tests were used to detect differences between groups with a significance level of $p<0.05$. Basal gene expression levels of undifferentiated MSCs were also measured.

Table 3.1 Primer sequences for qRT-PCR

Gene	Primer sequence	Product size (bp)
Sox9	F: 5' TCT ACA CAC AGC TCA CTC GAC CTT	83
	R: 5' TTC TTC GGT TAT TTT TAG GAT CAT CTC	
Aggrecan	F: 5' GCG AGT TGT CAT GGT CTG AA	122
	R: 5' TTC TTG GAG AAG GGA GTC CA	
Collagen II	RT2 qPCR Primer Assay, SABiosciences Corp.	
Collagen X	F: 5' CAG ATT TGA GCT ATC AGA CCA ACA A	85
	R: 5' AAA TTC AAG AGA GGC TTC ACA TAC G	
HIF-1alpha	F: 5' TTT ACC ATG CCC CAG ATT CAG	82
	R: 5' GAC TAT TAG GCT CAG GTG AAC TTT GTC	
Collagen I	F: 5' AAC CAA GGA TGC ACT ATG GA	162
	R: 5' GCT GCC AGC ATT GAT AGT TT	

3.3 Results

Cell Viability

Cell viability ranged between 80 – 85% within the bioreactors, with no significant differences due to length of culture time.

Histology

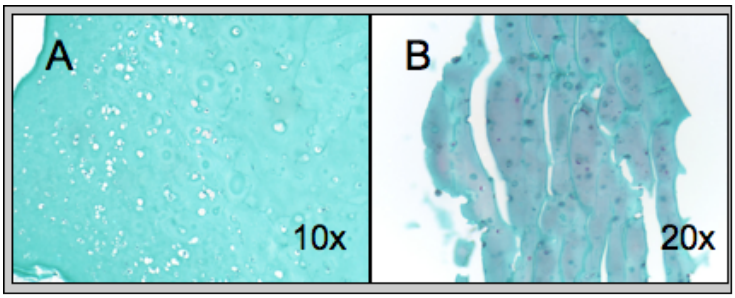

Figure 3.2 Safranin-O/Fast green staining of fibrin-cell pellets.
A) 2 weeks bioreactor culture B) 4 weeks bioreactor culture
Proteoglycan staining is not present until cells have been cultured for 4 weeks in the bioreactor; staining is diffuse rather than concentrated around individual cells.

Proteoglycan Quantification (Figure 3.3)

As culture time in the bioreactor increased, undifferentiated cells produced increasing amounts of proteoglycan, with four weeks of bioreactor culture (Table 3.2) resulting in significantly higher proteoglycan than any other time point ($p<0.05$).

Table 3.2 Average total GAG amount in bioreactors

Culture Time	Average total GAG content (ug)
1 week	41 ± 13 (n=5)
2 weeks	118 ± 66 (n=6)
3 weeks	150 ± 61 (n=5)
4 weeks	266 ± 39 (n=5)
5 weeks	203 ± 44 (n=5)

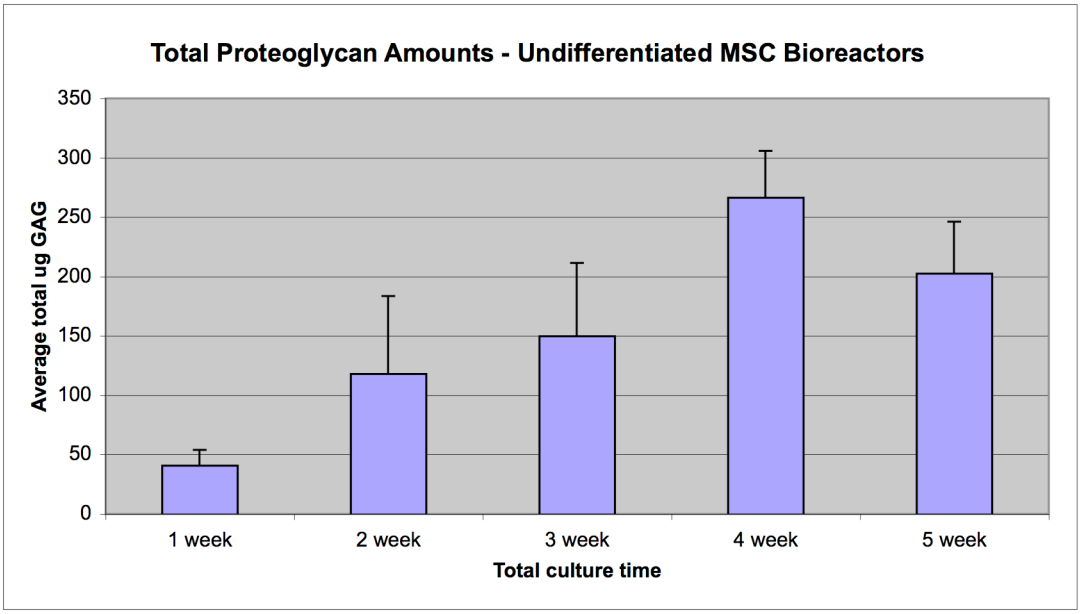

Figure 3.3 Total GAG amounts as measured by DMMB assay. Four weeks of bioreactor culture results in the highest amount of GAG production ($p<0.05$).

Gene Expression

There is no significant change in aggrecan expression with increased culture time in bioreactors or control bead culture. Not until 5 weeks of culture does aggrecan

expression in bioreactors exceed that of control beads, although the change is not significant (Figure 3.4). However, TGF-β3 culture results in consistently higher aggrecan expression levels, with significantly higher expression at all time points compared to control bead culture, and at 2 and 3 weeks compared to bioreactor culture.

TGF-β3 treatment results in an increase in collagen II expression by MSCs (Figure 3.5), with significant increases compared to baseline levels occurring after 4 and 5 weeks of treatment ($p<0.002$). Expression levels do not significantly change at any time point in control bead culture. When cultured in the bioreactor, collagen II expression is significantly increased from baseline ($p<0.02$) after 3 weeks of culture, with expression levels exceeding that of 3-week TGF-β3 beads.

Sox9 expression is not significantly altered by bioreactor culture or control bead culture (Figure 3.6). TGF-β3 treatment significantly upregulates Sox9 expression compared to baseline after 1, 2, 3, and 5 weeks of treatment, with the highest levels found after 2 weeks of culture ($p<0.02$).

Bioreactor culture of cells for two, three, four, or five weeks increases collagen X expression compared to control bead culture, with significant increases at 2 weeks ($p<0.02$) and 5 weeks ($p<0.04$) culture. Although bioreactor and control bead culture increase collagen X expression compared to baseline, increase in culture time does not result in significant differences. Collagen X expression is significantly increased by TGF-β3 treatment (Figure 3.7).

HIF-1α is not significantly regulated by TGF-β3 (Figure 3.8); at all time points, HIF-1α expression does not differ significantly from that of baseline MSCs. When cells are cultured in the bioreactor, however, HIF-1α expression is upregulated, with a

significant 2.3-fold increase from baseline occurring at 2 weeks of BR culture ($p<0.02$). At 3, 4, and 5 weeks of culture, expression levels drop down to levels that are not significantly different from basal levels of MSCs.

Collagen I expression does not significantly change from basal levels with TGF-β3 treatment, but expression is downregulated after 4 weeks of culture (Figure 3.9). Expression is significantly decreased from baseline levels by control bead culture ($p<0.05$), an effect that is not dependent on length of culture time. The effect of the bioreactor environment is even stronger on collagen I downregulation, with 2 weeks of BR culture resulting in significantly lower expression compared to control bead culture and TGF-β3 treatment ($p<0.03$).

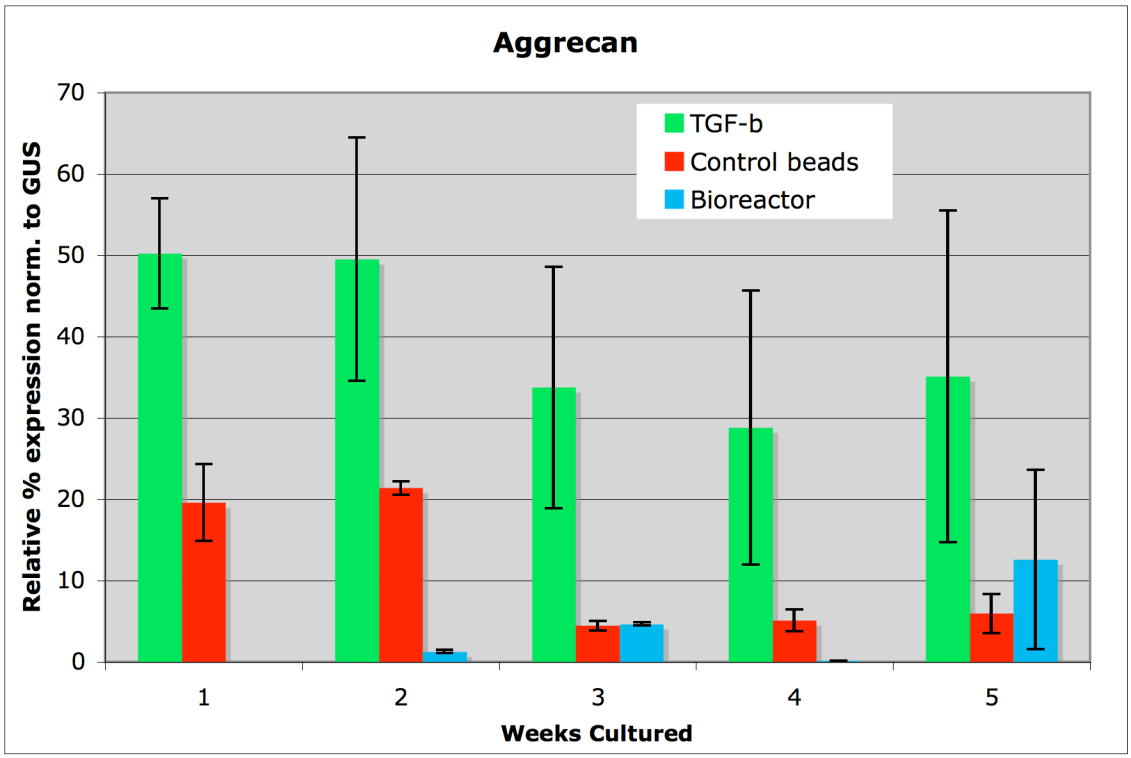

Figure 3.4 Gene expression levels of aggrecan normalized to GUS. Bioreactor culture for five weeks results in 2x increased aggrecan expression over control beads; expression levels are highest however, in TGF-β3 beads (2.5- to 7.5x higher than control beads).

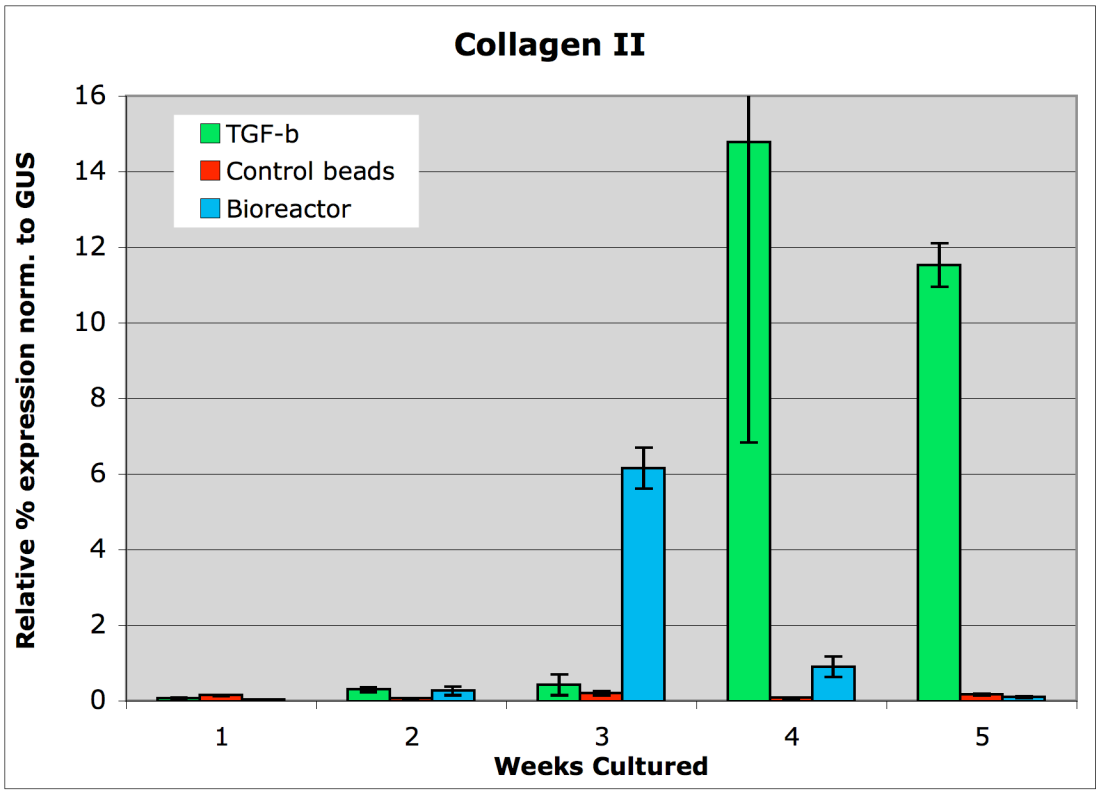

Figure 3.5 Gene expression levels of collagen II normalized to GUS. After three weeks of culture in the bioreactor, collagen II expression is significantly higher than in control beads or TGF-β3 beads. TGF-β3 treatment significantly increases expression at four and five weeks of culture ($p<0.002$). Baseline levels of collagen II expression in MSCs = 0.02% relative to GUS

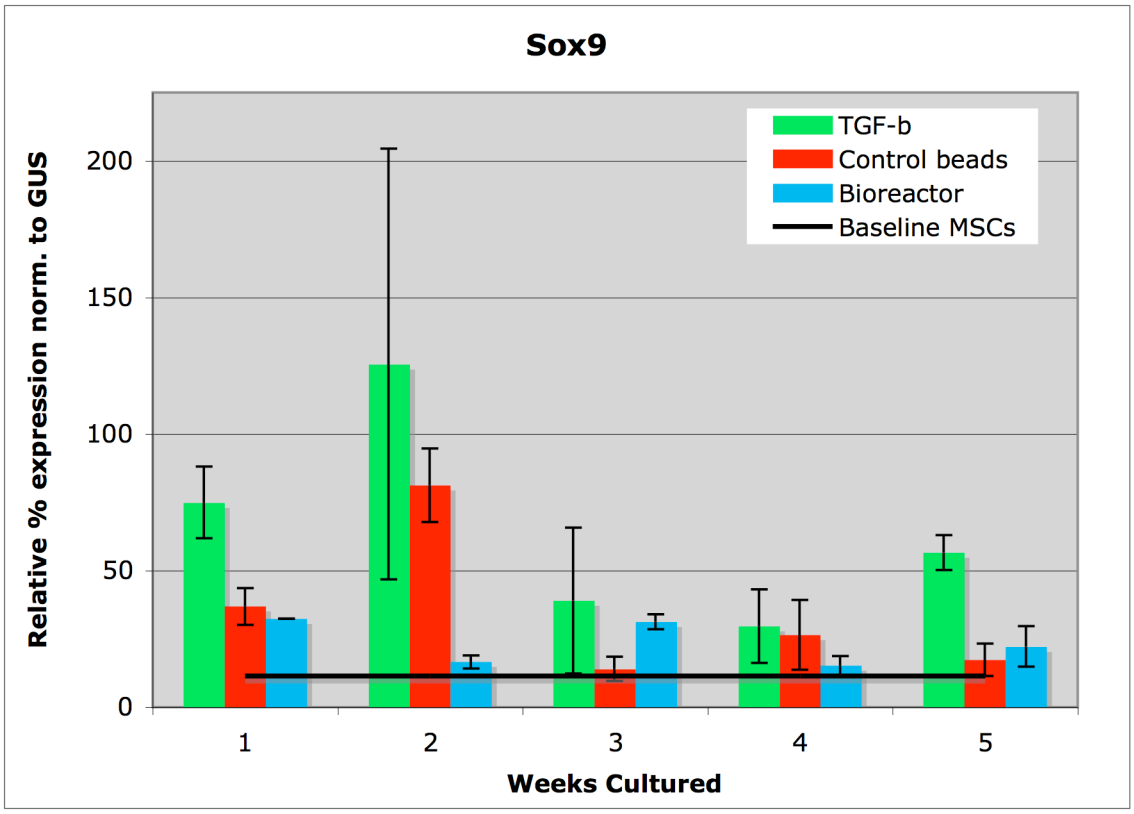

Figure 3.6 Gene expression levels of Sox9 normalized to GUS. Bioreactor and control bead culture do not significantly alter Sox9 expression compared to baseline levels. The highest levels of Sox9 expression result from 2 weeks of TGF-β3 treatment ($p<0.02$).

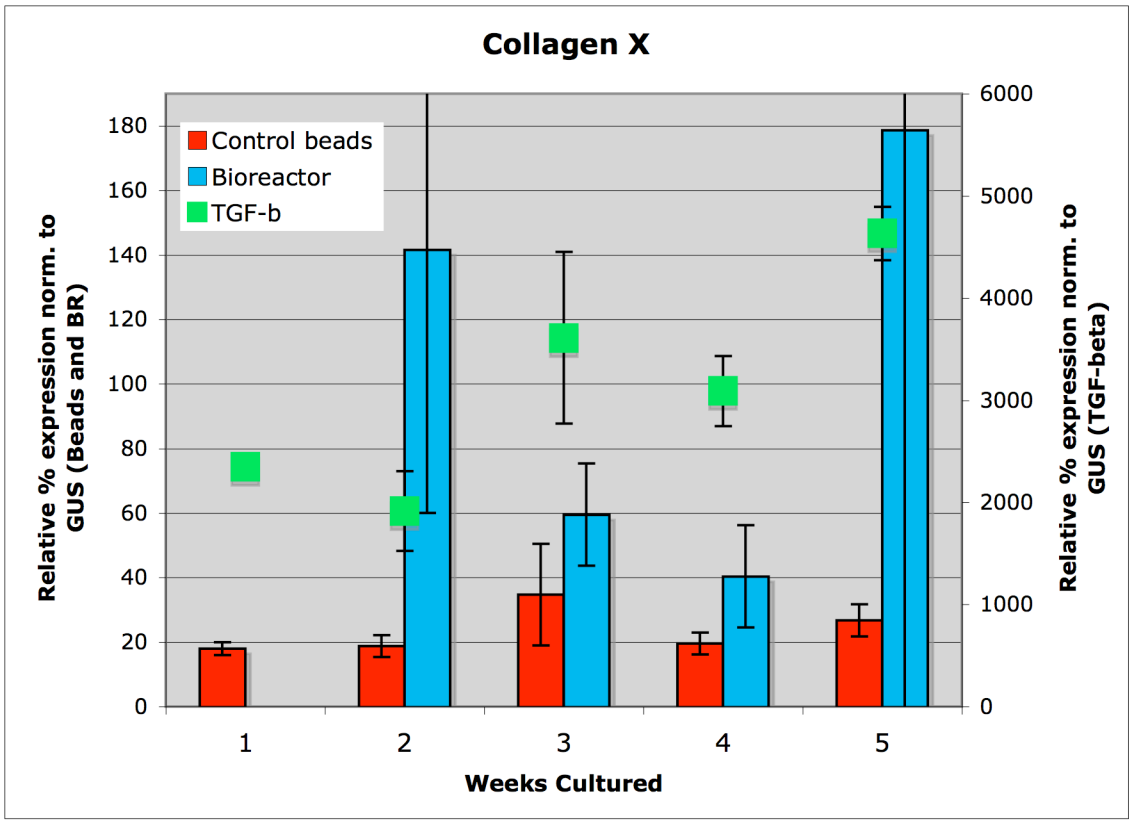

Figure 3.7 Gene expression levels of collagen X normalized to GUS. Collagen X expression is upregulated by TGF-β3 over 100-fold compared to control bead culture. Collagen X expression is significantly upregulated by bioreactor culture at 2 ($p<0.02$) and 5 ($p<0.04$) weeks compared to control bead culture. Baseline levels of collagen X expression in MSCs = 0.65% relative to GUS

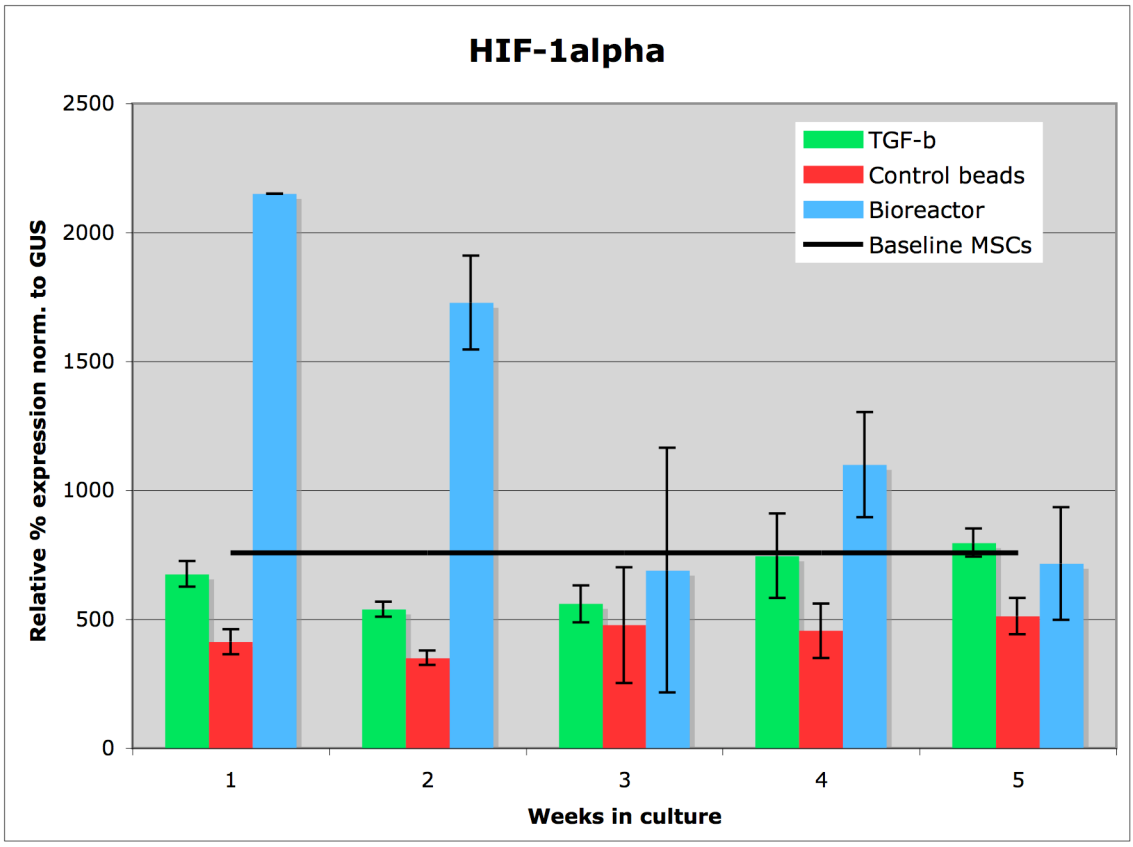

Figure 3.8 Gene expression levels of HIF-1α normalized to GUS. Two weeks of bioreactor culture results in a significant increase (2.3-fold) in expression from baseline levels ($p<0.02$). TGF-β3 treatment and control bead culture do not significantly change HIF-1α expression levels during any length of culture.

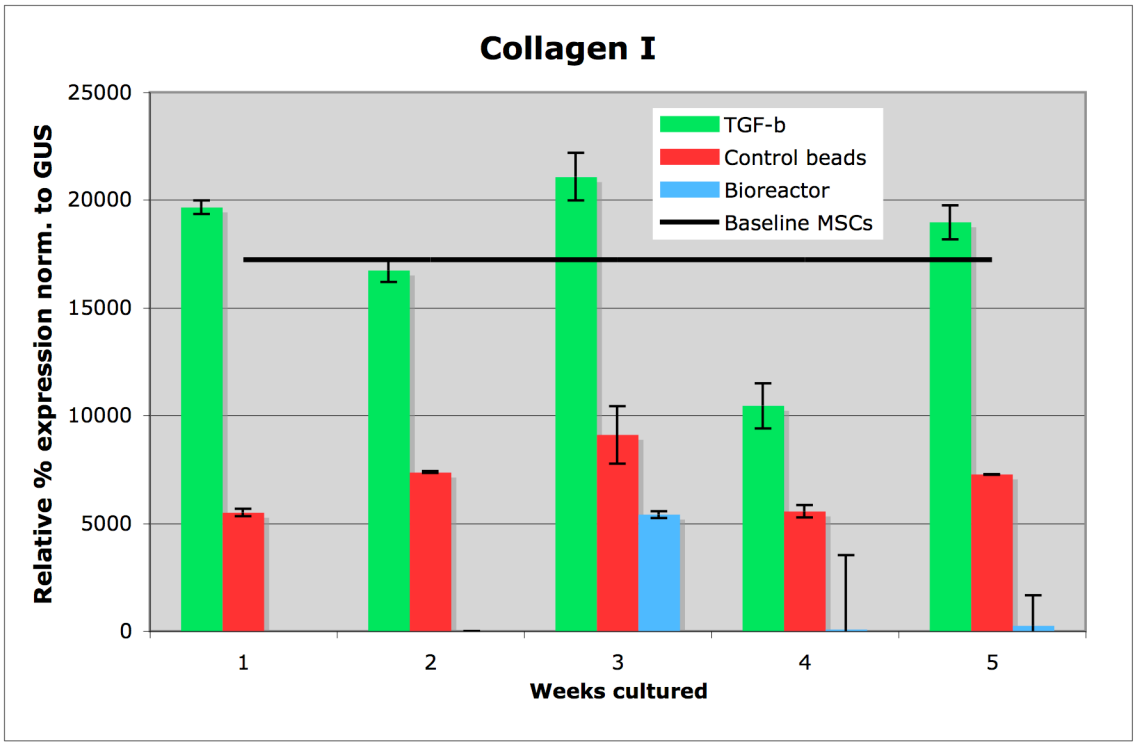

Figure 3.9 Gene expression levels of collagen I normalized to GUS. Control bead culture significantly decreases collagen I expression levels from baseline ($p<0.05$). Expression levels are not significantly affected by TGF-β3 treatment.

3.4 Discussion

We have described in this study a disc-mimetic bioreactor culture system that exposes injected MSCs to 4.8% oxygen tension and 0.12 MPa pressure. This environment is supportive of cell viability and proteoglycan production, and can induce expression of chondrogenic genes. The reported data support the idea that disc-mimetic conditions alone can induce MSC differentiation.

Induction of chondrogenic genes occurs on different timelines depending on the manner of differentiation (Table 3.3). Aggrecan expression is upregulated earlier in TGF-β3 beads than in the bioreactor. Conversely, significant increase in collagen II expression happens earlier in the bioreactor (3 weeks) than in TGF-β3 beads (4 and 5

weeks). Sox9 expression is significantly increased after 1 week of TGF-β3 bead culture, but does not significantly change in bioreactor culture at any time. Collagen X appears early in both bioreactors and TGF-β3 beads. HIF-1α is not regulated by TGF-β3 culture but is significantly increased after 2 weeks of bioreactor culture. Significant collagen I downregulation occurs earlier in the bioreactor (2 weeks) than in TGF-β3 beads (4 weeks).

Previous studies have established a timeline for chondrogenic gene expression during differentiation, with Sox9 induction occurring early at 2 days, induction of aggrecan at 4-5 days, induction of type II collagen after 7-8 days, early, and sustained detection of collagen X mRNA throughout the differentiation process [101, 155]. The TGF-β3 bead results follow this order, but at a slower pace. The bioreactor gene expression results loosely follow this order as well, with a few exceptions: Sox9 expression does not significantly change from baseline and significant aggrecan upregulation does not occur until 3 weeks, at the same time that collagen II is significantly upregulated. Sox9 is a transcription factor required for chondrocyte differentiation and the expression of genes such as Col2a1 and Aggrecan [156]; the fact that both aggrecan and collagen II expression levels increase in bioreactor culture without a significant increase in Sox9 expression should be noted. However, this could be a result of variation among the biological replicates; Sox9 expression in bioreactors was higher at 1 and 3 weeks than baseline MSCs levels (not significant, $p>0.10$).

Although GAG production in the bioreactor steadily increases with time, it does not peak until four weeks, perhaps as a result of the later surge in aggrecan gene

expression. Safranin-O staining also confirms this, as positive staining in the bioreactors is not seen until 4 weeks (Figure 3.2).

Table 3.3 Environment-dependent timeline of gene expression induction.

Gene	Environment	Weeks in Culture				
		1	2	3	4	5
Aggrecan	BR			⇧		
	TGF-b3	⇧	——	——	——	——▷
Collagen II	BR			⇧		
	TGF-b3				⇧	
Sox9	BR	-	-	-	-	-
	TGF-b3	⇧				
Collagen X	BR		⇧			
	TGF-b3	⇧				
HIF-1alpha	BR		⇧			
	TGF-b3	-	-	-	-	-
Collagen I	BR		⇩			
	TGF-b3				⇩	

Hypoxic environments induce expression of HIF-1α in both MSCs and chondrocytes [157, 158], and adult stromal cells with targeted deletion of the gene encoding HIF-1α have significantly reduced chondrogenic potential [142]. HIF-1α upregulates Sox9 under hypoxic conditions [159], and when HIF-1α is suppressed, there is a partial loss of aggrecan expression in rat NP cells [160]. This could perhaps explain how in the bioreactor, aggrecan and collagen II were upregulated in the absence of significant Sox9 upregulation, as HIF-1α was upregulated in the first two weeks of bioreactor culture. This upregulation did not persist after two weeks; it is possible that while mRNA expression was absent, the actual proteins were still present. It is also possible that as cells are differentiated by the bioreactor, HIF-1α upregulation is no longer needed; Risbud et al. demonstrated that nucleus pulposus cells produce HIF-1 proteins in normoxic conditions [161].

Although TGF-β3-mediated induction of MSCs may result in a gene expression profile similar to that of NP cells [102, 147], the molecular and histologic appearance of TGF-β3-treated MSCs is closer to fibrocartilage than that of hyaline cartilage because collagen I expression is enhanced. Bioreactor culture results in stronger downregulation (from baseline) of collagen I expression compared to control bead culture, suggesting cells cultured in the bioreactor may differentiate to a phenotype closer to NP cells rather than fibroblasts. Bioreactor culture also dampens and delays the increase in collagen X expression that is seen in TGF-β3 beads. Hypertrophic maturation of MSCs is characterized by the premature expression of collagen X, which can be detected early during MSC chondrogenesis, but it is debatable whether its expression signals true hypertrophic differentiation [162]. However, expression has been correlated with the unstable nature of transplanted tissue *in vivo*, which can lead to vascular invasion and calcification [163].

The disc-mimetic bioreactor is not only capable of inducing chondrogenic gene expression in MSCs, but can be used in place of a small animal model as a diagnostic tool to investigate behavior of various cell types after exposure to disc-mimetic conditions. It should be noted that the density of cells cultured in these bioreactor experiments is much lower than that of pellet or micromass culture. Cell-cell contact is important in chondrogenesis [164], and therefore use of the bioreactor to pre-differentiate cells might benefit from a higher cell density. However, it is preferable to represent the native disc conditions (including nucleus cellularity) when using the bioreactor as a diagnostic tool.

Based on our results, it may be possible for injected MSCs to differentiate and produce matrix once transplanted into the disc. The amount of time this would take,

however, coupled with the unpredictable nature of the degenerated disc, implies that cell transplantation into the disc would be more successful if cells are pre-differentiated prior to *in vivo* implantation.

Chapter 4: Effect of TGF-β3 Pre-treatment on Mesenchymal Stem Cell Behavior in a Disc-Mimetic Environment

4.1 Introduction

Current therapies for back pain patients with intervertebral disc degeneration are targeted at relieving symptoms of low back pain rather than targeting the underlying cause. As researchers start to develop an improved understanding of how disc degeneration develops, future possible therapies include less invasive regeneration strategies such as growth factor treatments, cell-based therapies, or tissue-engineering approaches [165].

Due to the relatively acellular nature of the intervertebral disc [12], autologous disc transplantation would not be feasible for tissue engineering applications, and researchers have investigated the use of mesenchymal stem cells for cell-based treatments. Mesenchymal stem cells (MSCs) can be differentiated into chondrocyte-like or disc-like cells *in vitro* [102, 147, 154, 166] but few studies have shown what the fate of these cells might be once implanted into the disc. Although MSCs have been used *in vivo* in a rabbit disc animal model [167], it is difficult to determine exactly to what extent the cells contribute to the healing process. Since loss of cellularity and reduced extracellular matrix production is a central feature of degenerative disc disease, the introduction of cells capable of surviving and producing normal extracellular matrix in a high pressure, low oxygen tension and low pH environment is critical for successful bioengineered disc regeneration.

Mechanical load helps maintain matrix homeostasis in intervertebral discs [150], and mechanical and hypoxic stress can affect chondrogenesis or the proliferative and

regenerative qualities of chondrocytes, MSCs, or disc cells [168-170]. We have developed a cell culture bioreactor that mimics the hydrostatic pressure and hypoxic conditions of the intervertebral disc in order to address several questions regarding the use of MSCs for cell-based IVD therapy. As described in Chapter 3, MSCs cultured in the bioreactor are able to produce proteoglycan and express chondrogenic markers such as increased aggrecan and collagen II gene expression. However, upregulation of chondrogenic genes occurred after three weeks of culture, and peak proteoglycan levels were found after four weeks. Based on these results and those from the animal study in Chapter 2, we believe a more differentiated MSC may be more responsive to the disc conditions and will be able to mount a more accelerated repair response. The goal of this study was to test this hypothesis by investigating the behavior of MSCs that are pre-treated with TGF-β3 in the disc-mimetic bioreactor. Cell response was characterized by proteoglycan production and chondrogenic gene expression. We also investigated what effect the disc environment may have on the persistence of TGF-β3-induced gene expression in MSCs.

4.2 Methods

Materials

Human bone marrow-derived MSCs, mesenchymal stem cell growth media (MSCGM), chondrogenic media (CM), and rhTGF-beta3 were purchased from Lonza Walkersville Inc. Slide-A-Lyzer dialysis cassettes (gamma-irradiated, 10,000 MWCO) were purchased from Pierce Biotechnology Inc. Fibrin glue (Tisseel VH) was purchased

from Baxter Biosciences. Sodium hyaluronate powder was purchased from Genzyme. Buffer RLT, Qiashredder columns, and RNeasy kits were purchased from Qiagen. Trizol reagent and PureLink RNA Mini kits were purchased from Invitrogen. Human Col2A1 primer was purchased from SABiosciences. All other primers were supplied by the UCSF Genome Analysis Core or manufactured by Integrated DNA Technologies.

Alginate Bead Culture

Mesenchymal stem cells from different donors were expanded up to passage seven in MSCGM. MSCs were suspended in a 1.2% alginate solution at a concentration of $4x10^6$ cells/mL. The alginate cell solution was dispensed dropwise from a syringe fitted with a 22-gauge needle into a 102mM $CaCl_2$ bath. Beads were allowed to cure at room temperature for 15 minutes, rinsed twice with PBS and then transferred to low-attachment 6-well culture plates. Beads were then cultured in chondrogenic media with 10 ng/mL TGF-β3 for one, two, or three weeks

At the end of the culture period, beads from each time point were split into three groups. One group was processed for qRT-PCR (described below) to serve as a baseline for our investigation on how the disc-mimetic bioreactor affects the persistence of genes regulated by TGF-β3. For the second group, beads were rinsed twice with PBS and then cultured in MSCGM for two weeks ("control beads"). The third group of beads were digested by a method previously described [171] to release cells and preserve cell-associated matrix. These cells were used for bioreactor culture (described below).

Bioreactor Construction

Bioreactor cassettes were prepared as previously described in Chapter 3. Cells (undifferentiated MSCs or cells released from alginate bead culture) were suspended in fibrin glue at a final concentration of 4 x 10^6 cells/mL and a 100 μL pellet of fibrin and cells was injected into the center of the media-equilibrated dialysis cassette. Cassettes were affixed with clips to prevent membrane rupture due to internal pressurization and then incubated in MSCGM at 37 degrees with 5% CO_2 for two weeks.

Cell Viability and Histology

At the end of the specified time point, two bioreactors were cut open and the fibrin-cell pellet was removed. The pellet was stained with Live-Dead Assay to obtain cell viability information. Five images in different sections of each pellet were captured and the percentage of live cells calculated and averaged from each section.
The pellets were then placed in 10% buffered formalin and processed in paraffin for histology. Seven-micron sections were cut and mounted onto glass slides. Slides were deparaffinized and hydrated before staining with fast green and Safranin-O to visualize collagen and proteoglycan.

DMMB Assay for Proteoglycan Quantification

After the two-week culture period, bioreactors were removed from media, and the fibrin-cell pellet was separated from the surrounding hyaluronan gel. The fibrin pellet was weighed and digested for 48 hours at 65 degrees in a papain solution (15 U/g of

tissue, 100 mg/mL solution). The hyaluronan gel was digested in 5 mL of 100 U/mL hyaluronidase solution for three hours at 37 degrees. Both the digested pellet and hyaluronan solutions were centrifuged for five minutes at 500*g* and the supernatant reserved for DMMB assay.

Standards were prepared with chondroitin sulfate A in a range of concentrations from 0 to 100 μg/mL. Pellet and hyaluronan gel samples were diluted 10-fold, and 40 μL of each sample was added to 250 μL of DMMB solution (21 mg DMMB, 5 mL absolute EtOH, 2 g sodium formate in total volume 800 mL ddH2O with pH 3.5) in a 96-well plate. Standards and samples were run in triplicate, and OD measured at 525 nm.

Real-time PCR Analysis of Gene Expression

All qRT-PCR experiments were performed on at least three biological replicates. For the TGF-β3 and control bead groups, alginate beads were washed three times in PBS and digested in a 55mM sodium citrate solution to release cells from alginate matrix. Cells were homogenized in buffer RLT with Qiashredder tubes and RNA extracted using the RNeasy kit according to manufacturer's protocol.

Bioreactors were flash-frozen in liquid nitrogen and homogenized using Trizol reagent; RNA was extracted using the PureLink Mini kit according to manufacturer's protocol.

RNA quantification, reverse transcription, and real-time PCR analyses were carried out at the UCSF Genome Analysis Core. All primers (Table 4.1) were optimized by the core facility. PCR reactions were carried out in triplicate, using BioRad SybrGreen

Mastermix, with no-RT and water controls. All data was analyzed using the $2^{-\Delta\Delta CT}$ method using the housekeeping gene GUS. Statistical analyses were performed on the ΔCt values; one-way ANOVA and Student t-tests were used to detect differences between groups with a significance level of $p<0.05$.

Table 4.1 Primers for qRT-PCR

Gene	Primer sequence	Product size (bp)
Sox9	F: 5' TCT ACA CAC AGC TCA CTC GAC CTT	83
	R: 5' TTC TTC GGT TAT TTT TAG GAT CAT CTC	
Aggrecan	F: 5' GCG AGT TGT CAT GGT CTG AA	122
	R: 5' TTC TTG GAG AAG GGA GTC CA	
Collagen II	RT2 qPCR Primer Assay, SABiosciences Corp.	
Collagen X	F: 5' CAG ATT TGA GCT ATC AGA CCA ACA A	85
	R: 5' AAA TTC AAG AGA GGC TTC ACA TAC G	
HIF-1alpha	F: 5' TTT ACC ATG CCC CAG ATT CAG	82
	R: 5' GAC TAT TAG GCT CAG GTG AAC TTT GTC	
Collagen I	F: 5' AAC CAA GGA TGC ACT ATG GA	162
	R: 5' GCT GCC AGC ATT GAT AGT TT	

4.3 Results

Cell Viability

Cell viability ranged between 90-97% within the bioreactors, with no significant difference due to length of culture time.

Proteoglycan Quantification and Histology

When cells were pre-treated with TGF-β3, total GAG amounts were higher than those found for undifferentiated cells cultured in the bioreactor. Two or three weeks of pre-treatment significantly enhanced total GAG content.

Table 4.2 Total GAG contents of undifferentiated MSCs and MSCS pre-treated with TGF-β3 after 2 weeks bioreactor culture.

TGF-beta	Average total GAG content (ug)
Undifferentiated	118 ± 66 (n=6)
1 week	190 ± 68 (n=6)
2 weeks	238 ± 57 (n=5)
3 weeks	218 ± 81 (n=5)

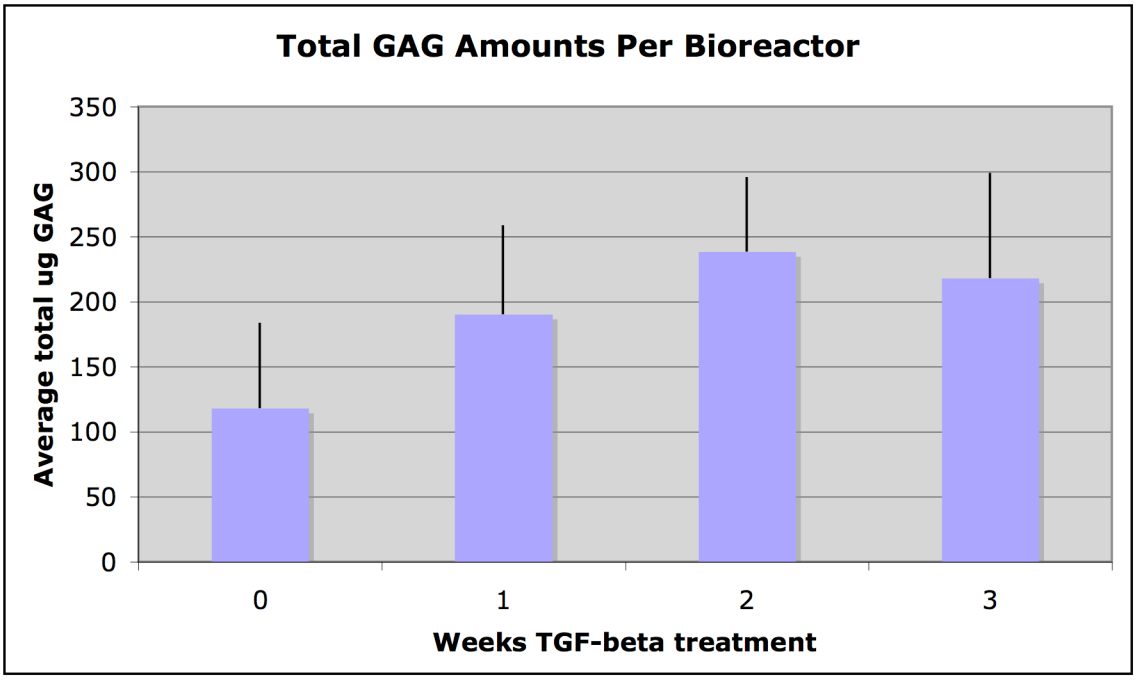

Figure 4.1 Total GAG amounts in bioreactors with TGF-β3 pre-treatment are higher than in bioreactors with undifferentiated cells. ($p<0.01$, 2 weeks pre-treatment, $p<0.05$, 3 weeks pre-treatment).

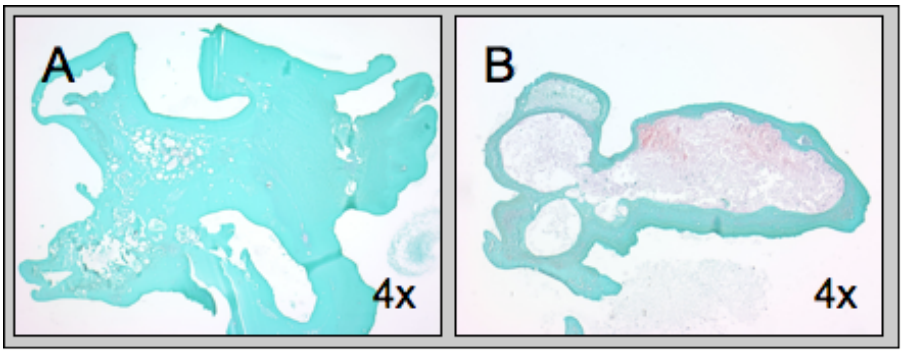

Figure 4.2 Safranin-O/fast green staining of fibrin-cell pellets. Proteoglycan staining is absent when cells are pre-treated with TGF-β3 for one week (A). Proteoglycan staining is observed in the center of the pellet when cells are pre-treated for two weeks with TGF-β3 (B).

Effect of TGF-β3 Pre-treatment on Gene Expression (Figures 4.3 – 4.8)

Gene expression levels in the following section are all compared to undifferentiated MSC values after 2 weeks culture in bioreactors or control beads.

In the bioreactor, TGF-β3 pre-treatment results in increased aggrecan expression (12.5-fold increase with 2 weeks pre-treatment, 5-fold increase with 3 weeks pre-treatment). Varying the length of pre-treatment time does not have a significant effect, but 2 weeks of pre-treatment results in the highest increase ($p<0.005$). In control beads, pre-treatment with TGF-β3 does not have as dramatic effects; 2 weeks of pre-treatment results in a 3.5-fold decrease in aggrecan expression ($p<0.02$) and 3 weeks of pre-treatment results in a 1.7-fold increase.

In both bioreactors and control beads, TGF-β3 pre-treatment upregulates collagen II expression. In bioreactors, 2 and 3 weeks pre-treatment result in 130-fold and 141-fold increase in expression ($p<0.02$, $p<0.001$, respectively) compared to undifferentiated MSC bioreactors. In control beads, 1 and 3 weeks pre-treatment significantly increases collagen II expression 4.3-fold and 19-fold ($p<0.001$ and $p<0.005$, respectively).

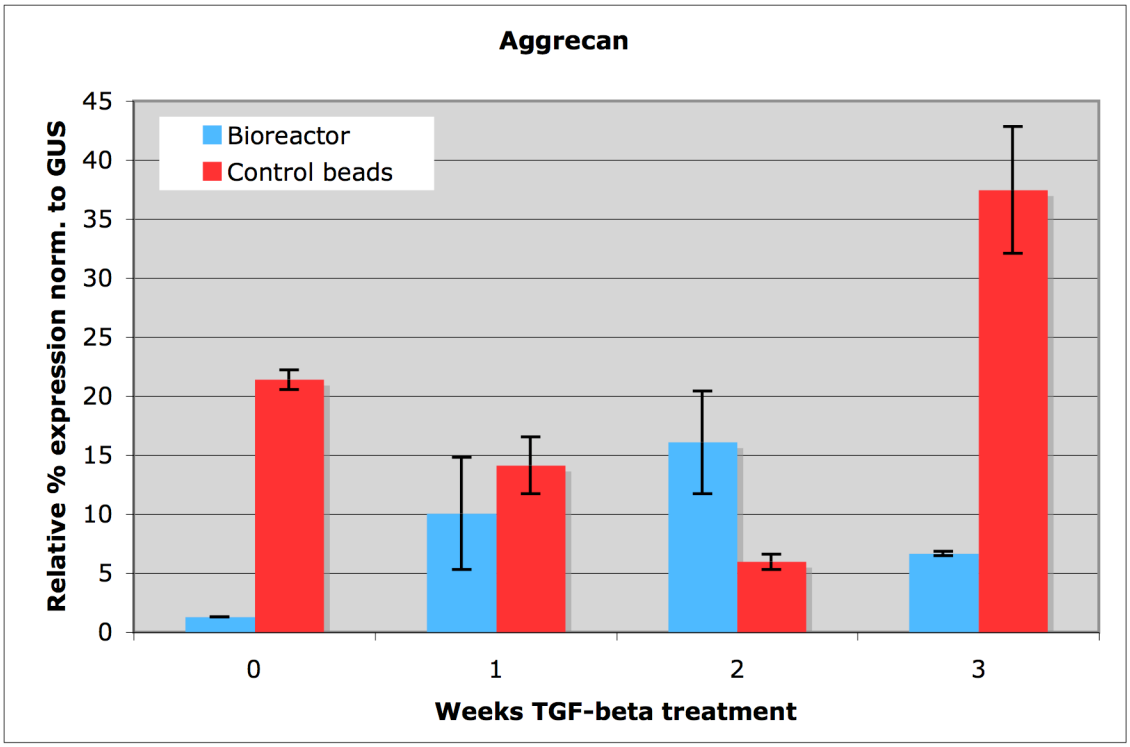

Figure 4.3 Effect of pre-treatment on aggrecan expression in bioreactors and control beads. In control bead culture, pre-treatment of one and two weeks results in decreased aggrecan expression. In bioreactors, pre-treatment of cells results in increased expression levels, with expression reaching the highest level after 2 weeks of pre-treament ($p<0.005$).

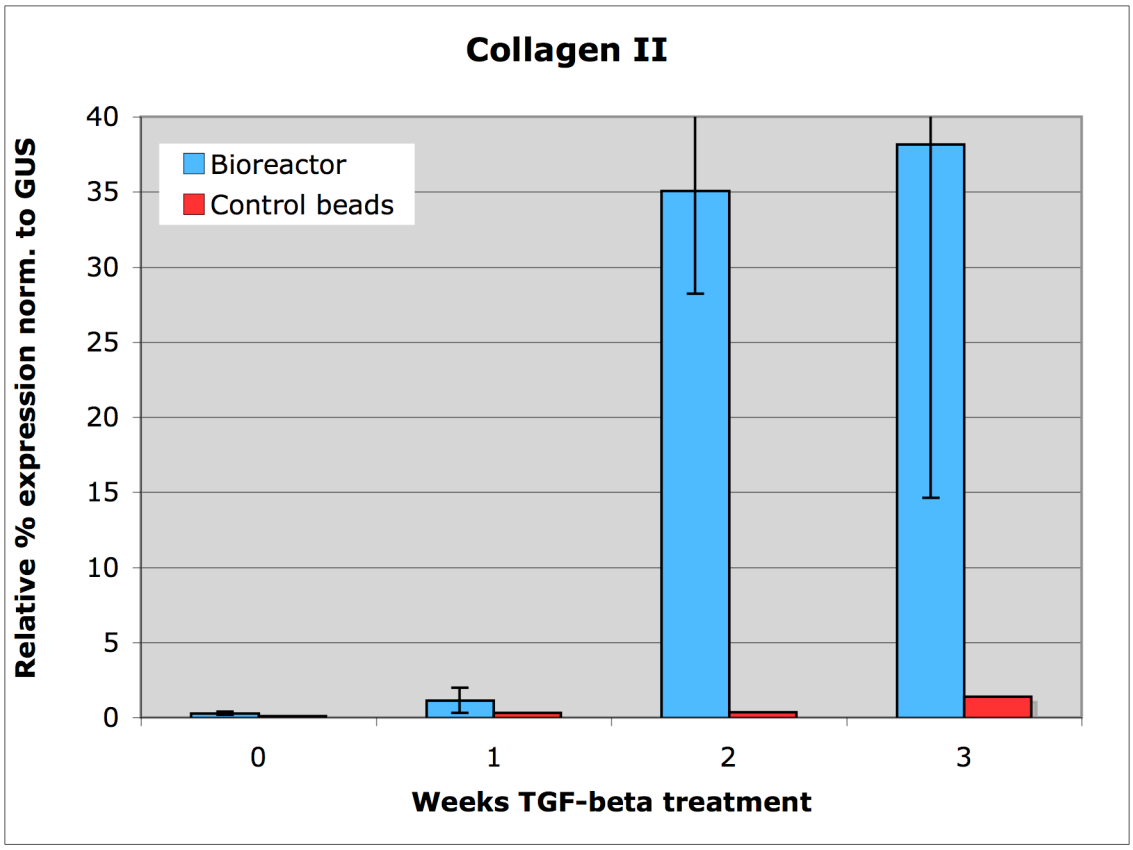

Figure 4.4 Effect of pre-treatment on collagen II expression in bioreactors and control beads. In the bioreactor, significant increases in collagen II expression occur with 2 and 3 weeks pre-treatment; compared to the equivalent control bead experiments, expression is 98-fold higher with 2 weeks pre-treatment and 28-fold higher with 3 weeks pre-treatment.

Pre-treatment of cells with TGF-β3 leads to a significant decrease in Sox9 expression at all lengths of pre-treatment time in control beads. In the bioreactor, 1 week of pre-treatment results in a 6.4-fold increase in sox9 expression ($p<0.01$).

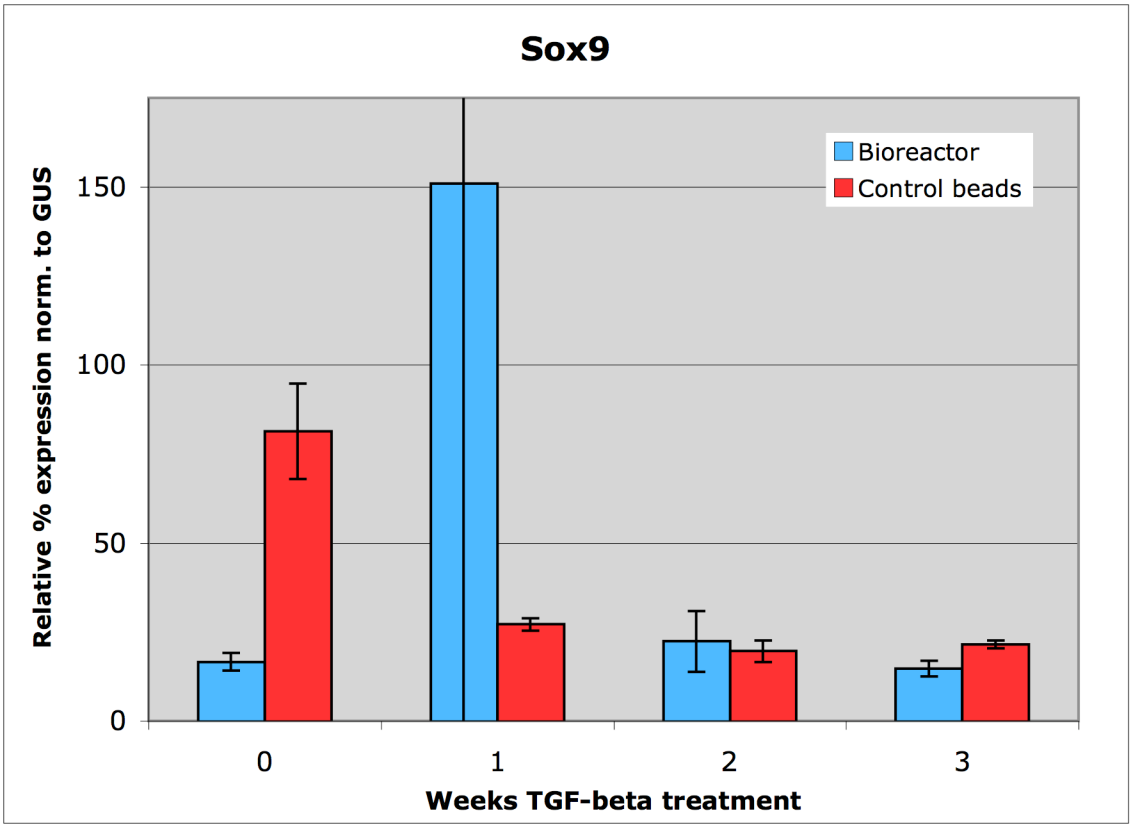

Figure 4.5 Effect of pre-treatment on Sox9 expression in bioreactors and control beads. In the bioreactor, one week of TGF-β3 pre-treatment results in significant increase in Sox9 expression. Pre-treatment with TGF-β3 (all time points) leads to significant decrease (3- to 4-fold, $p<0.02$) in expression in control beads.

Collagen X expression increases in both bioreactors and control beads with TGF-β3 pre-treatment. Three weeks of pre-treatment results in the largest increase compared to undifferentiated MSCs in both environments.

When MSCs are pre-treated with TGFβ3 prior to bioreactor culture, HIF-1α expression is downregulated, with a significant 3-fold decrease occurring after 1 week of pre-treatment ($p<0.05$). Pre-treatment of cells results in increased HIF-1α expression prior to control bead culture, with a significant 2-fold increasing occurring with 1 and 3 weeks pre-treatment ($p<0.02$).

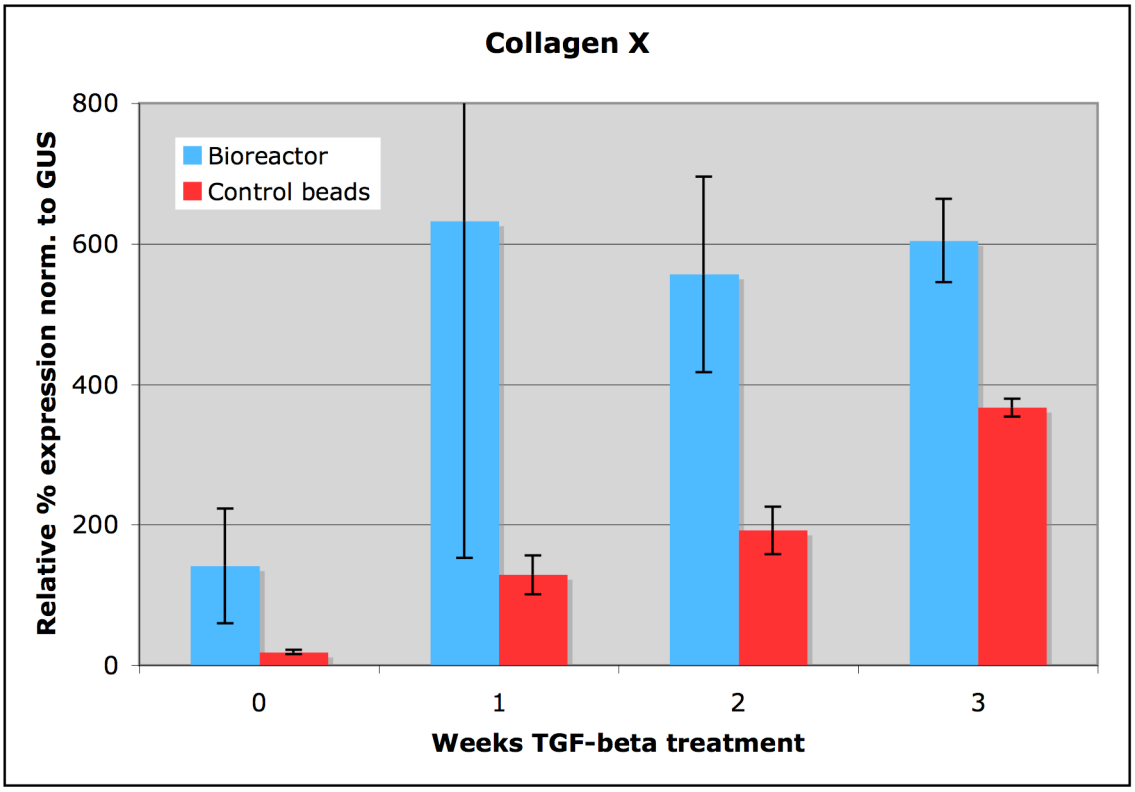

Figure 4.6 Effect of pre-treatment on collagen X expression in bioreactors and control beads. In the bioreactor, TGF-β3 pre-treatment for 3 weeks results in a 43-fold increase in collagen X expression ($p<0.001$). In control beads, 3 week pre-treatment results in a 19.6-fold increase ($p<0.05$).

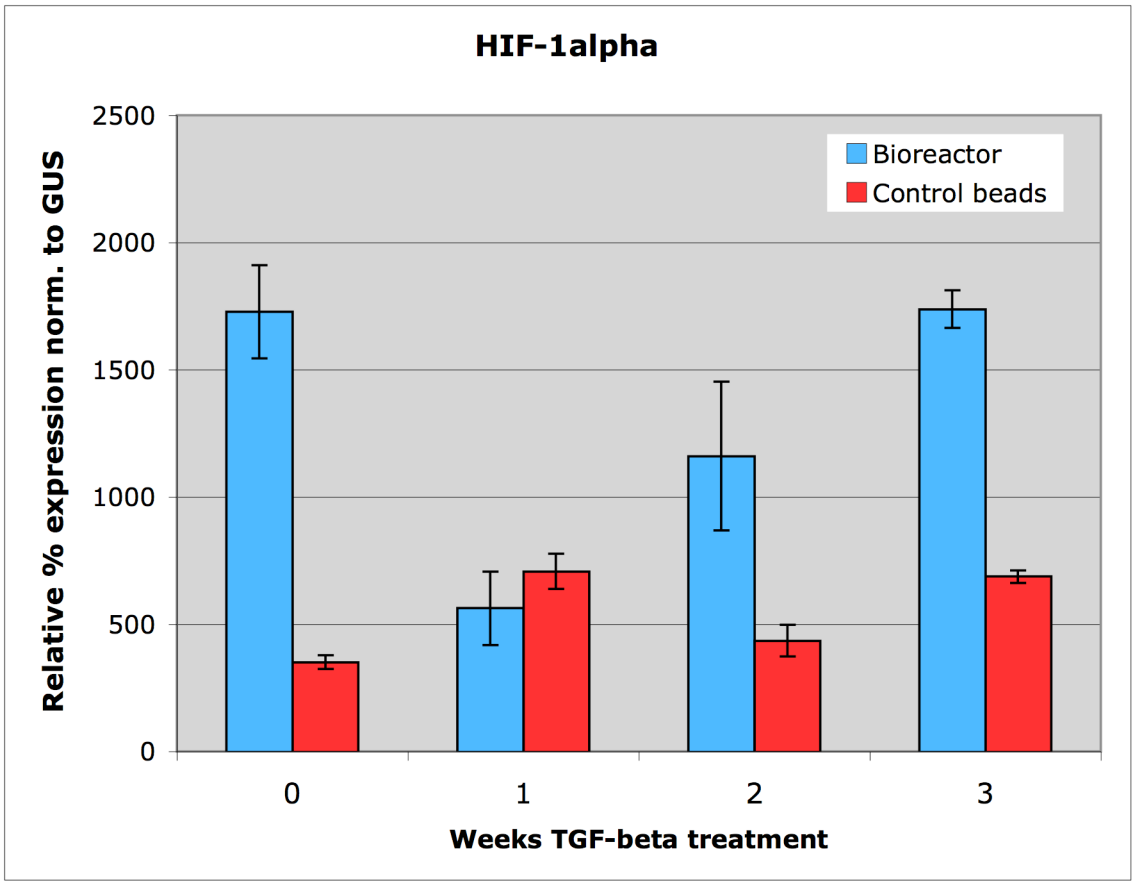

Figure 4.7 Effect of pre-treatment on HIF-1α expression in bioreactors and control beads. In the bioreactor, pre-treatment of cells with TGF-β3 leads to an overall decrease in HIF-1α expression, while expression is increased as a result of pre-treatment in control beads.

TGF-β3 pre-treatment results in significant increases in collagen I expression in the bioreactor environment (over 500-fold increase each time point, $p<0.05$). In control beads, pre-treatment does not have a significant affect except with 3 weeks pre-treatment, when expression is 1.5-fold increased ($p<0.04$).

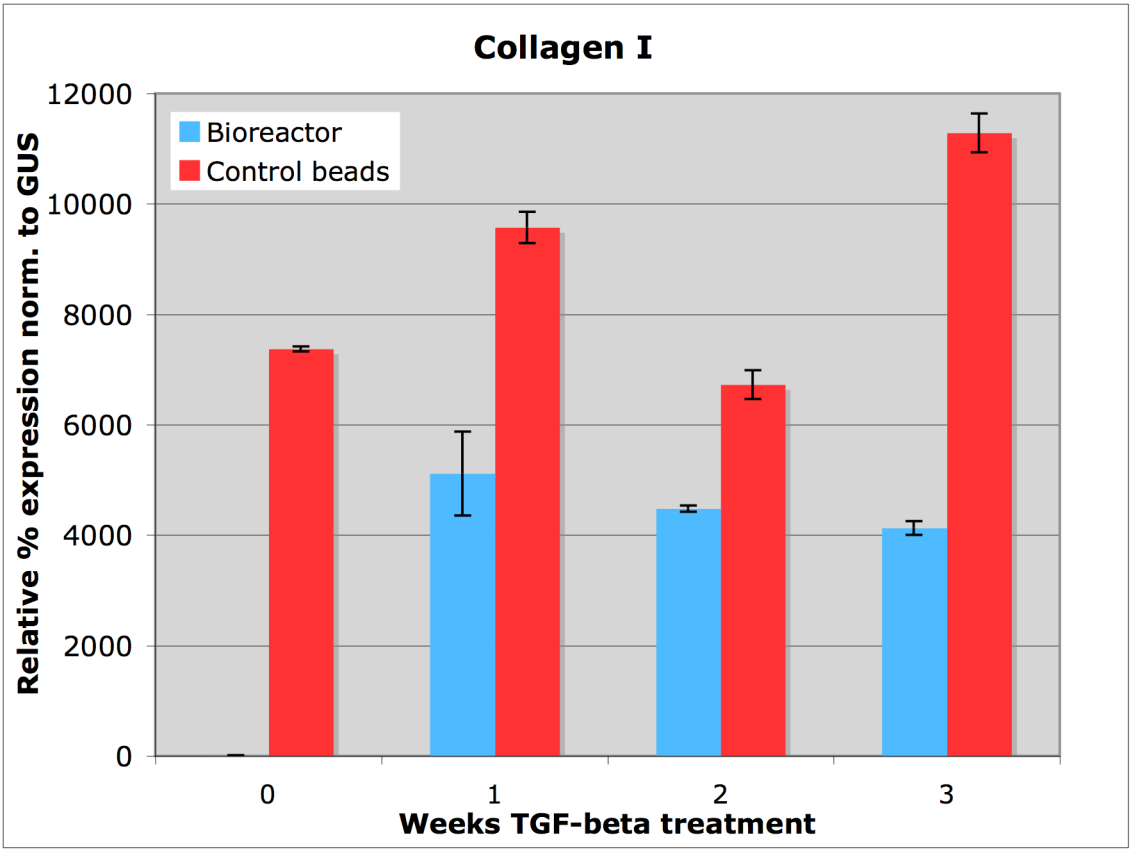

Figure 4.8 Effect of pre-treatment on collagen I expression in bioreactors and control beads. Pre-treatment with TGF-β3 does not have significant effect on collagen I expression in control beads. In bioreactors, expression is over 500-fold increased with pre-treatment compared to undifferentiated cells.

Persistence of TGF-β3-induced Gene Expression (Figs. 4.9 – 4.12)

Gene expression levels in the following section are comparisons made between expression levels in cells treated with TGF-β3 for 1, 2, or 3 weeks, and expression levels in cells that are pre-treated with TGF-β3 and then cultured for 2 weeks in either the bioreactor or in control beads.

Expression levels of collagen II indicate that the bioreactor environment amplifies upregulation induced by TGF-β3 (Figure 4.9). Although collagen II expression persists in control bead culture, it is not significantly changed. The largest bioreactor-induced

increase in collagen expression occurs with 2 weeks TGF-β3 pre-treatment (117-fold increase, $p<0.02$).

Generally, any increase in Sox9 expression induced by TGF-β3 is lost when cells are cultured in control beads or bioreactors (Figure 4.10). The exception is when cells are pre-treated with TGF-β3 for 1 week - bioreactor culture significantly increases Sox9 expression 1.4-fold ($p<0.01$). After one week of TGF-β3 treatment, two weeks of bioreactor culture significantly increases Sox9 expression 1.4-fold ($p<0.01$). In contrast, two weeks of traditional cell culture significantly decreases Sox9 expression 2.7-fold ($p<0.01$).

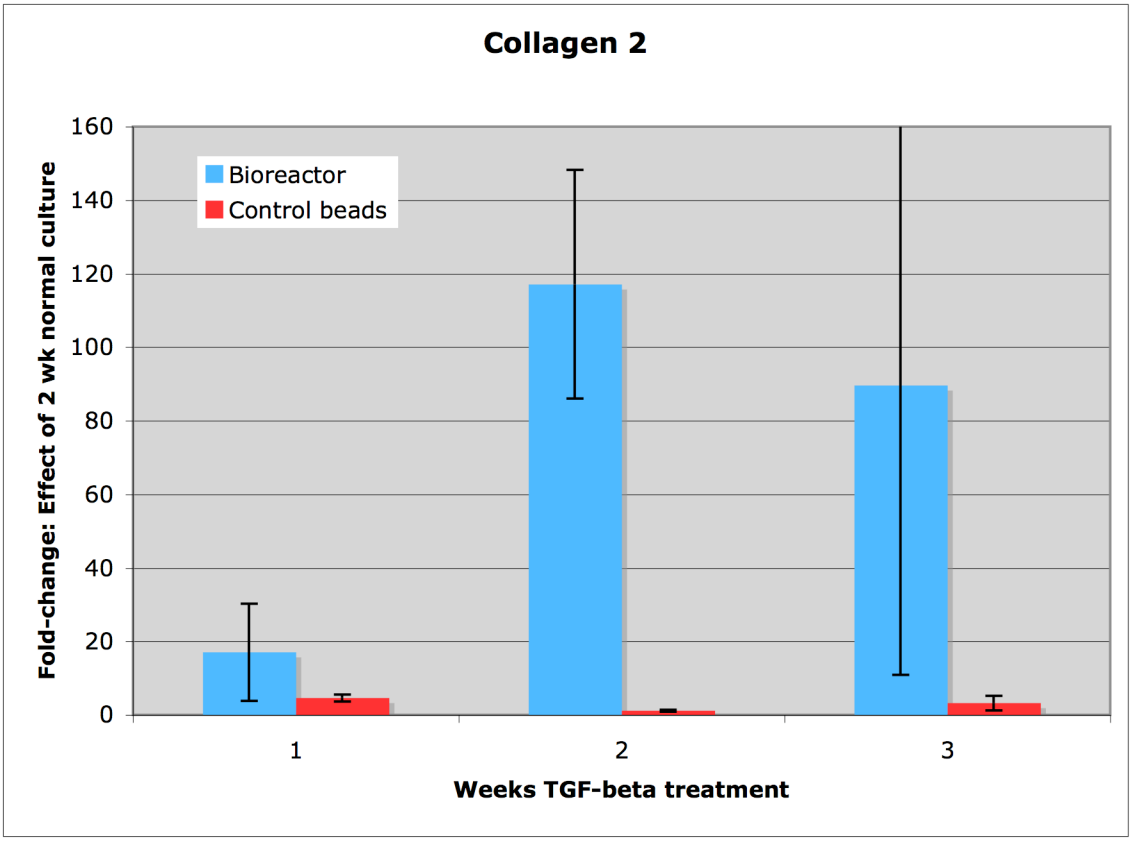

Figure 4.9 Persistence of collagen II expression after bioreactor or control bead culture. Two weeks of bioreactor culture significantly amplifies collagen II expression when cells have been pre-treated for 2 weeks ($p<0.02$). TGF-β3-induced gene expression does not significantly change after control bead culture.

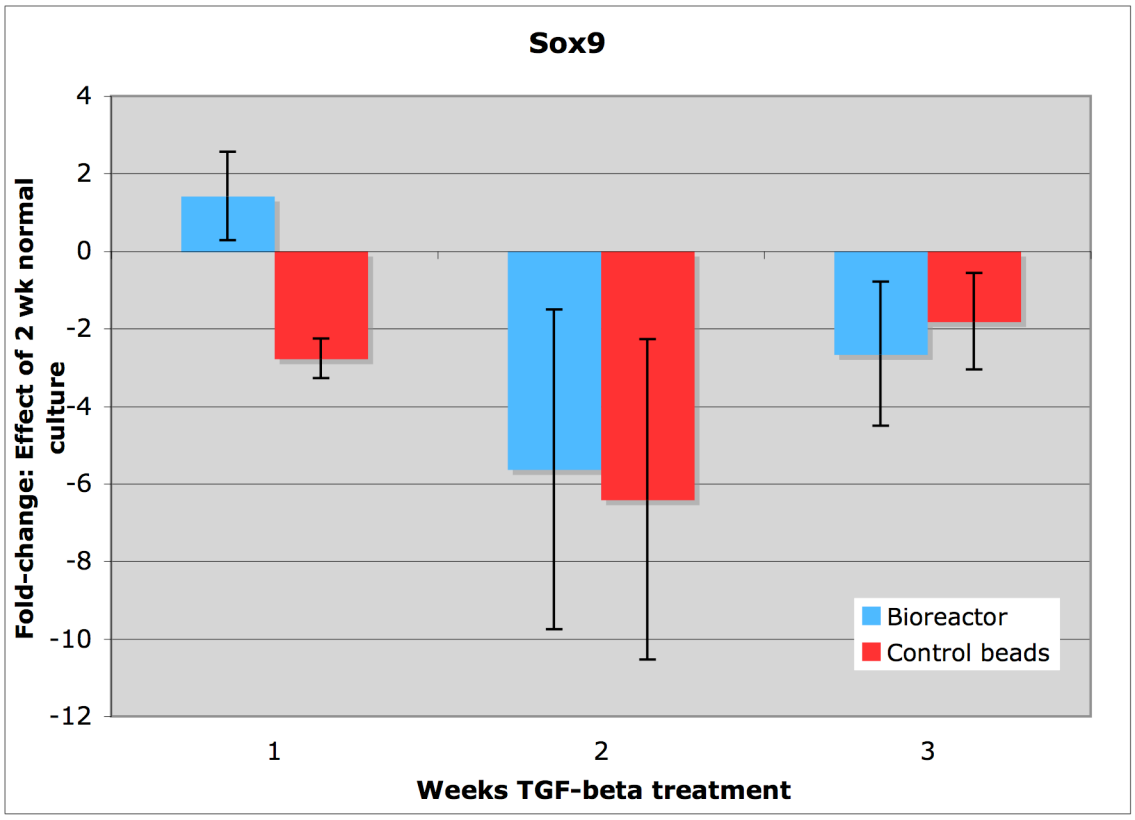

Figure 4.10 Persistence of Sox9 expression after bioreactor or control bead culture. After cells are pre-treated with TGF-β3 for one week, sox9 expression is increased by bioreactor culture ($p<0.01$) but decreased by control bead culture ($p<0.001$).

TGF-β3 significantly stimulates collagen X expression in cells, and this effect is reversed once cells are cultured in bioreactors or control beads (Figure 4.11).

Bioreactor culture significantly increases HIF-1α expression only when cells have been pre-treated for 3 weeks ($p<0.001$, Figure 4.12). Control bead culture does not significantly change HIF-α expression.

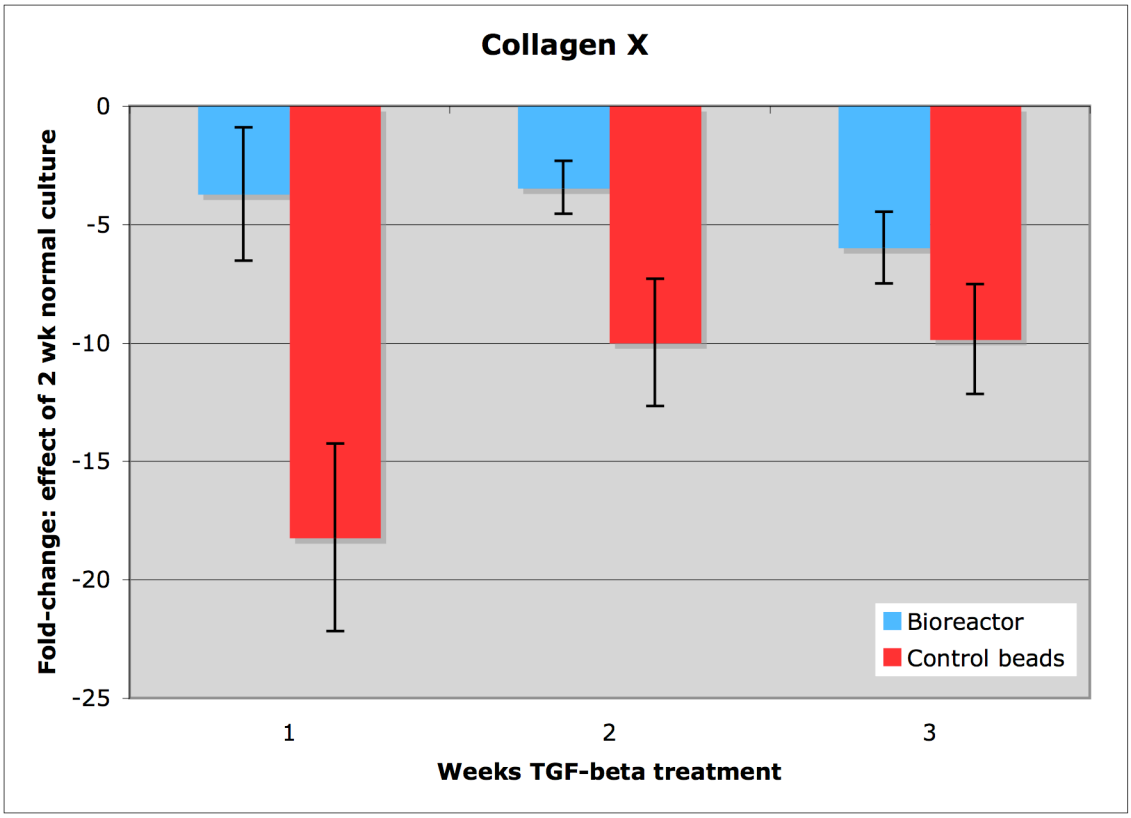

Figure 4.11 Persistence of collagen X expression after bioreactor or control bead culture. Control bead culture has a larger effect o decreasing collagen X expression than bioreactor culture.

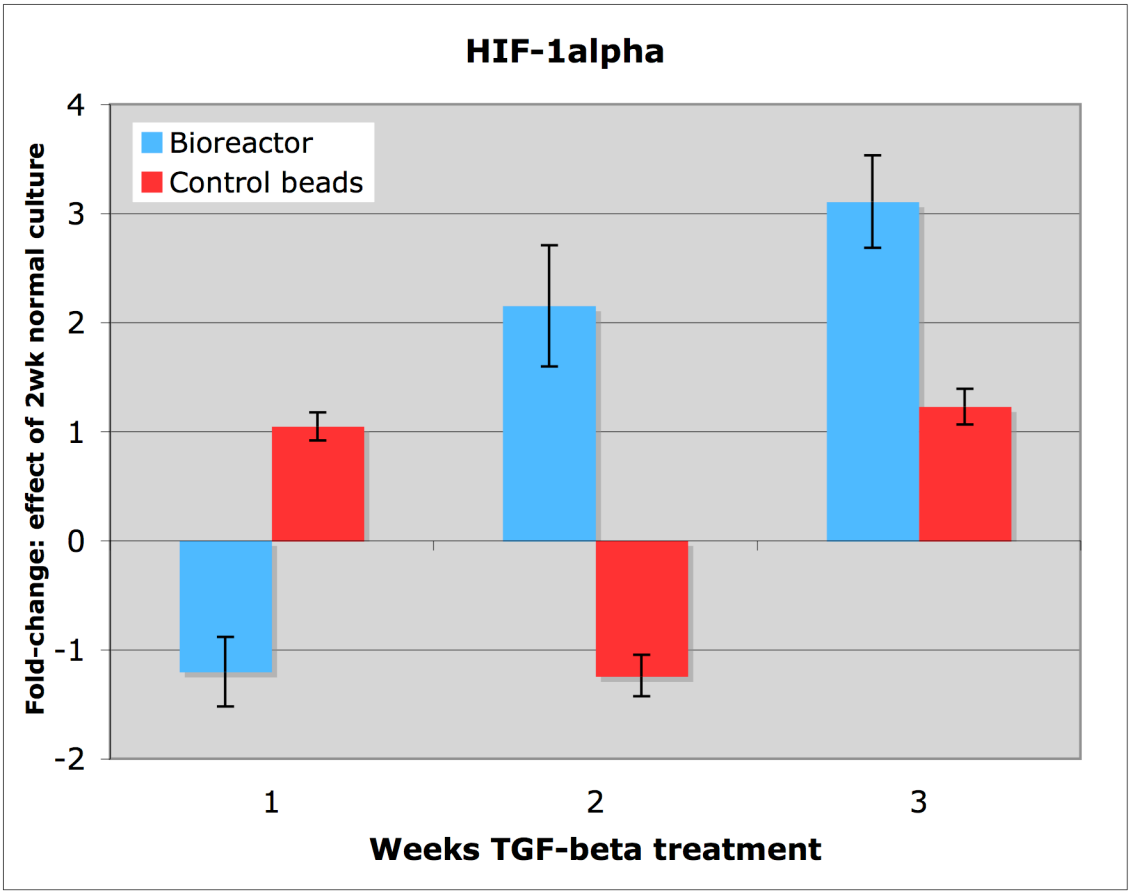

Figure 4.12 Persistence of HIF-1α expression after bioreactor or control bead culture. Bioreactor culture significantly increases HIF-1α expression when cells are pre-treated for 3 weeks.

4.4 Discussion

These results demonstrate that pre-treatment of MSCs with TGF-β3 may enhance cells' survival and function in a disc-mimetic environment. We previously established that disc-mimetic conditions alone are sufficient to induce expression of chondrogenic markers in MSCs, although this is accomplished at a slower rate than differentiation by chondrogenic growth factors. Gene expression profiles of aggrecan, collagen II, and Sox9 demonstrate that pre-treatment with TGF-β3 accelerates the process of bioreactor-mediated differentiation. When cells are pre-treated for 1 week with TGF-β3, expression

levels of aggrecan are twice as high as levels found in undifferentiated MSCs cultured in the bioreactor for 3 weeks, and Sox9 levels are 5 times higher. Two weeks of TGF-β3 treatment prior to bioreactor culture results in a 5-fold increase in collagen II expression compared to the highest levels found in bioreactor-cultured undifferentiated MSCs (data from Chapter 3).

Cell viability and GAG content data also suggest that pre-treating cells with TGF-β3 can improve their survival and function in disc-mimetic conditions. Pre-differentiated cells were 90-97% viable after bioreactor culture, while undifferentiated MSCs were 80-85% viable (Chapter 3). Total GAG amounts in bioreactors were doubled when cells were pre-treated for 2 weeks with TGF-β3, and undifferentiated MSCs would need to be cultured for 4 weeks in the bioreactor before reaching the GAG levels produced by these pre-treated MSCs. This observation is consistent with previous studies showing that differentiated MSCs and mature cell types such as chondrocytes have a more robust anabolic response to pressure than undifferentiated MSCs [151, 172].

The effect of TGF-β3 pre-treatment on aggrecan and Sox9 expression levels appears to be dependent on the disc-mimetic conditions of the bioreactor; bioreactor culture increases TGF-β3-induced aggrecan expression, but control bead culture decreases this expression. A similar result is seen for Sox9 expression. This could possibly be explained by the fact that the hypoxic environment within the bioreactor induced HIF-1α expression, and HIF-1α regulates Sox9 expression [159]. This result also highlights the significant effect that pre-differentiation of cells can have on cell behavior in the disc. Our previous bioreactor experiments indicated that neither bioreactor culture nor control bead culture have a significant effect on Sox9 expression,

yet two weeks of bioreactor culture significantly increases Sox9 expression when cells have been pre-treated with TGF-β3 for one week. The combined conditions of pressure and hypoxia also enhance collagen II expression; persistence of TGF-β3-induced collagen II expression occurs after both bioreactor and control bead culture, but expression is increased 141-fold after bioreactor culture compared to 19-fold after control bead culture. These results are consistent with previous observations in the literature concerning cell maturity and response to load – Scherer et al. found that a combination of low oxygen tension and pressure enhanced aggrecan and collagen production in chondrocytes, but did not have the same effect on bone marrow-derived stem cells [143].

It is also interesting to note that other genes that did not appear to be regulated by TGF-β3 (Chapter 3) were affected by pre-treatment prior to bioreactor or control bead culture. For example, we reported that HIF-1α espression by MSCs was not significantly affected by TGF-β3 stimulation, but was upregulated significantly after 2 weeks of bioreactor culture. However, HIF-1α expression was only significantly increased by 2 weeks of bioreactor culture when cells were pre-treated with TGF-β3 for 3 weeks. Collagen I expression was also reported to be unaffected significantly by TGF-β3 stimulation, but reduced significantly by control bead culture or bioreactor culture. When cultured in the bioreactor, pre-treatment of MSCs resulted in over 500-fold increase in collagen I expression compared to undifferentiated MSCs. However, due to culture in a disc-mimetic environment, the levels of collagen I expression were still far below that of baseline MSCs.

These data support the idea that differentiating MSCs prior to disc implantation can help counteract the challenges that would otherwise prevent cells from functioning

effectively within the disc environment. More importantly, the environment-dependent differences in gene expression highlight the necessity of mimicking several aspects of the disc environment in concert, especially when attempting to evaluate the fate of the cells post-implantation. The persistence of gene expression induced by TGF-β3 after bioreactor culture demonstrates that our bioreactor culture system mimics a healthier disc state rather than a chronically degenerated environment. Ultimately, cell therapy will target degenerated discs for repair, and degenerated discs have elevated levels of inflammatory cytokines. Therefore, future studies should incorporate inflammation into the bioreactor system to further our understanding of cell behavior and fate in the degenerated disc environment.

Chapter 5: Inflammation and the Disc-Mimetic Environment

5.1 Introduction

Current treatments of low back pain associated with intervertebral disc degeneration involve conservative management (physical therapy or medication) or surgical intervention, such as spinal fusion, discectomy, or total disc replacement [173]. However, these procedures not only reduce the mobility of the joint, increasing stress on adjacent discs [174], but only result in symptomatic relief by removing the disc tissue. The exact pathology of disc degeneration is unknown, but it can be characterized by a combination of changes in the matrix composition, altered biomechanics, and reduced cell number and activity [5, 22, 133]. As a result, researchers are investigating biologic treatment options to inhibit further degeneration that involve introducing therapeutic agents such as cells, scaffolds, and/or growth factors into the nucleus to restore disc functionality.

When developing cell-based therapies *in vitro*, it is important to represent the salient features of the anticipated *in vivo* environment. The intervertebral disc is recognized as a tissue with high pressure and low oxygen. Consequently, numerous authors have reported the role of mechanical and hypoxic stress on chondrogenesis and on proliferative/regenerative qualities of chondrocytes, MSCs, or disc cells [168-170]. However, it is becoming increasingly clear that degenerated discs have elevated levels of inflammatory cytokines, including TNF-α and interleukins [40, 44-46]. It is also well known that disc cells exposed to pro-inflammatory cytokines exhibit decreased proteoglycan and collagen production, and consequently, disc cytokines may inhibit matrix production and promote degeneration [175-177]. IL-1 exposure can result in

increased expression of matrix-degrading enzymes [43], and with TNF-α, can stimulate nerve growth factor production in human IVD cells [178], which can sensitize nociceptors and stimulate further cytokine production.

Ultimately, the use of autologous disc cells would not be feasible for cell transplantation therapies, due to the low number of cells in the disc and difficulties in expanding an appropriate number of cells for treatment. Therefore, we have investigated the use of mesenchymal stem cells, which are easily expanded and can be differentiated into chondrocyte-like cells, for cell-based disc therapy. Although there have been many *in vitro* studies confirming the suitability of MSCs for intervertebral disc repair, few have addressed the fate of these cells in an environment that mimics several of the harsh disc conditions in concert.

We have previously described a bioreactor that mimics the disc's low oxygen tension and high hydrostatic pressure, and have demonstrated that these features can have a significant effect on cell behavior. In particular, this system suggests that a disc-mimetic environment can induce MSC differentiation and result in increased proteoglycan synthesis. As both IL-1β and TNF-α are over-expressed in the degenerate IVD and implicated in matrix degradation, we have incorporated these cytokines into the bioreactor so as to more accurately represent the clinical site. Using this updated system, we report here how MSCs respond to the combined effects of low oxygen tension, high hydrostatic pressure, and presence of inflammatory cytokines, and whether MSC pre-differentiation toward a chondrocyte phenotype would improve its ability to function under these harsh conditions.

5.2 Materials and Methods

Materials

Human bone marrow-derived MSCs, mesenchymal stem cell growth media (MSCGM), chondrogenic media (CM), and rhTGF-β3 were purchased from Lonza Walkersville Inc. Slide-A-Lyzer dialysis cassettes (gamma-irradiated, 10,000 MWCO) were purchased from Pierce Biotechnology Inc. Fibrin glue (Tisseel VH) was purchased from Baxter Biosciences. Sodium hyaluronate powder was purchased from Genzyme. Human recombinant IL-1β and TNF-α were purchased from PeproTech Inc. Buffer RLT, Qiashredder columns, and RNeasy kits were purchased from Qiagen. Trizol reagent and PureLink RNA Mini kits were purchased from Invitrogen. Human Col2A1 primer was purchased from SABiosciences. All other primers were supplied by the UCSF Genome Analysis Core or manufactured by Integrated DNA Technologies.

Alginate Bead Culture

Mesenchymal stem cells from different donors were expanded up to passage seven in MSCGM. MSCs were suspended in a 1.2% alginate solution at a concentration of $4x10^6$ cells/mL. The alginate cell solution was dispensed dropwise from a syringe fitted with a 22-gauge needle into a 102mM $CaCl_2$ bath. Beads were allowed to cure at room temperature for 15 minutes, rinsed twice with PBS and then transferred to low-attachment 6-well culture plates. Beads were then cultured in chondrogenic media with TGF-β3 (10 ng/mL) for one, two, or three weeks.

At the end of the pre-differentiation culture period, beads from each time point

were split into two groups. For one group, beads were rinsed twice with PBS and then half were cultured in MSCGM ("control beads") and the other half cultured in MSCGM supplemented with 10 ng/mL each of human recombinant IL-1β and TNF-α ("inflammation beads"). These beads were cultured in low-attachment 6-well culture plates for two weeks. These bead experiments serve as a control to investigate the effects of bioreactor culture on the cells. The second group of beads were digested by a method previously described [171] to release cells and preserve cell-associated matrix. These cells were used for bioreactor culture (described below).

Bioreactor Construction

A 15% hyaluronan gel was made by dissolving sodium hyaluronate powder in MSCGM. For half of the bioreactors, the MSCGM was supplemented with IL-1β and TNF-α to a final concentration of 10ng/mL once the bioreactor's water content reached equilibrium based on osmotic pressure differences between the hyaluronan and culture media ("inflammation bioreactors") and the remaining bioreactors received gel without cytokine supplementation ("control bioreactors"). Three hundred microliters of gel were injected through the self-sealing silicone port of a dialysis cassette and excess air was removed from the cassette. The cassette was then incubated in MSCGM for four hours to allow for gel volume expansion and osmotic pressurization (approximately 0.12 MPa).

Cells (either undifferentiated MSCs or cells released from alginate bead culture) were suspended in fibrin glue at a final concentration of 4×10^6 cells/mL and a 100 μL pellet of fibrin and cells was injected into the center of the expanded cassette. An

autoclavable porous metal clip surrounds the device to permit fluid exchange but prevent membrane rupture due to internal pressurization. Cassettes were then incubated in MSCGM at 37 degrees with 5% CO_2 for two weeks.

Cell Viability

At the end of the specified time point, two bioreactors were cut open and the fibrin-cell pellet was removed. The pellet was stained with Live-Dead Assay to obtain cell viability information. Five images in different sections of each pellet were captured and the percentage of live cells calculated and averaged from each section.

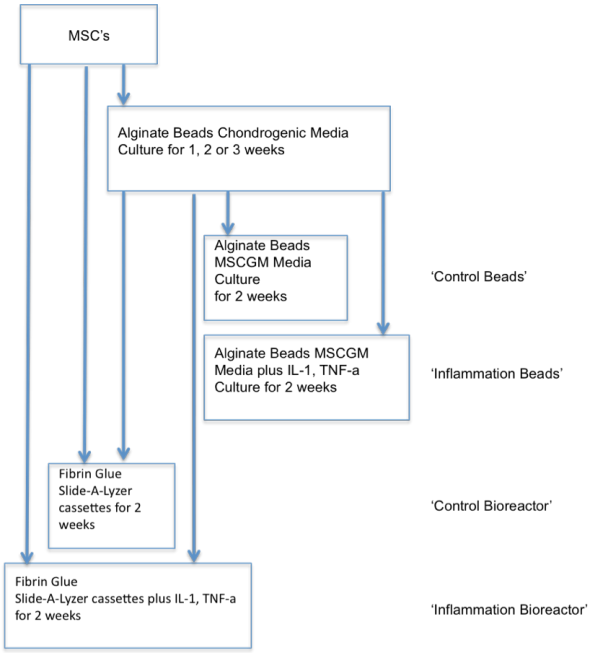

Figure 5.1. Study Design.

DMMB Assay for Proteoglycan Quantification

After the two-week culture period, bioreactors were removed from media, and the fibrin-cell pellet was separated from the surrounding hyaluronan gel. The fibrin pellet was weighed and digested for 48 hours at 65 degrees in a papain solution (15 U/g of tissue, 100 mg/mL solution). The hyaluronan gel was digested in 5 mL of 100 U/mL hyaluronidase solution for three hours at 37 degrees. Both the digested pellet and hyaluronan solutions were centrifuged for five minutes at 500*g* and the supernatant

reserved for DMMB assay.

Standards were prepared with chondroitin sulfate A in a range of concentrations from 0 to 100 μg/mL. Pellet and hyaluronan gel samples were diluted 10-fold, and 40 μL of each sample was added to 250 μL of DMMB solution (21mg DMMB, 5mL absolute EtOH, 2g sodium formate in total volume 800mL ddH2O with pH 3.5) in a 96-well plate. Standards and samples were run in triplicate, and OD measured at 525 nm.

Real-time PCR Analysis of Gene Expression

All qRT-PCR experiments were performed on at least three biological replicates. For the control and inflammation bead groups, beads were washed three times in PBS and digested in a 55 mM sodium citrate solution to release cells from alginate matrix. Cells were homogenized in buffer RLT with Qiashredder tubes and RNA extracted using the RNeasy kit according to manufacturer's protocol.

For the control and inflammation bioreactor groups, bioreactors were flash-frozen in liquid nitrogen and homogenized using Trizol reagent, and RNA was extracted using the PureLink Mini kit according to manufacturer's protocol.

RNA quantification, reverse transcription, and real-time PCR analyses were carried out at the UCSF Genome Analysis Core. All primers were optimized by the core facility. PCR reactions were carried out in triplicate, using BioRad SybrGreen Mastermix, with no-RT and water controls. All data was analyzed using the $2^{-\Delta\Delta CT}$ method using the housekeeping gene GUS. Statistical analyses were performed on the ΔCt values; one-way ANOVA and Student t-tests were used to detect differences

between groups with a significance level of $p<0.05$.

Table 5.1 Primer sequences for qRT-PCR

Gene	Primer sequence	Product size (bp)
Sox9	F: 5' TCT ACA CAC AGC TCA CTC GAC CTT	83
	R: 5' TTC TTC GGT TAT TTT TAG GAT CAT CTC	
Aggrecan	F: 5' GCG AGT TGT CAT GGT CTG AA	122
	R: 5' TTC TTG GAG AAG GGA GTC CA	
Collagen II	RT2 qPCR Primer Assay, SABiosciences Corp.	
Collagen X	F: 5' CAG ATT TGA GCT ATC AGA CCA ACA A	85
	R: 5' AAA TTC AAG AGA GGC TTC ACA TAC G	
HIF-1alpha	F: 5' TTT ACC ATG CCC CAG ATT CAG	82
	R: 5' GAC TAT TAG GCT CAG GTG AAC TTT GTC	
Collagen I	F: 5' AAC CAA GGA TGC ACT ATG GA	162
	R: 5' GCT GCC AGC ATT GAT AGT TT	
MMP9	F: 5' CCT GGA GAC CTG AGA ACC AAT C	79
	R: 5' CCA CCC GAG TGT AAC CAT AGC	
TSG-6	F: 5' TCA TGT CTG TGC TGC TGG ATG	67
	R: 5' GGG CCC TGG CTT CAC AA	

5.3 Results

Cell Viability

Inflammation did not affect cell viability; cells cultured in inflammation bioreactors maintained 83-92% viability, with no significant differences between groups.

Proteoglycan content

Pre-treatment of cells with TGF-β3 did not significantly affect the GAG amounts measured for each bioreactor (Table 5.2). GAG amounts in inflammation bioreactors were lower than amounts found in control bioreactors, with a significant difference when cells were pre-treated for 2 weeks ($p<0.03$, Figure 5.1).

Table 5.2 Total GAG amounts in inflammation bioreactors

TGF-beta	Average total GAG content (ug)
Undifferentiated	123 ± 51 (n=5)
1 week	148 ± 21 (n=7)
2 weeks	140 ± 58 (n=5)
3 weeks	123 ± 62 (n=5)

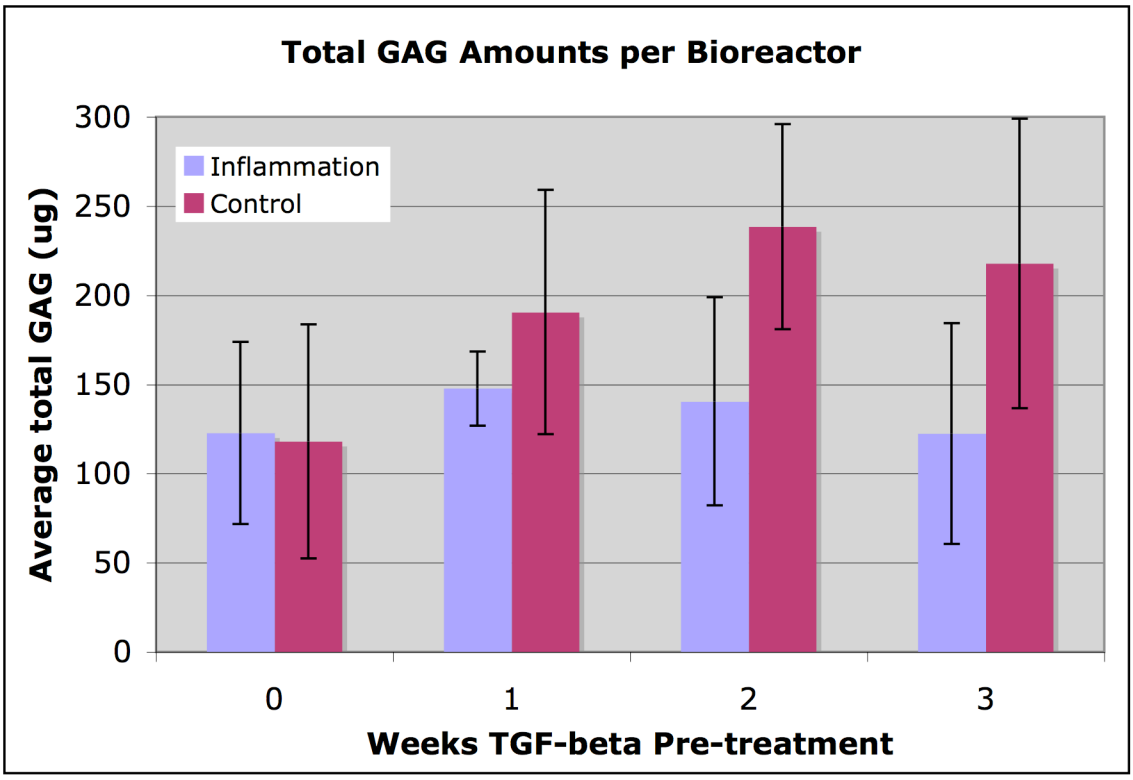

Figure 5.2 Total GAG amounts in inflammation and control bioreactors. Pre-treatment of cells with TGF-β3 increases GAG in control bioreactors but does not have a statistically significant effect in inflammation bioreactors.

Gene Expression – Effects of Inflammation and TGF-β3 Pre-treatment

To investigate the effect of inflammation, gene expression levels of inflammation bioreactors and beads were normalized to expression levels in control bioreactors and beads. To investigate the effect of TGF-β3 pre-treatment, pre-treated groups in all

bioreactors and beads were normalized to values for undifferentiated MSCs cultured in equivalent bioreactors and beads

Undifferentiated MSCs have 3.3-fold higher aggrecan expression in the inflammation bioreactor than in the control bioreactor. Inflammation results in a significant 13-fold decrease in aggrecan expression ($p<0.02$) when undifferentiated MSCs are cultured in beads. TGF-β3 pre-treatment results in significant upregulation of aggrecan in inflammation beads; in inflammation bioreactors, aggrecan expression is reduced, with a significant 4.3-fold reduction with 3 weeks pre-treatment ($p<0.03$).

When cells are cultured in bioreactors, inflammation reduces Sox9 expression, without significant differences between undifferentiated and pre-differentiated cells. In the bead environment, inflammation significantly reduces expression in all groups compared to control, with the most significant reduction (38-fold, $p<0.001$) occurring when the cells are undifferentiated. Pre-differentiation of cells increases expression of Sox9 compared to undifferentiated cells in both inflammation BRs and inflammation beads, an effect that is reversed in control beads. The highest increase in Sox9 expression occurs with one week of pre-differentiation – 5.8-fold in inflammation bioreactors ($p<0.02$) and 9-fold increase in control bioreactors ($p<0.01$).

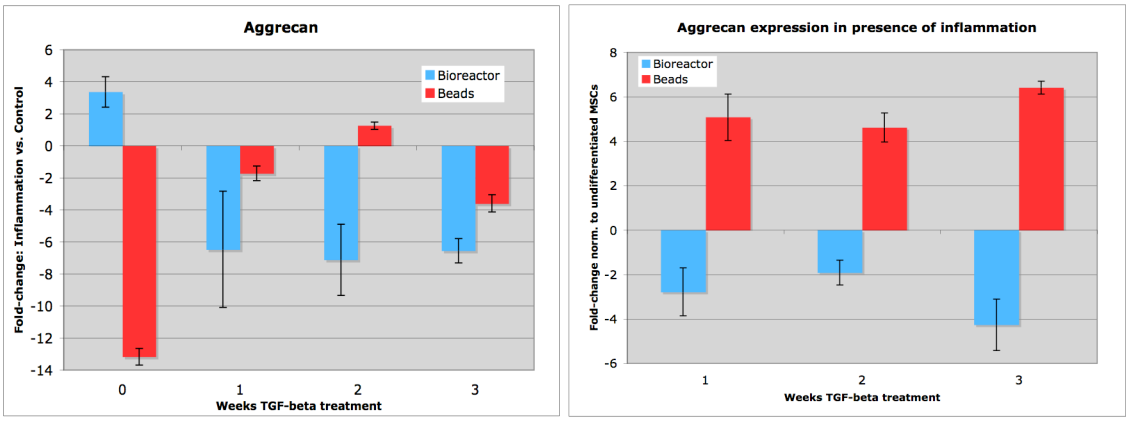

Figure 5.3 Effect of inflammation and pre-treatment on aggrecan gene expression as a function of culture type (bead versus bioreactor). In bead culture, pre-treatment increased aggrecan gene expression versus no-inflammation conditions. In bioreactor culture, pre-treatment reduced aggrecan gene expression versus no-inflammation conditions.

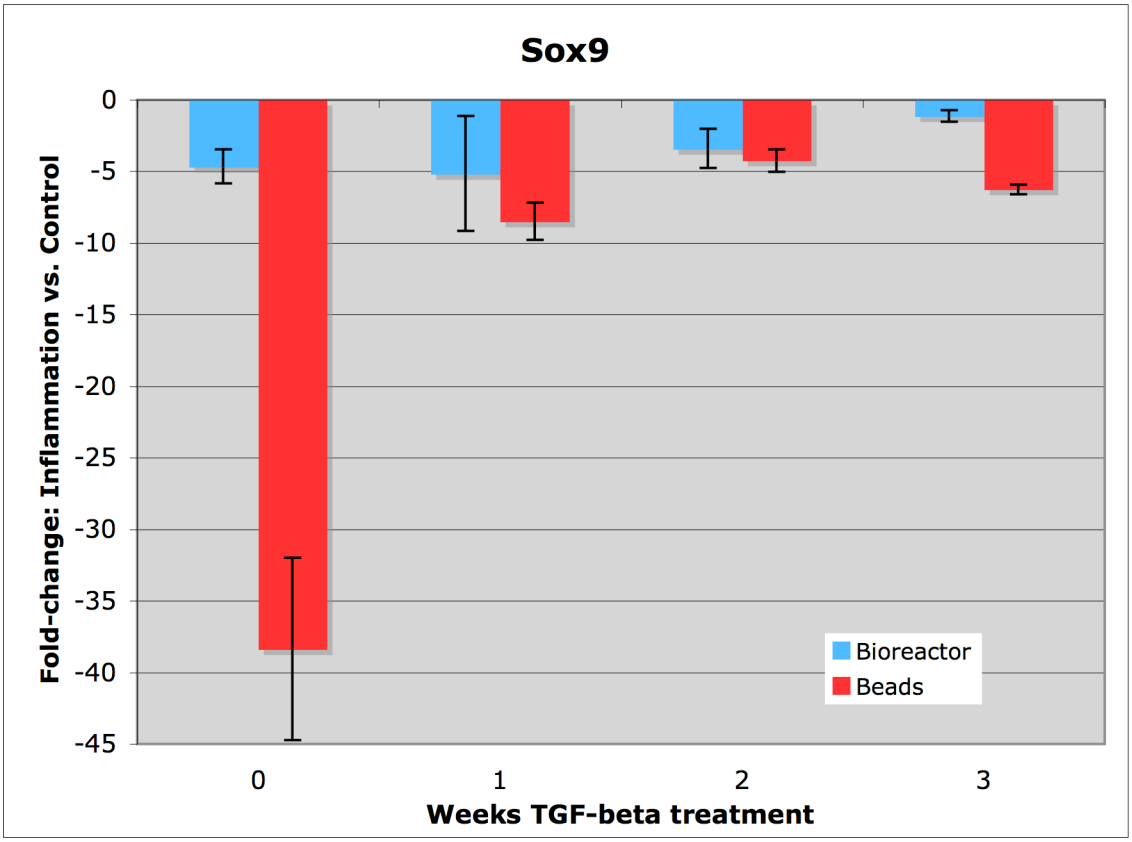

Figure 5.4 Effect of inflammation and pre-treatment on Sox9 gene expression as a function of culture type (bead versus bioreactor). In bead culture, pre-treatment had no effect on Sox9 gene expression versus no-inflammation conditions. In bioreactor culture, pre-treatment increased Sox9 gene expression versus no-inflammation conditions.

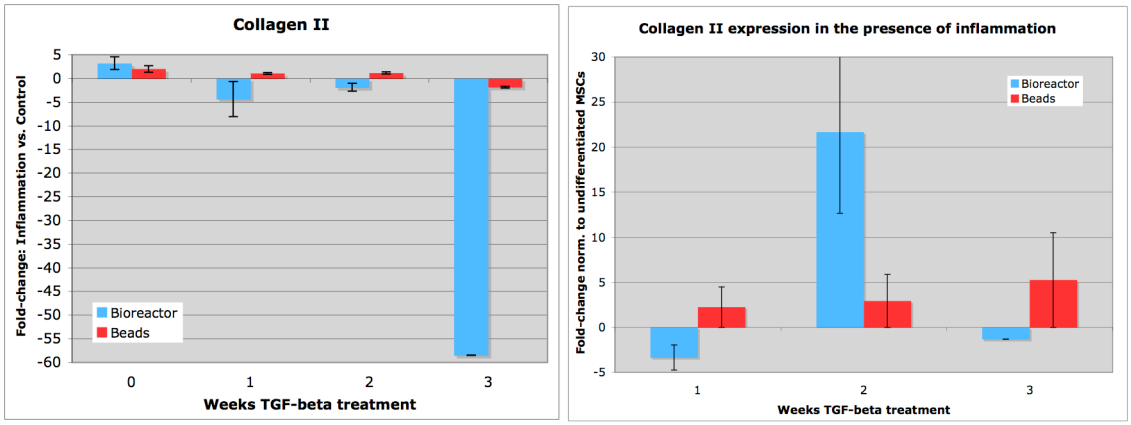

Figure 5.5 Effect of inflammation and pre-treatment on collagen II gene expression as a function of culture type (bead versus bioreactor). In inflammation bead culture, pre-treatment does not have a significant effect on expression. In bioreactor culture, pre-treatment for two weeks significantly increases collagen II expression in the presence of inflammation.

Similar to aggrecan, undifferentiated cells have a 3-fold higher expression of collagen II in the inflammation BR compared to the control BR. In inflammation bioreactors, collagen II expression is 21.6-fold increased when cells are pre-treated with TGF-β3 for 2 weeks ($p<0.01$). Pre-treatment does not have a significant effect on gene expression in inflammation beads.

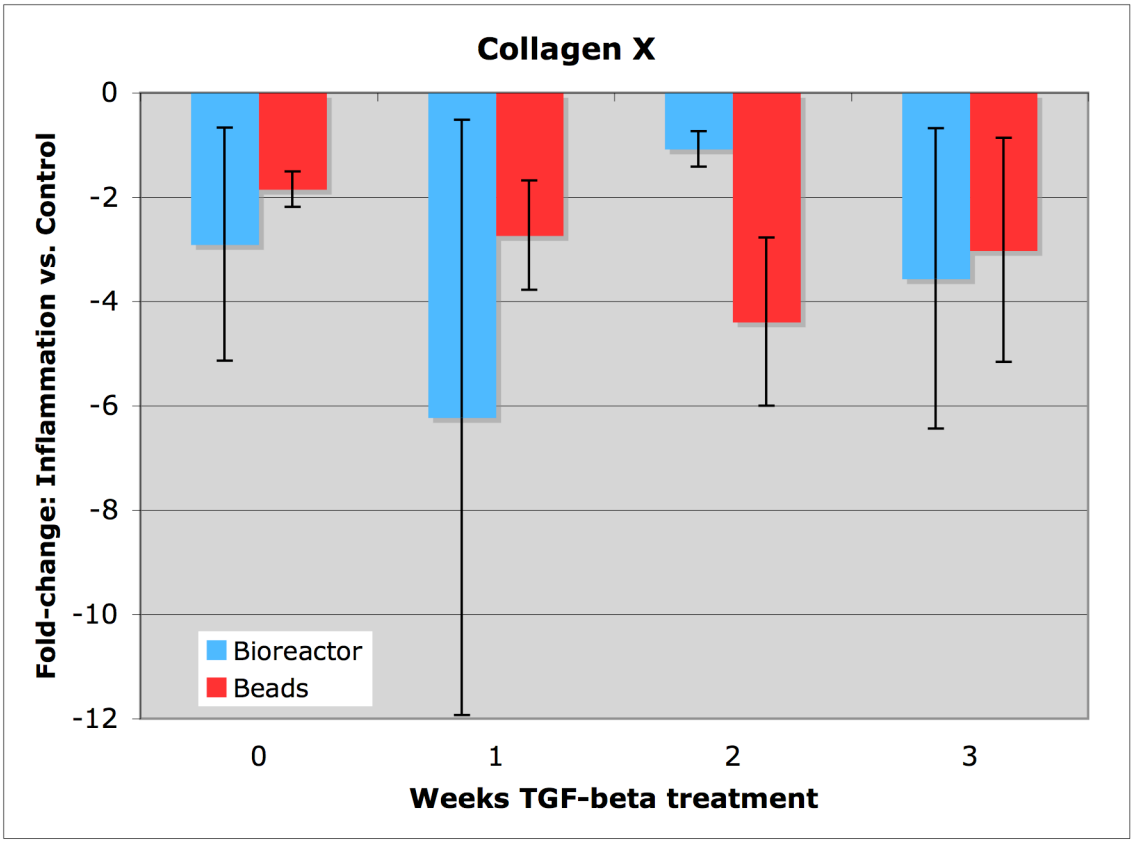

Figure 5.6 Effect of inflammation and pre-treatment on collagen X gene expression as a function of culture type (bead versus bioreactor). Inflammation decreases collagen X expression in both beads and bioreactors, and pre-treatment of TGF-β3 increases expression of collagen X in both beads and bioreactors when inflammation is present.

The presence of inflammation decreases collagen X expression in both bioreactors and beads compared to control. In the presence of inflammation, pre-differentiation of MSCs increases collagen 10 expression in both bioreactors and beads.

Inflammation results in an increase in HIF-1α expression compared to control in the bead environment. In bioreactors, inflammation results in decrease of HIF-1α expression when cells are undifferentiated, but the effect is not significant. When cells are pre-treated with TGF-β3 for 2 or 3 weeks prior to inflammation bioreactor culture,

expression is significantly increased 1.8- and 1.6-fold ($p<0.01$, $p<0.02$, respectively). Pre-treatment of cells does not have a significant effect in inflammation beads.

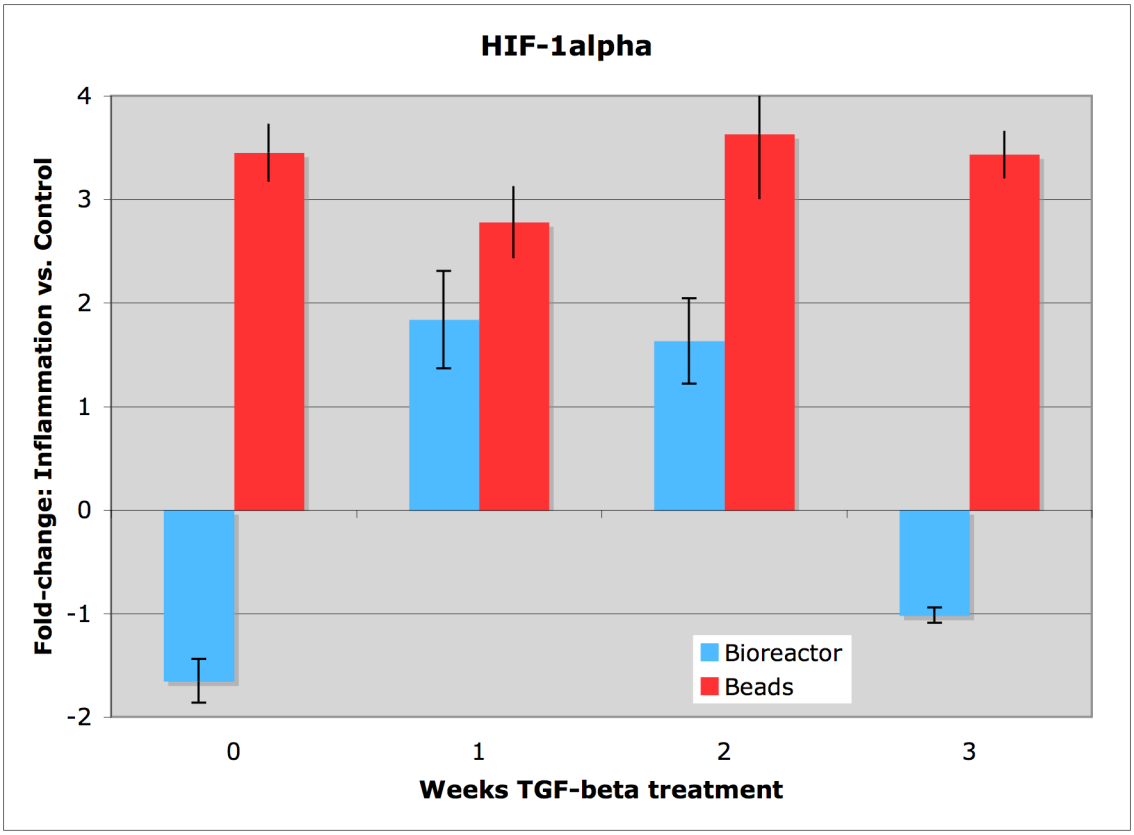

Figure 5.7 Effect of inflammation and pre-treatment on HIF-1α gene expression as a function of culture type (bead versus bioreactor). In inflammation bead culture, pre-treatment with TGF-β3 does not have a significant effect on expression. Two or three weeks of TGF-β3 pre-treatment in the presence of inflammation results in a significant increase in HIF-1α expression.

Collagen I expression is reduced by inflammation in bead culture. Inflammation does not have a significant effect on expression in bioreactor culture except when cells are undifferentiated; expression increases 364-fold compared to control bioreactors ($p<0.03$). In the presence of inflammation, pre-treatment of cells with TGF-β3 does not significantly change collagen I values from undifferentiated cells; in inflammation beads,

pre-treatment results in a significant increase in expression for all lengths of pre-treatment time.

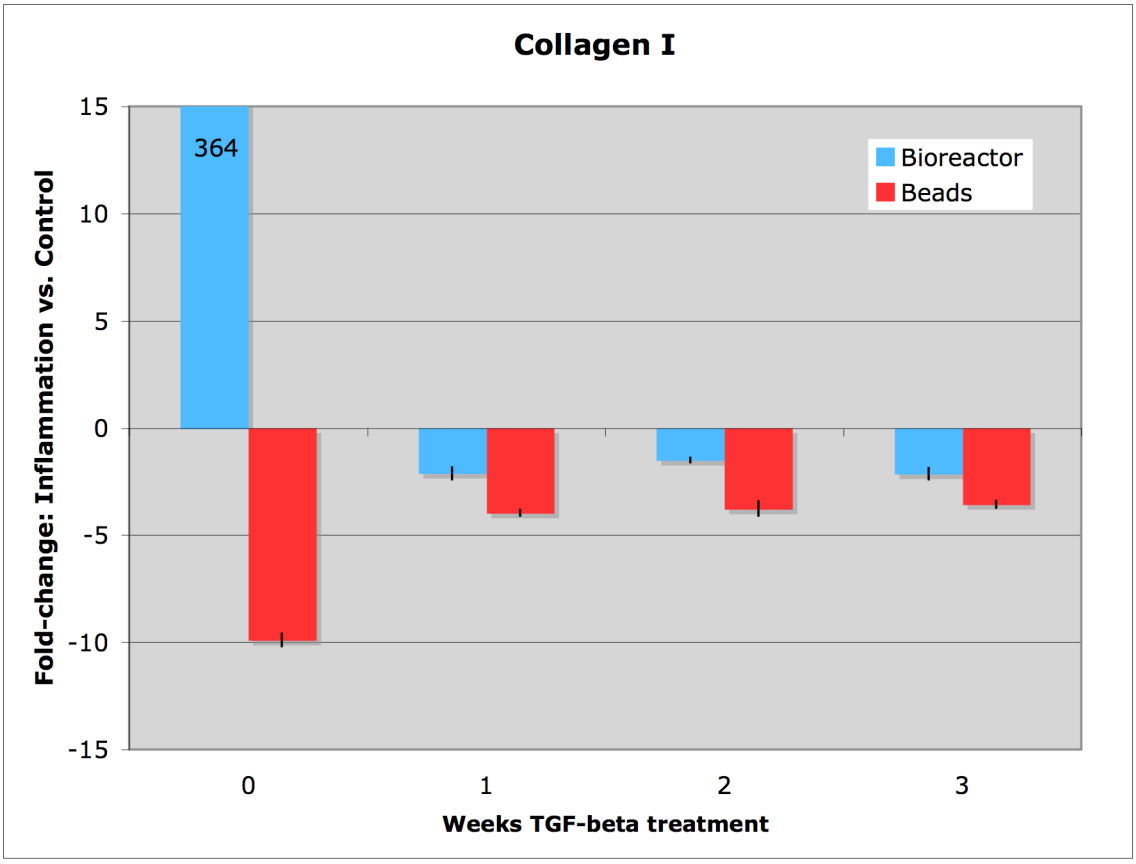

Figure 5.8 Effect of inflammation and pre-treatment on collagen I gene expression as a function of culture type (bead versus bioreactor). In bead culture, inflammation reduces collagen I. In bioreactor culture, inflammation only has a significant effect on undifferentiated cells. Pre-treatment of TGF-β3 does not significantly change collagen I expression in inflammation bioreactors, but results in a significant increase in inflammation beads.

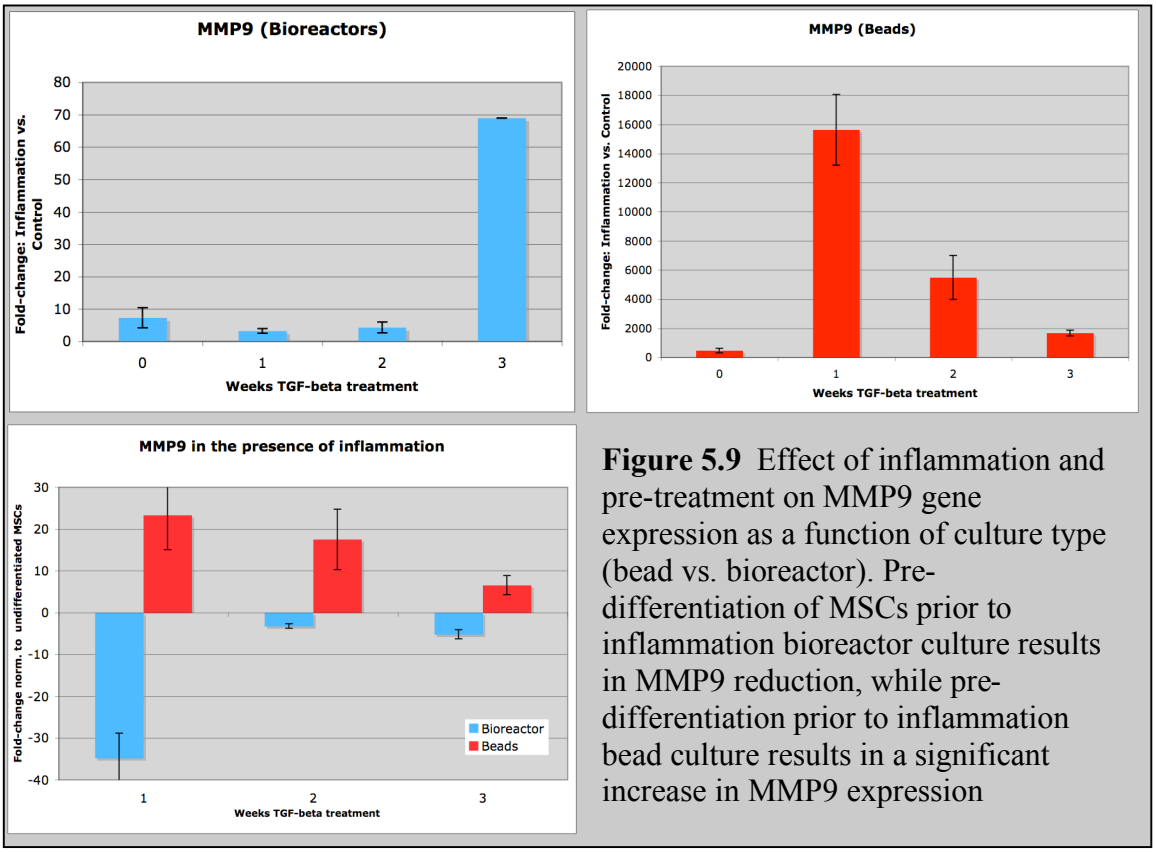

Figure 5.9 Effect of inflammation and pre-treatment on MMP9 gene expression as a function of culture type (bead vs. bioreactor). Pre-differentiation of MSCs prior to inflammation bioreactor culture results in MMP9 reduction, while pre-differentiation prior to inflammation bead culture results in a significant increase in MMP9 expression

The presence of inflammation results in an increase in MMP9 expression in both bioreactors (3 to 70-fold increase) and beads (476 to 15641-fold increase). Pre-differentiating cells for one or two weeks prior to inflammation BR culture results in significant reduction of MMP9 ($p<0.01$ and $p<0.02$, respectively.) Pre-treatment results in a significant increase in MMP9 expression in inflammation beads.

Pre-differentiation of MSCs before bead culture dampens the increase in TSG6 expression that results from exposure to inflammation. In the bioreactor environment, the

overall reactions to inflammation are lessened, with a reduction of TSG6 expression occurring for undifferentiated cells.

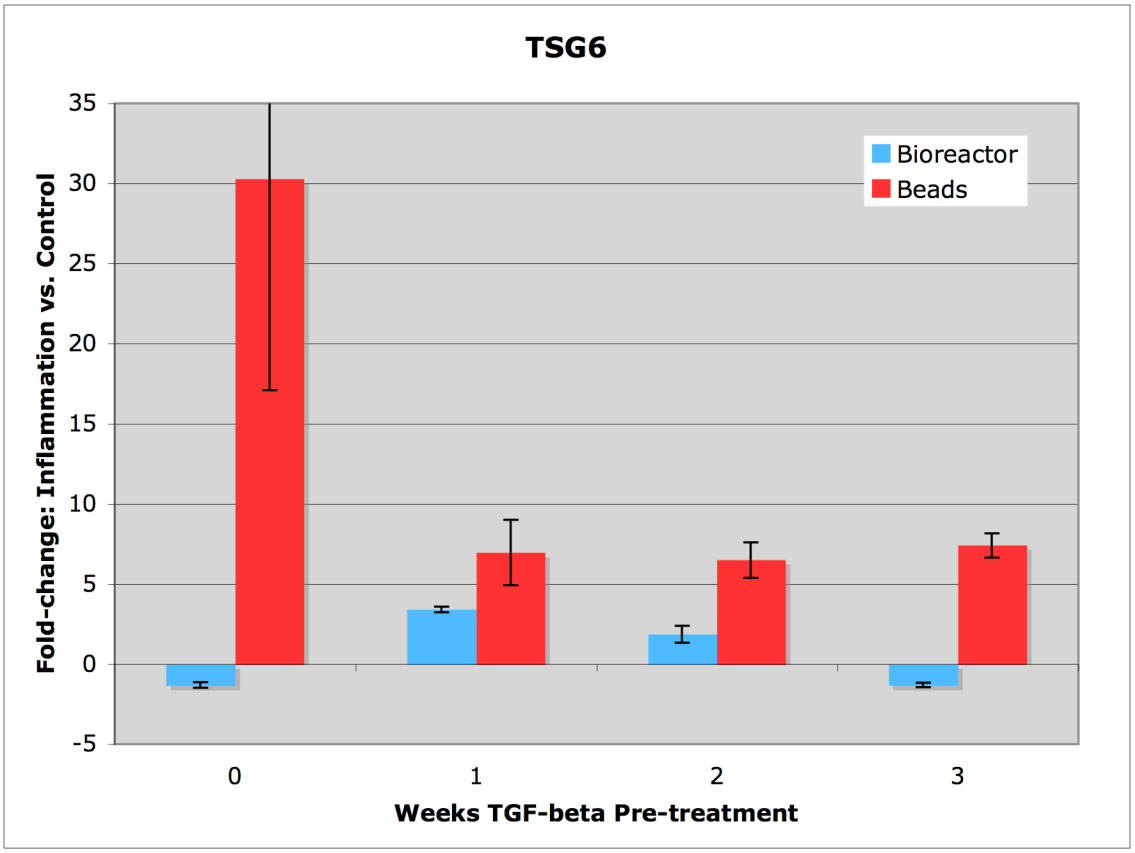

Figure 5.10 Effect of inflammation and pre-treatment on TSG6 gene expression as a function of culture type (bead versus bioreactor). In bead culture, pre-differentiation of MSCs dampens the increase in TSG6 expression that results from exposure to inflammation.

Gene Expression – Effect of Bioreactor Environment

To investigate the contribution of disc-mimetic conditions to changes in gene expression levels in the presence of inflammation, gene expression levels of inflammation bioreactors were normalized to levels in corresponding inflammation beads. These values were also compared to control values (control bioreactors normalized to control beads).

When inflammation is present, disc-mimetic conditions upregulate aggrecan expression in undifferentiated cells. For TGF-β3-treated cells, aggrecan expression is downregulated. Without inflammation, disc-mimetic conditions downregulate aggrecan expression in undifferentiated MSCs and do not have a significant effect on pre-treated cells.

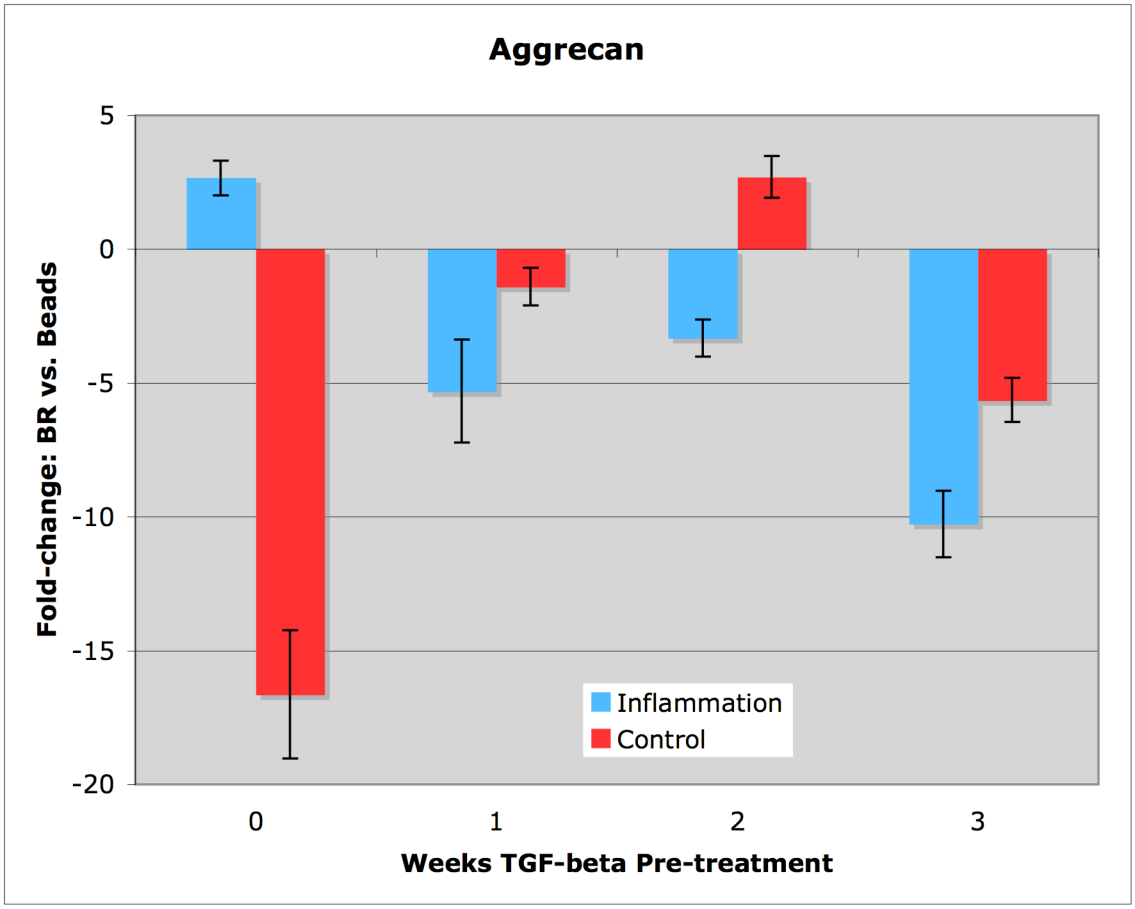

Figure 5.11 Effect of disc-mimetic conditions on aggrecan expression in the presence and absence of inflammation.

Disc-mimetic conditions increase Sox9 expression in all groups ($p<0.02$ for undifferentiated cells, $p<0.03$ for 1 week TGF-β3 pre-treatment) in the presence of

inflammation. Without inflammation, undifferentiated cells express a nearly 5-fold decrease in BR compared to bead culture ($p<0.01$).

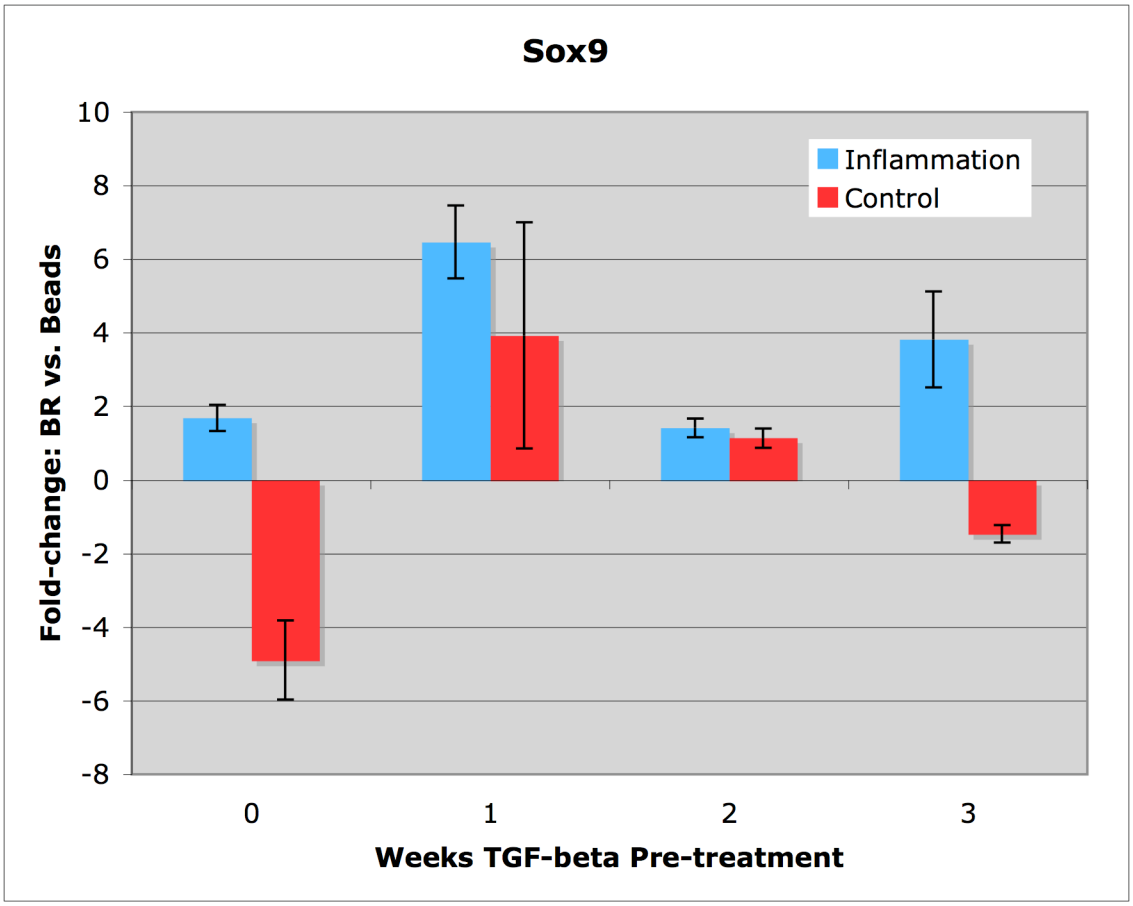

Figure 5.12 Effect of disc-mimetic conditions on Sox9 expression in the presence and absence of inflammation.

MMP9 expression by is significantly decreased by disc-mimetic conditions in the inflammation, particularly when cells have been pre-treated with TGF-β3. Expression is increased by disc-mimetic conditions when inflammation is not present.

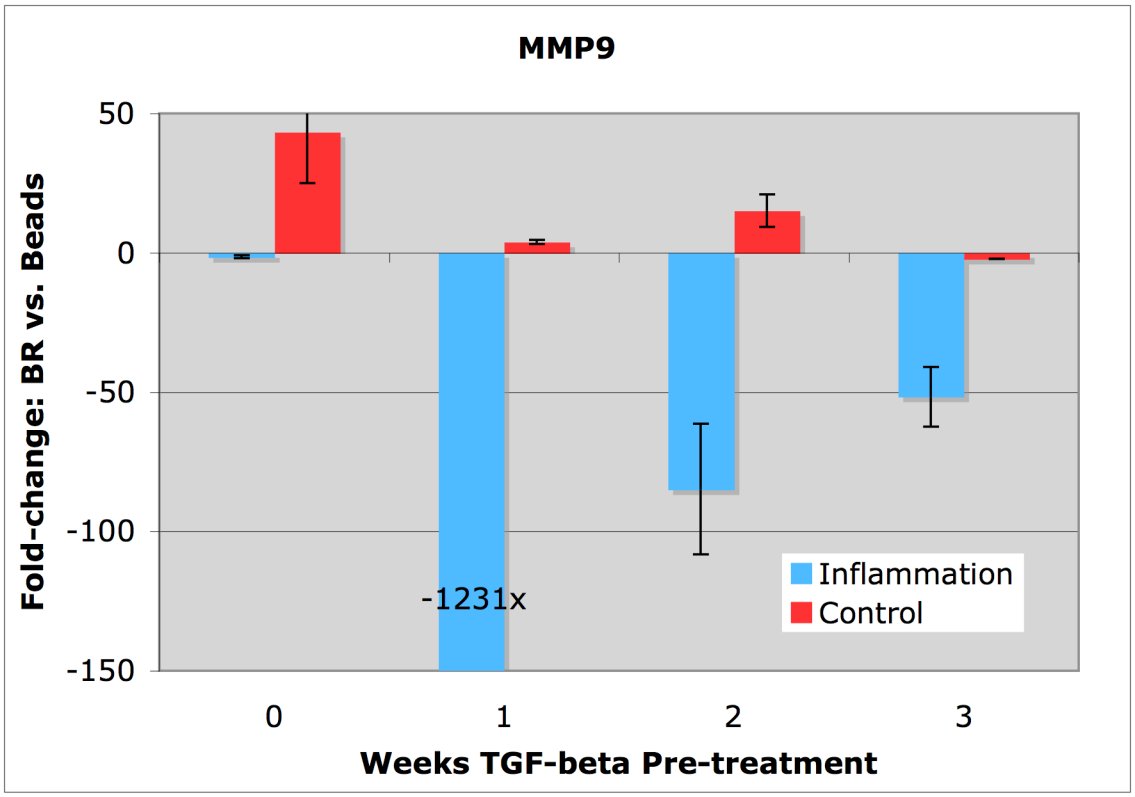

Figure 5.13 Effect of disc-mimetic conditions on MMP9 expression in the presence and absence of inflammation.

Without inflammation, bioreactor culture increases TSG6 expression compared to bead culture, with the largest increase occurring when cells are undifferentiated ($p<0.01$). Pre-differentiation of cells dampens the effect of bioreactor culture in the absence of inflammation. When inflammation is present, bioreactor culture does not have as significant effect on TSG6 expression – only the expression in undifferentiated cells is significantly reduced by disc-mimetic conditions ($p<0.03$), with a 1.1 to 1.6-fold reduction occurring in the groups.

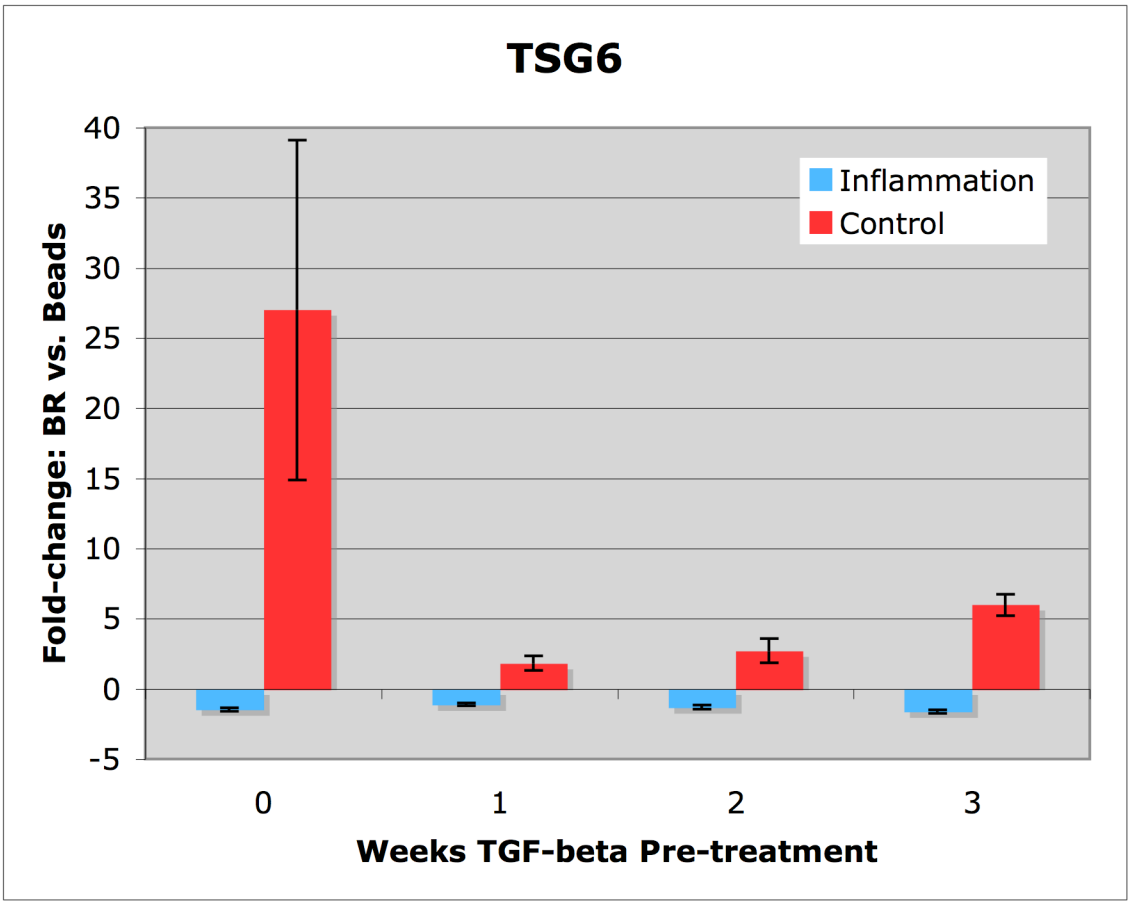

Figure 5.14 Effect of disc-mimetic conditions on TSG6 expression in the presence and absence of inflammation.

5.4 Discussion

This study characterized how inflammation affects the expression of certain chondrocyte- and inflammation-associated genes in undifferentiated and pre-differentiated MSCs in both a disc-mimetic and traditional cell culture environment. We report here that in a traditional cell culture environment, stimulation of undifferentiated MSCs with inflammatory cytokines results in decreased aggrecan, Sox9, collagen X, and collagen I expression, and increased collagen II, MMP9, and TSG6 expression. In a disc-

mimetic environment, aggrecan and collagen I expression are increased by inflammation, and HIF-1α and TSG6 expression are decreased.

Our results demonstrate that pre-treatment with TGF-β3 can have a profound effect on how MSCs react to inflammation. When cells are pre-treated before exposure to inflammation, aggrecan expression is increased in the bead environment and decreases in the disc-mimetic environment, both of which are contrary to the changes that occur in undifferentiated MSCs. This behavior is consistent with findings that hydrostatic pressure, like that in the disc-mimetic bioreactor, downregulates hydrostatic pressure in nucleus pulposus cells [179]. The proteoglycan amounts measured in inflammation bioreactors also confirm the trend seen in gene expression levels; the addition of inflammation does not result in a significant increase or decrease in GAG amount produced by undifferentiated cells, nor does pre-treatment with TGF-β3 enhance GAG production as it does in a non-inflammation environment.

Collagen II expression is also affected by pre-treatment in an inflammatory disc-mimetic environment. Two weeks of TGF-β3 treatment is sufficient to sustain gene expression after culture in inflammation bioreactors; one and three weeks of pre-treatment results in a decrease in expression after inflammatory bioreactor culture.

The effect of TGF-β3 treatment is strong enough to overcome inflammation-induced effects; two and three weeks of pre-treatment resulted in significant increases (1.8- and 1.6-fold, $p<0.002$) in HIF-1α expression after culture in inflammation bioreactors. When cells are undifferentiated and exposed to inflammatory bioreactor culture, HIF-1α expression is decreased. This result is surprising, as hypoxia increases expression (Chapter 3), and both IL-1β and TNF-α have been found to increase HIF-1α

expression [180]. This suggests that even though inflammation can strongly affect cells, the effect may be indirect or environment-dependent.

A significant potential hurdle for disc regeneration is the deleterious effect of pre-existing inflammation on injected cells. IL-1β and TNF-α have been shown to inhibit chondrogenesis of human mesenchymal stem cells [181], and prolonged exposure to an ischemic, nutrient-deprived microenvironment that resembles that of the degenerated IVD can lead to stem cell death [182, 183] and potentiate inflammation [184-186]. Cytokines secreted by the disc cells can stimulate wound healing, but at the same time cause damage to transplanted cells. TNF-α is a potent pro-death factor for MSCs [187].

Gene expression levels of aggrecan, collagen II, collagen X, MMP9, and TSG6 demonstrate that the effect of inflammation is context-dependent, and not always catabolic: inflammation can significantly enhance collagen 2 expression when cells are cultured in disc-mimetic conditions as opposed to in a traditional cell culture environment. Inflammation increases aggrecan expression in undifferentiated cells cultured in disc-mimetic conditions, but decreased in inflammation beads. Collagen X expression is heavily influenced by TGF-β3 stimulation (Chapter 3), yet expression is significantly reduced by inflammation in both beads and bioreactors. Collagen X is present in aged and scoliotic human intervertebral discs and degenerative discs, and is traditionally a marker of chondrocyte hypertrophy, indicating a role in matrix calcification [188, 189]. Hypertrophic chondrocytes secrete collagen X but also produce angiogenic factors [190]; inflammation could therefore have an initial protective effect on injected cells. IL-1β and TNF-α have both been shown to inhibit growth plate chondrogenesis [191]. MMP9 and TSG6 are normally upregulated in response to IL-1β

and TNF-α stimulation, but these effects are dampened when cells are cultured in disc-mimetic conditions as opposed to traditional cell culture conditions.

Our results suggest that inflammation does not necessarily have detrimental effects on injected cells, especially when cells are appropriately pre-conditioned, and highlight the importance of mimicking the *in situ* environment when investigating cell therapy efficacy.

Chapter 6: Conclusion and Future Directions

6.1 Research Summary

The overall goal of this dissertation was to investigate the use of mesenchymal stem cells to regenerate the nucleus pulposus. Specifically, we focused on advancing our understanding of how to optimally prepare the cells for transplantation to the disc, and investigated the fate of MSCs after transplantation into an *in vivo* disc environment or an *in vitro* disc-mimetic environment.

Undifferentiated MSCs and juvenile chondrocytes were injected into a rat coccygeal disc model to determine how cell maturity can affect its function once transplanted into the disc. Discs injected with undifferentiated MSCs had greater initial loss of disc height than JC-injected discs, and at 4 weeks post-transplantation, most MSC-injected discs displayed disrupted annular architecture while less than one-fifth of JC-injected discs showed evidence of annular disruption around the wound tract. At 12 weeks post-injection, discs injected with fibrin only showed degeneration and loss of proteoglycan staining while more than 80% of JC-injected discs presented with normal nucleus size.

The *in vivo* experiments demonstrated that a mature cell phenotype would function more effectively within the disc environment. However, MSCs are a more practical choice for cell therapy as they are easily harvested, expanded, and can differentiate into a number of mature phenotypes, and do not present the same challenges that arise from harvesting and expanding autologous disc cells or chondrocytes. Therefore, we investigated the use of pre-differentiated MSCs for cell-mediated nucleus regeneration. Traditionally, biochemical agents such as TGF-β3 are used to induce MSC

chondrogenesis *in vitro*, and while nucleus pulposus cells share some of the same phenotypic characteristics as chondrocytes, they cannot be classified as such. It has been demonstrated that the *in vivo* disc environment plays a role in the differentiation and metabolism of disc cells, and may have a significant effect on MSC chondrogenesis. Therefore, we developed a novel disc-mimetic bioreactor culture system that exposes cells to physiologically relevant levels of hypoxia (4.8%) and hydrostatic pressure (0.12 MPa), and used this system to determine if the physiochemical environment of the disc, absent native disc cells and chondrogenic growth factors, can induce differentiation of MSCs. MSCs cultured in this bioreactor were produced proteoglycan, and showed upregulation in aggrecan, collagen II, Sox9, and collagen X, in a pattern similar to what has been previously reported in the literature for TGF-β3-induced chondrogenesis. However, the overall timeline of bioreactor-induced differentiation occurs on the order of weeks, rather than days, further suggesting that pre-differentiation of cells prior to disc implantation is necessary to overcome the challenges of the disc environment.

As few experiments have investigated the fate of pre-differentiated MSCs in either an *in vivo* or *in vitro* disc environment, we utilized the disc-mimetic bioreactor as a diagnostic tool to advance our understanding of what might happen to these cells after transplantation into the disc. MSCs were stimulated with TGF-β3 to varying levels of differentiation before transplantation into the disc-mimetic bioreactor. Pre-differentiated MSCs had improved cell viability and increased GAG production compared to undifferentiated MSCs after two weeks of bioreactor culture. Gene expression profiles of aggrecan, collagen II, and Sox9 demonstrated that pre-treatment with TGF-β3 accelerates the process of disc environment-mediated differentiation, and MSCs that were pre-

differentiated prior to bioreactor culture displayed higher levels of collagen II and Sox9 than the highest levels induced by TGF-β3 stimulation.

The persistence of TGF-β3-induced gene expression after bioreactor culture implied that the bioreactor mimics a healthier disc state than that found in a chronically degenerated environment. The environment-dependent differences in gene expression in the previous experiments highlighted the necessity of mimicking several aspects of the disc environment in concert when attempting to evaluate the fate of the cells post-implantation. Therefore, IL-1β and TNF-α were incorporated into the bioreactor to evaluate the effects of inflammation on undifferentiated and pre-differentiated MSCs in disc-mimetic conditions. Inflammation can have deleterious effects on disc cells and chondrocytes, and our experiments indicated that undifferentiated MSCs also suffered these effects when cultured in a traditional cell culture environment, with decreased aggrecan and sox9 expression and increased MMP9 and TSG6 expression. The effects of inflammation also affect pre-treated MSCs, as seen by gene expression levels and total GAG amounts. However, some of the traditional responses to inflammation were reversed when cells were cultured in the disc-mimetic environment. Aggrecan and collagen II expression are increased when pre-differentiated prior to bioreactor culture, and expression levels of collagen X, MMP9, and TSG also demonstrated that the effect of inflammation is context-dependent and not necessarily detrimental. The results of this study confirm the importance of accurately mimicking the conditions of the disc environment, and taken together with the findings from the other research aims of this dissertation, demonstrate that MSCs can be optimized for nucleus pulposus regeneration.

6.2 Future Directions

The challenges of the disc environment, and the environment-dependent changes seen in MSCs during transplantation to the disc suggest several different areas where future research can focus to optimize nucleus pulposus regeneration.

Modification of Bioreactor for Future Diagnostic Studies

A useful feature of the disc-mimetic bioreactor developed for this research is the ease with which it can be modified to incorporate additional features of the disc environment. A major obstacle to tissue engineering strategies for regenerating the nucleus pulposus is the overall lack of knowledge of not only the genetic phenotype of disc cells, but also how phenotype can change with degeneration and pain.

One problem of attempting to regenerate the nucleus pulposus *in situ* is identifying the difference between painful and nonpainful discs. The appropriate candidate for cell therapy will be one with moderate degeneration (no greater than Thompson grade 3) who most likely presents with axial back pain (not due to herniation). Therefore, an important step in advancing this research is to use human tissue samples to help elucidate the factors that not only make up a degenerated painful cell phenotype, but that contribute to its cause. Previous studies have been able to find differences between normal and degenerate discs without the ability to identify which discs are painful. Features that distinguish degenerated non-painful discs from degenerated painful discs are unclear. Recent work suggests that painful discs have an increased density of nociceptors as part of the vertebral endplate and outer annulus, perhaps as part of the granulation tissue formed as a result of damaged extracellular matrix [66, 192, 193].

Another recent study reported that painful disc tissue differs from degenerated non-painful disc tissue in their lactate-to-proteoglycan ratios, with pain patients having an increased ratio [194].

Using a combination of gene array, environmental measurements such as oxygen and pH, lactate concentration, and ELISA data for concentrations of cytokines, differences in biochemical and cellular phenotype between degenerated painful and degenerated non-painful discs can be determined. Using this data, the bioreactor can be modified accordingly to accurately mimic the degenerated painful disc phenotype, providing an efficient method to screen cell responses to this environment.

Appropriate Cell Type for Disc Repair

When considering MSCs for tissue engineering applications, we have described the importance of environmental conditions. It has been hypothesized that a successful approach would involve mimicking specific cellular events that occur during embryonic tissue development (reviewed in [195]). Researchers have looked at pellet co-culture of MSCs and nucleus pulposus cells to mimic embryonic processes such as tissue induction and condensation. Co-culture generally resulted in increased matrix synthesis and/or induction of chondrogenic genes in the MSCs [135, 154, 196].

In young humans, a second population of cells, known as notochordal cells, resides in the nucleus pulposus. These cells are presumed to be remnants of the embryonic tissue that initially guided formation of the spine [197, 198]; as these cells play a role in formation of the spine, it can be hypothesized that they also influence repair of the degenerated or damaged disc. However, the exact role played by notochordal cells

in nucleus pulposus formation remains unknown. Some researchers have suggested that notochordal cells directly synthesize the nucleus and then differentiate into a chondrocytic cell. Others suggest that the notochordal cells direct migration of cells from the surrounding mesenchyme, and these migrated cells themselves synthesize nucleus matrix. Once synthesis is complete, the notochordal cells undergo necrosis or apoptosis [197, 199]. Although the exact role of the notochordal cell during development is unknown, loss of notochordal cells seems to be consistent with disc degeneration, and may even be the first stage in early degeneration [199]. The two theories regarding the role of notochordal cells in development assign two possible roles to the notochordal cell: either as a primary stem cell source, or as an "organizer" cell [200]. The exact genetic phenotype of a notochordal cell has yet to be identified; researchers have identified molecular differences between notochordal cells and nucleus pulposus cells, such as presence of CD44s, galectin 3, vimentin, and cytokeratins 8 and 19 [201-204]. However, like nucleus pulposus cells, it is difficult to coax differentiation of MSCs into a notochordal cell phenotype without knowing that exact phenotype, and also because the notochordal cells may themselves act as stem cells. Restoring the notochordal cell population to the disc could act to recruit other cells to synthesize new matrix. With the notochordal cell acting as an "organizer" in this case, it may also be possible to identify the relevant signals that direct the cell recruitment and matrix synthesis process, and researchers can inject a cocktail of these cell-signaling factors unique to notochordal cells directly into the disc.

The results presented in this dissertation highlight the importance of taking into account several different environmental factors when identifying appropriate cell types

for nucleus pulposus regeneration. In light of this research, it is most likely that pre-conditioning MSCs in the disc-mimetic bioreactor, in addition to TGF-β3 pre-treatment or notochordal cell signaling factor stimulation, will result in optimal cell function when implanted into human discs.

Delivery of Cells

An oft-overlooked challenge to nucleus pulposus regeneration by cell therapy is the manner in which the cells will be transplanted and retained in the human disc. The importance of cellular scaffolds has been previously reviewed [205, 206], but the majority of studies have focused on the ability of the scaffolds to maintain native disc cell phenotype [207, 208] and direct differentiation [153, 209-211]. Very few researchers have addressed the issue of engineering a scaffold that is optimized for retention inside the disc. Without a method to prevent cell extrusion after initial implantation into the disc, any research devoted to cell optimization is less relevant. With the level of research that is devoted to cell optimization, research should also be devoted towards engineering a scaffold that is biologically inert (preventing an inflammatory response), easily injectable (therefore, thermoregulated or similar), and stiff enough to withstand the pressures of daily activity, maximizing cell retention.

Appendix A: Cell Retention After Injection into the Rat Coccygeal Disc

A.1 Introduction

A previous experiment in our lab demonstrated that retention of cells injected into the rat coccygeal disc is significantly reduced seven and 14 days after initial injection when cells are delivered in a hyaluronan gel carrier [212]. The activities of daily living (an average of 1 MPa in humans [213]) can generate significant internal pressures on injected cells, and an appropriate carrier should be used that will maximize cell retention but allow the cells to survive and produce extracellular matrix. In this experiment, we investigated the retention properties of a fibrin glue carrier.

A.2 Methods

Fluorescent Microspheres as Cell Analogs for Retention Studies

In order to quantify how many cells might be retained in the disc upon injection, polystyrene microsphere beads (FluoSpheres, 15um diameter, Invitrogen) were used as a cell analog. When dissolved in 2-ethoxyethyl acetate, the beads release a red fluorescent dye (excitation 570, emission 598) that can be detected with a fluorescent plate reader. The number of beads can be detected by calibrating the readings against a standard curve.

Bead Injections

A 15% hyaluronan (HA) gel was made by dissolving hyaluronic acid powder (Genzyme) in PBS. The PBS had fluorescent microspheres mixed in at a concentration of 10 million beads/mL. Twenty microliters of gel was injected into six separate rat coccygeal discs under fluoroscopic guidance for each time point. Three discs injected

with blank HA gel served as a control. For fibrin carrier injections, similar experiments were carried out. First, 10 microliters of fibrinogen (34 mg/mL) mixed with beads (10 million/mL) was injected into the rat coccygeal disc, followed by 10 microliters of thrombin (333 U/mL) mixed with beads (10 million/mL). Three discs injected with blank fibrin served as a control.

Bead Quantification

For both carrier types, discs were excised immediately, 7 days, or 28 days after injection. The tissue was minced, then dissolved in 2-ethoxyethyl acetate to release the fluorescent dye. The number of beads retained in each disc was calculated against a standard curve with a range of 2,000 to 10 million beads/mL. The background fluorescence of the control discs was subtracted from the measurements, and the percentage of beads retained was calculated for each disc.

A.3 Results and Conclusions

At day zero, an average of 26% of the injected beads delivered in HA gel were retained in the disc. At seven days, 16% of injected beads were retained. Only 6% of injected beads were detected at 28 days

When beads were delivered in fibrin carrier, an average of 55% were retained at day zero. At seven days, 33% of injected beads were retained. Twelve percent of injected beads were retained at 28 days.

Using a fibrin carrier resulted in an overall higher retention of injected beads than using a hyaluronan gel carrier (Figure A.1). The needle entry point can still be visualized

up to two weeks after injection, meaning a cross-linked carrier may be more suitable to reduce carrier extrusion due to low viscosity or enzymatic degradation. Fibrin sealant is FDA-approved for use as a surgical adhesive, and the mechanical properties have been widely characterized [214-217]. For future experiments, the injection technique will need to be refined as to maximize the amount of fibrinogen and thrombin that come into contact with each other, and a higher concentration of fibrinogen and thrombin should be used to speed polymerization time, reducing the amount of carrier that can extrude from the needle entry point, increasing initial cell retention.

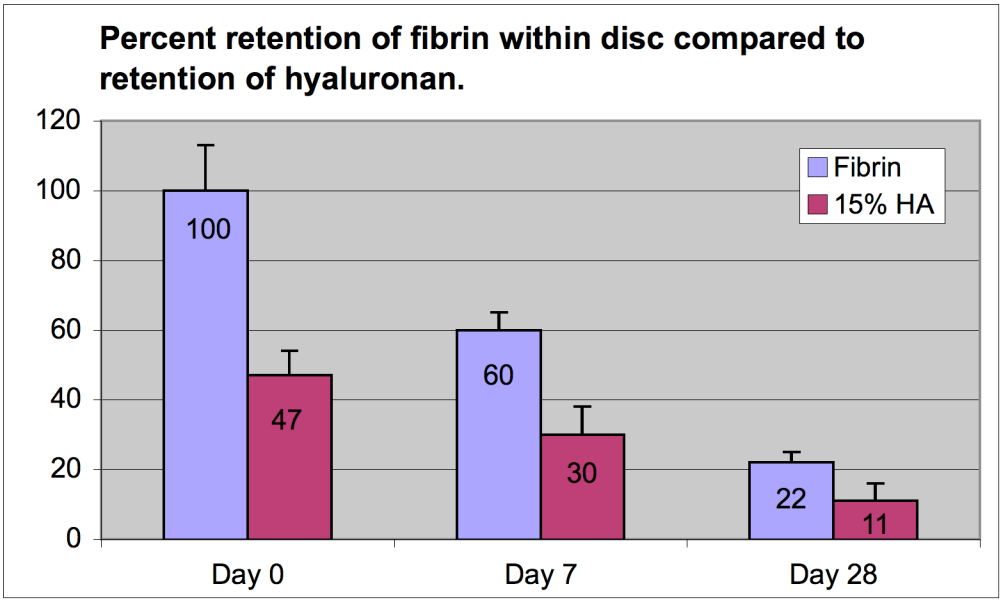

Figure A.1 Retention of beads in fibrin and hyaluronan carriers.

Appendix B: Morphological Effects of Rat Mesenchymal Stem Cell Injection into a Rat Model of Disc Degeneration

B.1 Introduction

Previous experiments in our lab have shown cell retention in a hyaluronan gel carrier to be significantly reduced at 7 and 14 days after transplantation [212]. After investigating a different carrier for improved cell retention (Appendix A), we looked at whether or not rat MSC injection could improve the morphology of degenerated rat coccygeal discs using an animal model developed in our lab [218] .

B.2 Methods

Animals

Male Inbred Fisher rats (250-300 g) were used. All procedures were approved by the Institutional Animal Care and Use Committee of the University of California at San Francisco.

Rat Mesenchymal Stem Cell Isolation and Culture

Rats were euthanized by CO_2 asphyxiation and bilateral thoracotomy. Femora and tibiae were excised and cleaned with PBS. The condyles and heads of the bones were removed, and the lumen of each bone was flushed with Dulbecco's Modified Eagle's Medium (DMEM) using a 19-gauge needle. The bone marrow-DMEM mixture was centrifuged for 5 minutes at 1800 rpm. The supernatant was aspirated and remaining cell pellet treated with ammonium Chloride Potassium (ACK) lysis buffer to lyse red blood cells. The cell-buffer mixture was again centrifuged for 5 minutes at 1800 rpm,

and the supernatant was aspirated. The cell pellet was resuspended in cell growth media (DMEM, 10% FBS, 1% pen-strep) before straining through a 40 μm mesh filter. Cells were then counted with a hemocytometer and plated on tissue culture-treated flasks at a density of $2x10^7$ cells/100 cm^2. After 24 hours, non-adherent hematopoietic cells were discarded and the remaining attached cells were rinsed with PBS, incubated at 37 ° C/5% CO2 and cultured for two passages, with media changed three times a week.

Single Annular Stab for Rat Disc Degeneration

Six rats were each anesthetized using ketamine (90 mg/kg IP) and xylazine (10 mg/kg IP). Buprenorphine (0.01 mg/kg SQ) was administered once before recovery and then as needed to control postoperative pain. Atipamezole HCL (0.2 mg/kg IP) was used for anesthesia reversal. Food, drink, and activity were unrestricted post-operatively. A 2.5 cm longitudinal incision was made along the tail to expose the lateral portion of tail discs Co5/Co6, Co6/Co7, and Co7/Co8. Lateral stabs were performed so that the incision would be on the primary plane of motion for tail discs. A number 11 blade was inserted 1.5 mm into the disc to depressurize the nucleus. A clamp was placed on the blade to prevent the blade from penetrating the disc more than 1.5 mm and radiographic images were captured to ensure the blade was parallel to the endplates to avoid endplate damage. The blade was then removed and the tail skin was closed using interrupted stitches.

Rat MSC Injection

Adherent cells were removed from flasks by washing with 0.25% trypsin in

EDTA for 5 minutes. Cells were labeled with CM-DiI membrane stain (Invitrogen) and suspended in 50 mg/mL fibrinogen at a concentration of 10^7 cells/mL. Labeled cells were also suspended in thrombin (400 IU/mL) at a concentration of 10^7 cells/mL. Twenty-eight days after the initial stab injury, two of the degenerated discs in each rat were injected with 20uL of cells suspended in fibrin. The remaining degenerated disc in each rat was injected with 20uL of blank fibrin as a control.

Confirmation of Cell Retention and Histology

Twenty-eight days after the cell or fibrin control injections, rats were euthanized and each injected disc with a section of adjacent vertebrae was harvested. Of the 12 cell-injected discs, three were frozen in OCT tissue-freezing medium, and sectioned 70 um thick along the transverse plane. CM-DiI-stained cells were visualized under fluorescence microscopy using a Texas Red filter under 40x magnification. The remaining control and cell-injected discs were fixed in formalin, decalcified in formic acid, dehydrated, and embedded in paraffin. Six-micron sections were cut through the nucleus pulposus parallel to the direction of the stab. Sections were stained with Safranin-O, fast green, and hematoxylin. Disc and endplate architecture was examined at 2x magnification. Nuclear and annular cellular and extracellular aspects were analyzed using 10x and 20x magnification.

B.3 Results

Frozen transverse sections revealed cells were present in the disc, but sparsely dispersed throughout the nucleus and annulus.

All discs, regardless of treatment, had severe morphological changes, including loss of nucleus pulposus, decreased disc height, and disorganized collagen lamellae (Figure B.1). Some discs showed disrupted endplate architecture, and two of the disc motion segments had complete loss of movement when excised upon sacrifice. These discs were all severely degenerated compared to discs that had been stabbed and left to recover for 4 or 6 weeks (Figure B.2). These control stab-recovery discs showed nucleus representing one-fourth to one-half of the disc area, continuous endplates, and discs that recover for 8 weeks have a more "normal" morphological presentation than discs that recover for 4 weeks.

B.4 Discussion

Injection of rat MSCs does not have a positive effect on disc morphology after injection into a rat degeneration model. Looking at the histology for the stab-injured discs, there is no evidence that suggests the disc morphology is degenerated beyond repair prior to cell or fibrin injection. However, discs injected only with fibrin carrier have similar severe morphological changes to those seen in cell-injected discs, so we cannot determine which component (cells or fibrin) contributed to the increase degeneration. A possible explanation is that the initial stab injury was too severe or damaged the endplate, which has been shown to induce degeneration in a rabbit organ culture model [219], and can also lead to adjacent disc degeneration [36].

Another problem is the difficulty in differentiating rat MSCs towards a chondrogenic phenotype. Although bone marrow-derived stem cells from 1-week-old rats can form cartilage matrix *in vitro*, proteoglycan staining for cell aggregates from 12-week-old or 1-year-old rats is largely negative [220]. Rat mesenchymal stem cells have difficulty producing proteoglycan in pellet culture compared to human MSCs [personal communication, Brian Johnstone, Oregon Health & Science University] and therefore would not be able to produce matrix upon implantation into a degenerated disc, and it has only be recently shown that synovium-derived rat MSCs have the best chondrogenic differentiation potential compared to cells derived from other tissue types [221]. Future animal studies should utilize human MSCs, which form proteoglycan when differentiated along a chondrogenic lineage.

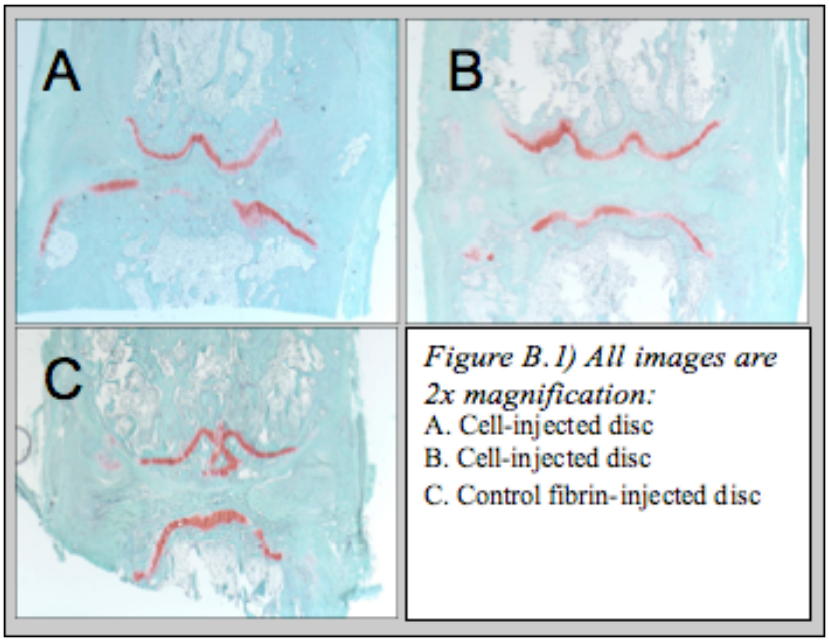

Figure B.1) All images are 2x magnification:
A. Cell-injected disc
B. Cell-injected disc
C. Control fibrin-injected disc

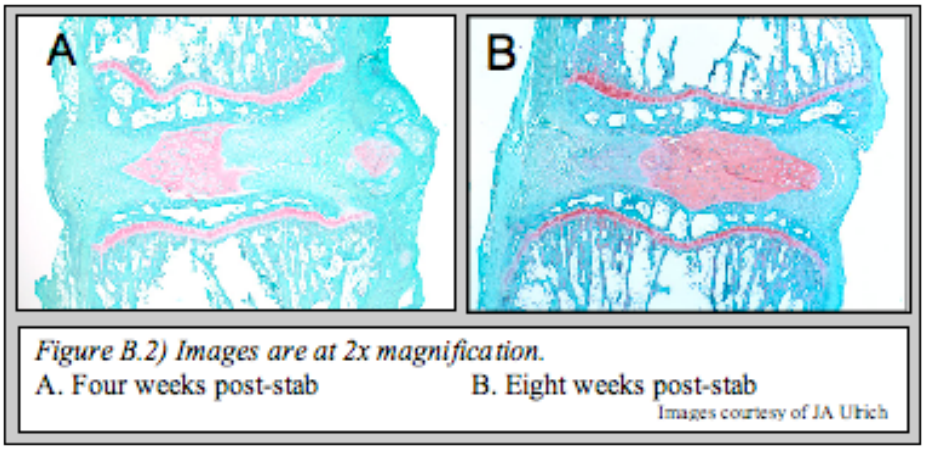

Figure B.2) Images are at 2x magnification.
A. Four weeks post-stab B. Eight weeks post-stab
Images courtesy of JA Ulrich

References

1. Humzah, M.D. and R.W. Soames, *Human intervertebral disc: structure and function.* Anat Rec, 1988. **220**(4): p. 337-56.
2. Roberts, S., *Disc morphology in health and disease.* Biochem Soc Trans, 2002. **30**(Pt 6): p. 864-9.
3. Roughley, P.J., *Biology of intervertebral disc aging and degeneration: involvement of the extracellular matrix.* Spine, 2004. **29**(23): p. 2691-9.
4. Walker, M.H. and D.G. Anderson, *Molecular basis of intervertebral disc degeneration.* Spine J, 2004. **4**(6 Suppl): p. 158S-166S.
5. Adams, M.A. and P.J. Roughley, *What is intervertebral disc degeneration, and what causes it?* Spine, 2006. **31**(18): p. 2151-61.
6. Cs-Szabo, G., et al., *Changes in mRNA and protein levels of proteoglycans of the anulus fibrosus and nucleus pulposus during intervertebral disc degeneration.* Spine, 2002. **27**(20): p. 2212-9.
7. Bibby, S.R., et al., *The pathophysiology of the intervertebral disc.* Joint Bone Spine, 2001. **68**(6): p. 537-42.
8. Gruber, H.E. and E.N. Hanley, Jr., *Recent advances in disc cell biology.* Spine, 2003. **28**(2): p. 186-93.
9. Bruehlmann, S.B., et al., *Regional variations in the cellular matrix of the annulus fibrosus of the intervertebral disc.* J Anat, 2002. **201**(2): p. 159-71.
10. Chelberg, M.K., et al., *Identification of heterogeneous cell populations in normal human intervertebral disc.* J Anat, 1995. **186 (Pt 1)**: p. 43-53.

11. Sive, J.I., et al., *Expression of chondrocyte markers by cells of normal and degenerate intervertebral discs.* Mol Pathol, 2002. **55**(2): p. 91-7.

12. Maroudas, A., et al., *Factors involved in the nutrition of the human lumbar intervertebral disc: cellularity and diffusion of glucose in vitro.* J Anat, 1975. **120**(Pt 1): p. 113-30.

13. Urban, J.P., S. Smith, and J.C. Fairbank, *Nutrition of the intervertebral disc.* Spine, 2004. **29**(23): p. 2700-9.

14. Roberts, S., J. Menage, and J.P. Urban, *Biochemical and structural properties of the cartilage end-plate and its relation to the intervertebral disc.* Spine, 1989. **14**(2): p. 166-74.

15. Gronblad, M., J.N. Weinstein, and S. Santavirta, *Immunohistochemical observations on spinal tissue innervation. A review of hypothetical mechanisms of back pain.* Acta Orthop Scand, 1991. **62**(6): p. 614-22.

16. Fagan, A., et al., *ISSLS prize winner: The innervation of the intervertebral disc: a quantitative analysis.* Spine, 2003. **28**(23): p. 2570-6.

17. Bogduk, N., W. Tynan, and A.S. Wilson, *The nerve supply to the human lumbar intervertebral discs.* J Anat, 1981. **132**(Pt 1): p. 39-56.

18. Ahmed, M., et al., *Neuropeptide Y, tyrosine hydroxylase and vasoactive intestinal polypeptide-immunoreactive nerve fibers in the vertebral bodies, discs, dura mater, and spinal ligaments of the rat lumbar spine.* Spine, 1993. **18**(2): p. 268-73.

19. Boos, N., et al., *Classification of age-related changes in lumbar intervertebral discs: 2002 Volvo Award in basic science.* Spine, 2002. **27**(23): p. 2631-44.

20. Edelson, J.G. and H. Nathan, *Stages in the natural history of the vertebral end-plates.* Spine, 1988. **13**(1): p. 21-6.

21. Miller, J.A., C. Schmatz, and A.B. Schultz, *Lumbar disc degeneration: correlation with age, sex, and spine level in 600 autopsy specimens.* Spine, 1988. **13**(2): p. 173-8.

22. Buckwalter, J.A., *Aging and degeneration of the human intervertebral disc.* Spine, 1995. **20**(11): p. 1307-14.

23. Roberts, S., et al., *Histology and pathology of the human intervertebral disc.* J Bone Joint Surg Am, 2006. **88 Suppl 2**: p. 10-4.

24. Ishihara, H. and J.P. Urban, *Effects of low oxygen concentrations and metabolic inhibitors on proteoglycan and protein synthesis rates in the intervertebral disc.* J Orthop Res, 1999. **17**(6): p. 829-35.

25. Martin, M.D., C.M. Boxell, and D.G. Malone, *Pathophysiology of lumbar disc degeneration: a review of the literature.* Neurosurg Focus, 2002. **13**(2): p. E1.

26. Haefeli, M., et al., *The course of macroscopic degeneration in the human lumbar intervertebral disc.* Spine, 2006. **31**(14): p. 1522-31.

27. Bernick, S., J.M. Walker, and W.J. Paule, *Age changes to the anulus fibrosus in human intervertebral discs.* Spine, 1991. **16**(5): p. 520-4.

28. Umehara, S., et al., *Effects of degeneration on the elastic modulus distribution in the lumbar intervertebral disc.* Spine, 1996. **21**(7): p. 811-9; discussion 820.

29. Mimura, M., et al., *Disc degeneration affects the multidirectional flexibility of the lumbar spine.* Spine, 1994. **19**(12): p. 1371-80.

30. Lotz, J.C., et al., *Mechanobiology in intervertebral disc degeneration and regeneration.* Conf Proc IEEE Eng Med Biol Soc, 2004. **7**: p. 5459.

31. Handa, T., et al., *Effects of hydrostatic pressure on matrix synthesis and matrix metalloproteinase production in the human lumbar intervertebral disc.* Spine, 1997. **22**(10): p. 1085-91.

32. Ishihara, H., et al., *Effects of hydrostatic pressure on matrix synthesis in different regions of the intervertebral disk.* J Appl Physiol, 1996. **80**(3): p. 839-46.

33. Neidlinger-Wilke, C., et al., *Regulation of gene expression in intervertebral disc cells by low and high hydrostatic pressure.* Eur Spine J, 2006. **15 Suppl 3**: p. S372-8.

34. Takahashi, I., et al., *Compressive force promotes sox9, type II collagen and aggrecan and inhibits IL-1beta expression resulting in chondrogenesis in mouse embryonic limb bud mesenchymal cells.* J Cell Sci, 1998. **111 (Pt 14)**: p. 2067-76.

35. Liu, G.Z., et al., *Nitric oxide mediates the change of proteoglycan synthesis in the human lumbar intervertebral disc in response to hydrostatic pressure.* Spine, 2001. **26**(2): p. 134-41.

36. Adams, M.A., et al., *Mechanical initiation of intervertebral disc degeneration.* Spine, 2000. **25**(13): p. 1625-36.

37. Pelletier, J.P., et al., *Cytokines and inflammation in cartilage degradation.* Rheum Dis Clin North Am, 1993. **19**(3): p. 545-68.

38. Murata, Y., et al., *Distribution and appearance of tumor necrosis factor-alpha in the dorsal root ganglion exposed to experimental disc herniation in rats.* Spine, 2004. **29**(20): p. 2235-41.

39. Kang, J.D., et al., *Herniated lumbar intervertebral discs spontaneously produce matrix metalloproteinases, nitric oxide, interleukin-6, and prostaglandin E2.* Spine, 1996. **21**(3): p. 271-7.

40. Weiler, C., et al., *Expression and distribution of tumor necrosis factor alpha in human lumbar intervertebral discs: a study in surgical specimen and autopsy controls.* Spine, 2005. **30**(1): p. 44-53; discussion 54.

41. Takahashi, H., et al., *Inflammatory cytokines in the herniated disc of the lumbar spine.* Spine, 1996. **21**(2): p. 218-24.

42. Specchia, N., et al., *Cytokines and growth factors in the protruded intervertebral disc of the lumbar spine.* Eur Spine J, 2002. **11**(2): p. 145-51.

43. Le Maitre, C.L., A.J. Freemont, and J.A. Hoyland, *The role of interleukin-1 in the pathogenesis of human intervertebral disc degeneration.* Arthritis Res Ther, 2005. **7**(4): p. R732-45.

44. Ahn, S.H., et al., *mRNA expression of cytokines and chemokines in herniated lumbar intervertebral discs.* Spine, 2002. **27**(9): p. 911-7.

45. Olmarker, K. and K. Larsson, *Tumor necrosis factor alpha and nucleus-pulposus-induced nerve root injury.* Spine, 1998. **23**(23): p. 2538-44.

46. Miyamoto, H., et al., *The role of cyclooxygenase-2 and inflammatory cytokines in pain induction of herniated lumbar intervertebral disc.* Kobe J Med Sci, 2000. **46**(1-2): p. 13-28.

47. Burke, J.G., et al., *Spontaneous production of monocyte chemoattractant protein-1 and interleukin-8 by the human lumbar intervertebral disc.* Spine, 2002. **27**(13): p. 1402-7.

48. Studer, R.K., et al., *p38 MAPK inhibition in nucleus pulposus cells: a potential target for treating intervertebral disc degeneration.* Spine, 2007. **32**(25): p. 2827-33.

49. Grang, L., et al., *Intervertebral disk degeneration and herniation: the role of metalloproteinases and cytokines.* Joint Bone Spine, 2001. **68**(6): p. 547-53.

50. Goldring, M.B. and F. Berenbaum, *The regulation of chondrocyte function by proinflammatory mediators: prostaglandins and nitric oxide.* Clin Orthop Relat Res, 2004(427 Suppl): p. S37-46.

51. Adams, M.A. and W.C. Hutton, *The effect of fatigue on the lumbar intervertebral disc.* J Bone Joint Surg Br, 1983. **65**(2): p. 199-203.

52. Lotz, J.C., et al., *Compression-induced degeneration of the intervertebral disc: an in vivo mouse model and finite-element study.* Spine, 1998. **23**(23): p. 2493-506.

53. Maclean, J.J., et al., *Anabolic and catabolic mRNA levels of the intervertebral disc vary with the magnitude and frequency of in vivo dynamic compression.* J Orthop Res, 2004. **22**(6): p. 1193-200.

54. Chen, J., W. Yan, and L.A. Setton, *Static compression induces zonal-specific changes in gene expression for extracellular matrix and cytoskeletal proteins in intervertebral disc cells in vitro.* Matrix Biol, 2004. **22**(7): p. 573-83.

55. Shinmei, M., et al., *Interleukin 1, tumor necrosis factor, and interleukin 6 as mediators of cartilage destruction.* Semin Arthritis Rheum, 1989. **18**(3 Suppl 1): p. 27-32.

56. Fujita, K., et al., *Neutral proteinases in human intervertebral disc. Role in degeneration and probable origin.* Spine, 1993. **18**(13): p. 1766-73.

57. Benneker, L.M., et al., *2004 Young Investigator Award Winner: vertebral endplate marrow contact channel occlusions and intervertebral disc degeneration.* Spine, 2005. **30**(2): p. 167-73.

58. Holm, S., et al., *Experimental disc degeneration due to endplate injury.* J Spinal Disord Tech, 2004. **17**(1): p. 64-71.

59. Cinotti, G., et al., *Degenerative changes of porcine intervertebral disc induced by vertebral endplate injuries.* Spine, 2005. **30**(2): p. 174-80.

60. Boden, S.D., et al., *Abnormal magnetic-resonance scans of the cervical spine in asymptomatic subjects. A prospective investigation.* J Bone Joint Surg Am, 1990. **72**(8): p. 1178-84.

61. Jensen, M.C., et al., *Magnetic resonance imaging of the lumbar spine in people without back pain.* N Engl J Med, 1994. **331**(2): p. 69-73.

62. Suarez-Almazor, M.E., et al., *Use of lumbar radiographs for the early diagnosis of low back pain. Proposed guidelines would increase utilization.* Jama, 1997. **277**(22): p. 1782-6.

63. Vanharanta, H., et al., *The relationship of pain provocation to lumbar disc deterioration as seen by CT/discography.* Spine, 1987. **12**(3): p. 295-8.

64. Palmgren, T., et al., *An immunohistochemical study of nerve structures in the anulus fibrosus of human normal lumbar intervertebral discs.* Spine, 1999. **24**(20): p. 2075-9.

65. Cavanaugh, J.M., *Neural mechanisms of lumbar pain.* Spine, 1995. **20**(16): p. 1804-9.

66. Freemont, A.J., et al., *Nerve growth factor expression and innervation of the painful intervertebral disc.* J Pathol, 2002. **197**(3): p. 286-92.

67. Johnson, W.E., et al., *Human intervertebral disc aggrecan inhibits nerve growth in vitro.* Arthritis Rheum, 2002. **46**(10): p. 2658-64.

68. Miller, R.J., et al., *C-reactive protein and interleukin 6 receptor in post-traumatic stress disorder: a pilot study.* Cytokine, 2001. **13**(4): p. 253-5.

69. Burke, J.G., et al., *Intervertebral discs which cause low back pain secrete high levels of proinflammatory mediators.* J Bone Joint Surg Br, 2002. **84**(2): p. 196-201.

70. Kawaguchi, S., et al., *Chemokine profile of herniated intervertebral discs infiltrated with monocytes and macrophages.* Spine, 2002. **27**(14): p. 1511-6.

71. Woertgen, C., R.D. Rothoerl, and A. Brawanski, *Influence of macrophage infiltration of herniated lumbar disc tissue on outcome after lumbar disc surgery.* Spine, 2000. **25**(7): p. 871-5.

72. Coppes, M.H., et al., *Innervation of "painful" lumbar discs.* Spine, 1997. **22**(20): p. 2342-9; discussion 2349-50.

73. Moneta, G.B., et al., *Reported pain during lumbar discography as a function of anular ruptures and disc degeneration. A re-analysis of 833 discograms.* Spine, 1994. **19**(17): p. 1968-74.

74. Buirski, G. and M. Silberstein, *The symptomatic lumbar disc in patients with low-back pain. Magnetic resonance imaging appearances in both a symptomatic and control population.* Spine, 1993. **18**(13): p. 1808-11.

75. Walker, B.F., *The prevalence of low back pain: a systematic review of the literature from 1966 to 1998.* J Spinal Disord, 2000. **13**(3): p. 205-17.

76. Ehrlich, G.E., *Low back pain.* Bull World Health Organ, 2003. **81**(9): p. 671-6.

77. Deyo, R.A. and Y.J. Tsui-Wu, *Descriptive epidemiology of low-back pain and its related medical care in the United States.* Spine, 1987. **12**(3): p. 264-8.

78. Andersson, G.B., *Epidemiological features of chronic low-back pain.* Lancet, 1999. **354**(9178): p. 581-5.

79. Nelemans, P.J., et al., *Injection therapy for subacute and chronic benign low back pain.* Spine, 2001. **26**(5): p. 501-15.

80. Fritzell, P., et al., *2001 Volvo Award Winner in Clinical Studies: Lumbar fusion versus nonsurgical treatment for chronic low back pain: a multicenter randomized controlled trial from the Swedish Lumbar Spine Study Group.* Spine, 2001. **26**(23): p. 2521-32; discussion 2532-4.

81. Fairbank, J., et al., *Randomised controlled trial to compare surgical stabilisation of the lumbar spine with an intensive rehabilitation programme for patients with chronic low back pain: the MRC spine stabilisation trial.* Bmj, 2005. **330**(7502): p. 1233.

82. Levin, D.A., J.J. Hale, and J.A. Bendo, *Adjacent segment degeneration following spinal fusion for degenerative disc disease.* Bull NYU Hosp Jt Dis, 2007. **65**(1): p. 29-36.

83. Blumenthal, S., et al., *A prospective, randomized, multicenter Food and Drug Administration investigational device exemptions study of lumbar total disc replacement with the CHARITE artificial disc versus lumbar fusion: part I: evaluation of clinical outcomes.* Spine, 2005. **30**(14): p. 1565-75; discussion E387-91.

84. Bertagnoli, R., et al., *The treatment of disabling multilevel lumbar discogenic low back pain with total disc arthroplasty utilizing the ProDisc prosthesis: a prospective study with 2-year minimum follow-up.* Spine, 2005. **30**(19): p. 2192-9.

85. Di Martino, A., et al., *Nucleus pulposus replacement: basic science and indications for clinical use.* Spine, 2005. **30**(16 Suppl): p. S16-22.

86. Meisel, H.J., et al., *Clinical experience in cell-based therapeutics: disc chondrocyte transplantation A treatment for degenerated or damaged intervertebral disc.* Biomol Eng, 2007. **24**(1): p. 5-21.

87. Ganey, T., et al., *Disc chondrocyte transplantation in a canine model: a treatment for degenerated or damaged intervertebral disc.* Spine, 2003. **28**(23): p. 2609-20.

88. Gorensek, M., et al., *Nucleus pulposus repair with cultured autologous elastic cartilage derived chondrocytes.* Cell Mol Biol Lett, 2004. **9**(2): p. 363-73.

89. Okuma, M., et al., *Reinsertion of stimulated nucleus pulposus cells retards intervertebral disc degeneration: an in vitro and in vivo experimental study.* J Orthop Res, 2000. **18**(6): p. 988-97.

90. Watanabe, K., et al., *Effect of reinsertion of activated nucleus pulposus on disc degeneration: an experimental study on various types of collagen in degenerative discs.* Connect Tissue Res, 2003. **44**(2): p. 104-8.

91. Sharma, B. and J.H. Elisseeff, *Engineering structurally organized cartilage and bone tissues.* Ann Biomed Eng, 2004. **32**(1): p. 148-59.

92. Nomura, T., et al., *Nucleus pulposus allograft retards intervertebral disc degeneration.* Clin Orthop Relat Res, 2001(389): p. 94-101.

93. Le Maitre, C.L., A.J. Freemont, and J.A. Hoyland, *Accelerated cellular senescence in degenerate intervertebral discs: a possible role in the pathogenesis of intervertebral disc degeneration.* Arthritis Res Ther, 2007. **9**(3): p. R45.

94. Heathfield, S.K., C.L. Le Maitre, and J.A. Hoyland, *Caveolin-1 expression and stress-induced premature senescence in human intervertebral disc degeneration.* Arthritis Res Ther, 2008. **10**(4): p. R87.

95. Bianco, P. and P.G. Robey, *Stem cells in tissue engineering.* Nature, 2001. **414**(6859): p. 118-21.

96. Pittenger, M.F., J.D. Mosca, and K.R. McIntosh, *Human mesenchymal stem cells: progenitor cells for cartilage, bone, fat and stroma.* Curr Top Microbiol Immunol, 2000. **251**: p. 3-11.

97. Eridani, S., *Stem cells for all seasons? Experimental and clinical issues.* J R Soc Med, 2002. **95**(1): p. 5-8.

98. Prockop, D.J., *Marrow stromal cells as stem cells for nonhematopoietic tissues.* Science, 1997. **276**(5309): p. 71-4.

99. Mauney, J.R., V. Volloch, and D.L. Kaplan, *Role of adult mesenchymal stem cells in bone tissue engineering applications: current status and future prospects.* Tissue Eng, 2005. **11**(5-6): p. 787-802.

100. Caplan, A.I., et al., *Principles of cartilage repair and regeneration.* Clin Orthop Relat Res, 1997(342): p. 254-69.

101. Barry, F., et al., *Chondrogenic differentiation of mesenchymal stem cells from bone marrow: differentiation-dependent gene expression of matrix components.* Exp Cell Res, 2001. **268**(2): p. 189-200.

102. Steck, E., et al., *Induction of intervertebral disc-like cells from adult mesenchymal stem cells.* Stem Cells, 2005. **23**(3): p. 403-11.

103. Rajpurohit, R., et al., *Phenotypic characteristics of the nucleus pulposus: expression of hypoxia inducing factor-1, glucose transporter-1 and MMP-2.* Cell Tissue Res, 2002. **308**(3): p. 401-7.

104. Lee, C.R., et al., *A phenotypic comparison of intervertebral disc and articular cartilage cells in the rat.* Eur Spine J, 2007. **16**(12): p. 2174-85.

105. Freed, L.E., I. Martin, and G. Vunjak-Novakovic, *Frontiers in tissue engineering. In vitro modulation of chondrogenesis.* Clin Orthop Relat Res, 1999(367 Suppl): p. S46-58.

106. Mauck, R.L., et al., *Functional tissue engineering of articular cartilage through dynamic loading of chondrocyte-seeded agarose gels.* J Biomech Eng, 2000. **122**(3): p. 252-60.

107. Le Blanc, K., et al., *HLA expression and immunologic properties of differentiated and undifferentiated mesenchymal stem cells.* Exp Hematol, 2003. **31**(10): p. 890-6.

108. Traggiai, E., et al., *Bone marrow-derived mesenchymal stem cells induce both polyclonal expansion and differentiation of B cells isolated from healthy donors and systemic lupus erythematosus patients.* Stem Cells, 2008. **26**(2): p. 562-9.

109. Spaggiari, G.M., et al., *Mesenchymal stem cell-natural killer cell interactions: evidence that activated NK cells are capable of killing MSCs, whereas MSCs can inhibit IL-2-induced NK-cell proliferation.* Blood, 2006. **107**(4): p. 1484-90.

110. Bartholomew, A., et al., *Mesenchymal stem cells suppress lymphocyte proliferation in vitro and prolong skin graft survival in vivo.* Exp Hematol, 2002. **30**(1): p. 42-8.

111. Jones, S., et al., *The antiproliferative effect of mesenchymal stem cells is a fundamental property shared by all stromal cells.* J Immunol, 2007. **179**(5): p. 2824-31.

112. Glennie, S., et al., *Bone marrow mesenchymal stem cells induce division arrest anergy of activated T cells.* Blood, 2005. **105**(7): p. 2821-7.

113. Liu, H., et al., *The immunogenicity and immunomodulatory function of osteogenic cells differentiated from mesenchymal stem cells.* J Immunol, 2006. **176**(5): p. 2864-71.

114. Sato, K., et al., *Nitric oxide plays a critical role in suppression of T-cell proliferation by mesenchymal stem cells.* Blood, 2007. **109**(1): p. 228-34.

115. Ren, G., et al., *Mesenchymal stem cell-mediated immunosuppression occurs via concerted action of chemokines and nitric oxide.* Cell Stem Cell, 2008. **2**(2): p. 141-50.

116. Yamamoto, Y., et al., *Upregulation of the viability of nucleus pulposus cells by bone marrow-derived stromal cells: significance of direct cell-to-cell contact in coculture system.* Spine, 2004. **29**(14): p. 1508-14.

117. Caplan, A.I. and J.E. Dennis, *Mesenchymal stem cells as trophic mediators.* J Cell Biochem, 2006. **98**(5): p. 1076-84.

118. Turner, J.A., et al., *Patient outcomes after lumbar spinal fusions.* Jama, 1992. **268**(7): p. 907-11.

119. Gruber, H.E., et al., *Autologous intervertebral disc cell implantation: a model using Psammomys obesus, the sand rat.* Spine, 2002. **27**(15): p. 1626-33.

120. Zhang, Y., et al., *Cell therapy using articular chondrocytes overexpressing BMP-7 or BMP-10 in a rabbit disc organ culture model.* Spine, 2008. **33**(8): p. 831-8.

121. Xu, J., et al., *Chondrogenic differentiation of human mesenchymal stem cells in three-dimensional alginate gels.* Tissue Eng Part A, 2008. **14**(5): p. 667-80.

122. Kim, P.K. and C.L. Branch, Jr., *The lumbar degenerative disc: confusion, mechanics, management.* Clin Neurosurg, 2006. **53**: p. 18-25.

123. Marcacci, M., et al., *Arthroscopic second generation autologous chondrocyte implantation.* Knee Surg Sports Traumatol Arthrosc, 2007. **15**(5): p. 610-9.

124. Adkisson, H.D., et al., *In vitro generation of scaffold independent neocartilage.* Clin Orthop Relat Res, 2001(391 Suppl): p. S280-94.

125. Nochi, H., et al. *Chondrocytes fail to induce allogenic T-lymphocyte proliferation in presence of inflammatory cytokines*. in *Transactions of the 50th Orthopaedic Research Society* 2004. San Francisco, CA.

126. Latorre, A., et al., *Experimental model of multidirectional disc hernia in rats.* Int Orthop, 1998. **22**(1): p. 44-8.

127. He, X.H., L.H. Xu, and Y. Liu, *Procedure for preparing peptide-major histocompatibility complex tetramers for direct quantification of antigen-specific cytotoxic T lymphocytes.* World J Gastroenterol, 2005. **11**(27): p. 4180-7.

128. Kim, A.J., et al. *Juvenile chondrocytes may facilitate disc repair*. in *Transactions of the 53rd Orthopaedic Research Society*. 2007. San Diego, CA.

129. Hidaka, C., et al., *Acceleration of cartilage repair by genetically modified chondrocytes over expressing bone morphogenetic protein-7.* J Orthop Res, 2003. **21**(4): p. 573-83.

130. Jin, E.J., et al., *BMP-2-enhanced chondrogenesis involves p38 MAPK-mediated down-regulation of Wnt-7a pathway.* Mol Cells, 2006. **22**(3): p. 353-9.

131. Estes, B.T., A.W. Wu, and F. Guilak, *Potent induction of chondrocytic differentiation of human adipose-derived adult stem cells by bone morphogenetic protein 6.* Arthritis Rheum, 2006. **54**(4): p. 1222-32.

132. Zhang, Y., et al., *Transduced bovine articular chondrocytes affect the metabolism of cocultured nucleus pulposus cells in vitro: implications for chondrocyte transplantation into the intervertebral disc.* Spine, 2005. **30**(23): p. 2601-7.

133. Antoniou, J., et al., *The human lumbar intervertebral disc: evidence for changes in the biosynthesis and denaturation of the extracellular matrix with growth, maturation, ageing, and degeneration.* J Clin Invest, 1996. **98**(4): p. 996-1003.

134. Ohshima, H. and J.P. Urban, *The effect of lactate and pH on proteoglycan and protein synthesis rates in the intervertebral disc.* Spine, 1992. **17**(9): p. 1079-82.

135. Le Visage, C., et al., *Interaction of human mesenchymal stem cells with disc cells: changes in extracellular matrix biosynthesis.* Spine, 2006. **31**(18): p. 2036-42.

136. Richardson, S.M., et al., *Intervertebral disc cell-mediated mesenchymal stem cell differentiation.* Stem Cells, 2006. **24**(3): p. 707-16.

137. Buschmann, M.D., et al., *Mechanical compression modulates matrix biosynthesis in chondrocyte/agarose culture.* J Cell Sci, 1995. **108 (Pt 4)**: p. 1497-508.

138. Mauck, R.L., X. Yuan, and R.S. Tuan, *Chondrogenic differentiation and functional maturation of bovine mesenchymal stem cells in long-term agarose culture.* Osteoarthritis Cartilage, 2006. **14**(2): p. 179-89.

139. Mohamed-Ali, H., *Influence of interleukin-1 beta, tumour necrosis factor alpha and prostaglandin E2 on chondrogenesis and cartilage matrix breakdown in vitro.* Rheumatol Int, 1995. **14**(5): p. 191-9.

140. Murakami, S., V. Lefebvre, and B. de Crombrugghe, *Potent inhibition of the master chondrogenic factor Sox9 gene by interleukin-1 and tumor necrosis factor-alpha.* J Biol Chem, 2000. **275**(5): p. 3687-92.

141. Roman-Blas, J.A., D.G. Stokes, and S.A. Jimenez, *Modulation of TGF-beta signaling by proinflammatory cytokines in articular chondrocytes.* Osteoarthritis Cartilage, 2007. **15**(12): p. 1367-77.

142. Malladi, P., et al., *Effect of reduced oxygen tension on chondrogenesis and osteogenesis in adipose-derived mesenchymal cells.* Am J Physiol Cell Physiol, 2006. **290**(4): p. C1139-46.

143. Scherer, K., et al., *The influence of oxygen and hydrostatic pressure on articular chondrocytes and adherent bone marrow cells in vitro.* Biorheology, 2004. **41**(3-4): p. 323-33.

144. Johnstone, B., et al., *In vitro chondrogenesis of bone marrow-derived mesenchymal progenitor cells.* Exp Cell Res, 1998. **238**(1): p. 265-72.

145. Majumdar, M.K., E. Wang, and E.A. Morris, *BMP-2 and BMP-9 promotes chondrogenic differentiation of human multipotential mesenchymal cells and overcomes the inhibitory effect of IL-1.* J Cell Physiol, 2001. **189**(3): p. 275-84.

146. Bartels, E.M., et al., *Oxygen and lactate concentrations measured in vivo in the intervertebral discs of patients with scoliosis and back pain.* Spine, 1998. **23**(1): p. 1-7; discussion 8.

147. Risbud, M.V., et al., *Differentiation of mesenchymal stem cells towards a nucleus pulposus-like phenotype in vitro: implications for cell-based transplantation therapy.* Spine, 2004. **29**(23): p. 2627-32.

148. Kanichai, M., et al., *Hypoxia promotes chondrogenesis in rat mesenchymal stem cells: a role for AKT and hypoxia-inducible factor (HIF)-1alpha.* J Cell Physiol, 2008. **216**(3): p. 708-15.

149. Pilgaard, L., et al., *Transcriptional signature of human adipose tissue-derived stem cells (hASCs) preconditioned for chondrogenesis in hypoxic conditions.* Exp Cell Res, 2009.

150. Holm, S. and A. Nachemson, *Variations in the nutrition of the canine intervertebral disc induced by motion.* Spine, 1983. **8**(8): p. 866-74.

151. Miyanishi, K., et al., *Dose- and time-dependent effects of cyclic hydrostatic pressure on transforming growth factor-beta3-induced chondrogenesis by adult human mesenchymal stem cells in vitro.* Tissue Eng, 2006. **12**(8): p. 2253-62.

152. Wagner, D.R., et al., *Hydrostatic pressure enhances chondrogenic differentiation of human bone marrow stromal cells in osteochondrogenic medium.* Ann Biomed Eng, 2008. **36**(5): p. 813-20.

153. Sakai, D., et al., *Differentiation of mesenchymal stem cells transplanted to a rabbit degenerative disc model: potential and limitations for stem cell therapy in disc regeneration.* Spine, 2005. **30**(21): p. 2379-87.

154. Vadala, G., et al., *Coculture of bone marrow mesenchymal stem cells and nucleus pulposus cells modulate gene expression profile without cell fusion.* Spine, 2008. **33**(8): p. 870-6.

155. Sekiya, I., et al., *In vitro cartilage formation by human adult stem cells from bone marrow stroma defines the sequence of cellular and molecular events during chondrogenesis.* Proc Natl Acad Sci U S A, 2002. **99**(7): p. 4397-402.

156. Akiyama, H., et al., *The transcription factor Sox9 has essential roles in successive steps of the chondrocyte differentiation pathway and is required for expression of Sox5 and Sox6.* Genes Dev, 2002. **16**(21): p. 2813-28.

157. Schipani, E., et al., *Hypoxia in cartilage: HIF-1alpha is essential for chondrocyte growth arrest and survival.* Genes Dev, 2001. **15**(21): p. 2865-76.

158. Pfander, D., et al., *HIF-1alpha controls extracellular matrix synthesis by epiphyseal chondrocytes.* J Cell Sci, 2003. **116**(Pt 9): p. 1819-26.

159. Amarilio, R., et al., *HIF1alpha regulation of Sox9 is necessary to maintain differentiation of hypoxic prechondrogenic cells during early skeletogenesis.* Development, 2007. **134**(21): p. 3917-28.

160. Agrawal, A., et al., *Normoxic stabilization of HIF-1alpha drives glycolytic metabolism and regulates aggrecan gene expression in nucleus pulposus cells of the rat intervertebral disk.* Am J Physiol Cell Physiol, 2007. **293**(2): p. C621-31.

161. Risbud, M.V., et al., *Nucleus pulposus cells express HIF-1alpha under normoxic culture conditions: a metabolic adaptation to the intervertebral disc microenvironment.* J Cell Biochem, 2006. **98**(1): p. 152-9.

162. Mwale, F., et al., *Limitations of using aggrecan and type X collagen as markers of chondrogenesis in mesenchymal stem cell differentiation.* J Orthop Res, 2006. **24**(8): p. 1791-8.

163. Pelttari, K., et al., *Premature induction of hypertrophy during in vitro chondrogenesis of human mesenchymal stem cells correlates with calcification and vascular invasion after ectopic transplantation in SCID mice.* Arthritis Rheum, 2006. **54**(10): p. 3254-66.

164. Grassel, S. and N. Ahmed, *Influence of cellular microenvironment and paracrine signals on chondrogenic differentiation.* Front Biosci, 2007. **12**: p. 4946-56.

165. Richardson, S.M., et al., *Intervertebral disc biology, degeneration and novel tissue engineering and regenerative medicine therapies.* Histol Histopathol, 2007. **22**(9): p. 1033-41.

166. Shen, B., et al., *BMP-2 Enhances TGF-beta3-Mediated Chondrogenic Differentiation of Human Bone Marrow Multipotent Mesenchymal Stromal Cells in Alginate Bead Culture.* Tissue Eng Part A, 2008.

167. Sakai, D., et al., *Regenerative effects of transplanting mesenchymal stem cells embedded in atelocollagen to the degenerated intervertebral disc.* Biomaterials, 2006. **27**(3): p. 335-45.

168. Zuscik, M.J., et al., *Regulation of chondrogenesis and chondrocyte differentiation by stress.* J Clin Invest, 2008. **118**(2): p. 429-38.

169. Angele, P., et al., *Cyclic, mechanical compression enhances chondrogenesis of mesenchymal progenitor cells in tissue engineering scaffolds.* Biorheology, 2004. **41**(3-4): p. 335-46.

170. Bibby, S.R., et al., *Metabolism of the intervertebral disc: effects of low levels of oxygen, glucose, and pH on rates of energy metabolism of bovine nucleus pulposus cells.* Spine, 2005. **30**(5): p. 487-96.

171. Masuda, K., et al., *A novel two-step method for the formation of tissue-engineered cartilage by mature bovine chondrocytes: the alginate-recovered-chondrocyte (ARC) method.* J Orthop Res, 2003. **21**(1): p. 139-48.

172. Ikenoue, T., et al., *Mechanoregulation of human articular chondrocyte aggrecan and type II collagen expression by intermittent hydrostatic pressure in vitro.* J Orthop Res, 2003. **21**(1): p. 110-6.

173. An, H., et al., *Summary statement: emerging techniques for treatment of degenerative lumbar disc disease.* Spine, 2003. **28**(15 Suppl): p. S24-5.

174. Phillips, F.M., J. Reuben, and F.T. Wetzel, *Intervertebral disc degeneration adjacent to a lumbar fusion. An experimental rabbit model.* J Bone Joint Surg Br, 2002. **84**(2): p. 289-94.

175. Takegami, K., et al., *Osteogenic protein-1 enhances matrix replenishment by intervertebral disc cells previously exposed to interleukin-1.* Spine, 2002. **27**(12): p. 1318-25.

176. Shen, B., et al., *Induction of matrix metalloproteinase-2 and -3 activity in ovine nucleus pulposus cells grown in three-dimensional agarose gel culture by interleukin-1beta: a potential pathway of disc degeneration.* Eur Spine J, 2003. **12**(1): p. 66-75.

177. Seguin, C.A., et al., *Tumor necrosis factor-alpha modulates matrix production and catabolism in nucleus pulposus tissue.* Spine, 2005. **30**(17): p. 1940-8.

178. Abe, Y., et al., *Proinflammatory cytokines stimulate the expression of nerve growth factor by human intervertebral disc cells.* Spine, 2007. **32**(6): p. 635-42.

179. Neidlinger-Wilke, C., et al., *Mechanical stimulation alters pleiotrophin and aggrecan expression by human intervertebral disc cells and influences their capacity to stimulate endothelial migration.* Spine, 2009. **34**(7): p. 663-9.

180. Hellwig-Burgel, T., et al., *Interleukin-1beta and tumor necrosis factor-alpha stimulate DNA binding of hypoxia-inducible factor-1.* Blood, 1999. **94**(5): p. 1561-7.

181. Wehling, N., et al., *Interleukin-1beta and tumor necrosis factor alpha inhibit chondrogenesis by human mesenchymal stem cells through NF-kappaB-dependent pathways.* Arthritis Rheum, 2009. **60**(3): p. 801-12.

182. Potier, E., et al., *Prolonged hypoxia concomitant with serum deprivation induces massive human mesenchymal stem cell death.* Tissue Eng, 2007. **13**(6): p. 1325-31.

183. Wuertz, K., et al., *Behavior of mesenchymal stem cells in the chemical microenvironment of the intervertebral disc.* Spine, 2008. **33**(17): p. 1843-9.

184. Early, S.B., et al., *Hypoxia stimulates inflammatory and fibrotic responses from nasal-polyp derived fibroblasts.* Laryngoscope, 2007. **117**(3): p. 511-5.

185. Westra, J., et al., *Regulation of cytokine-induced HIF-1alpha expression in rheumatoid synovial fibroblasts.* Ann N Y Acad Sci, 2007. **1108**: p. 340-8.

186. Ahn, J.K., et al., *Role of hypoxia-inducible factor-1alpha in hypoxia-induced expressions of IL-8, MMP-1 and MMP-3 in rheumatoid fibroblast-like synoviocytes.* Rheumatology (Oxford), 2008. **47**(6): p. 834-9.

187. Fan, V.H., et al., *Tethered epidermal growth factor provides a survival advantage to mesenchymal stem cells.* Stem Cells, 2007. **25**(5): p. 1241-51.

188. Aigner, T., et al., *Variation with age in the pattern of type X collagen expression in normal and scoliotic human intervertebral discs*. Calcif Tissue Int, 1998. **63**(3): p. 263-8.

189. Roberts, S., et al., *Type X collagen in the human invertebral disc: an indication of repair or remodelling?* Histochem J, 1998. **30**(2): p. 89-95.

190. Bonnet, C.S. and D.A. Walsh, *Osteoarthritis, angiogenesis and inflammation.* Rheumatology (Oxford), 2005. **44**(1): p. 7-16.

191. De Luca, F., *Impaired growth plate chondrogenesis in children with chronic illnesses.* Pediatr Res, 2006. **59**(5): p. 625-9.

192. Brown, M.F., et al., *Sensory and sympathetic innervation of the vertebral endplate in patients with degenerative disc disease.* J Bone Joint Surg Br, 1997. **79**(1): p. 147-53.

193. Freemont, A.J., et al., *Nerve ingrowth into diseased intervertebral disc in chronic back pain.* Lancet, 1997. **350**(9072): p. 178-81.

194. Keshari, K.R., et al., *Lactic acid and proteoglycans as metabolic markers for discogenic back pain.* Spine, 2008. **33**(3): p. 312-7.

195. Solchaga, L.A., V.M. Goldberg, and A.I. Caplan, *Cartilage regeneration using principles of tissue engineering.* Clin Orthop Relat Res, 2001(391 Suppl): p. S161-70.

196. Niu, C.C., et al., *Mesenchymal Stem Cell and Nucleus Pulposus Cell Coculture Modulates Cell Profile.* Clin Orthop Relat Res, 2008.

197. Trout, J.J., J.A. Buckwalter, and K.C. Moore, *Ultrastructure of the human intervertebral disc: II. Cells of the nucleus pulposus.* Anat Rec, 1982. **204**(4): p. 307-14.

198. Trout, J.J., et al., *Ultrastructure of the human intervertebral disc. I. Changes in notochordal cells with age.* Tissue Cell, 1982. **14**(2): p. 359-69.

199. Aguiar, D.J., S.L. Johnson, and T.R. Oegema, *Notochordal cells interact with nucleus pulposus cells: regulation of proteoglycan synthesis.* Exp Cell Res, 1999. **246**(1): p. 129-37.

200. Hunter, C.J., J.R. Matyas, and N.A. Duncan, *The notochordal cell in the nucleus pulposus: a review in the context of tissue engineering.* Tissue Eng, 2003. **9**(4): p. 667-77.

201. Stevens, J.W., et al., *CD44 expression in the developing and growing rat intervertebral disc.* Dev Dyn, 2000. **219**(3): p. 381-90.

202. Gotz, W., et al., *Detection and distribution of the carbohydrate binding protein galectin-3 in human notochord, intervertebral disc and chordoma.* Differentiation, 1997. **62**(3): p. 149-57.

203. Maiorano, E., et al., *Expression of intermediate filaments in chordomas. An immunocytochemical study of five cases.* Pathol Res Pract, 1992. **188**(7): p. 901-7.

204. Persson, S., L.G. Kindblom, and L. Angervall, *Classical and chondroid chordoma. A light-microscopic, histochemical, ultrastructural and immunohistochemical analysis of the various cell types.* Pathol Res Pract, 1991. **187**(7): p. 828-38.

205. Richardson, S.M. and J.A. Hoyland, *Stem cell regeneration of degenerated intervertebral discs: current status.* Curr Pain Headache Rep, 2008. **12**(2): p. 83-8.

206. O'Halloran, D.M. and A.S. Pandit, *Tissue-engineering approach to regenerating the intervertebral disc.* Tissue Eng, 2007. **13**(8): p. 1927-54.

207. Chiba, K., et al., *Metabolism of the extracellular matrix formed by intervertebral disc cells cultured in alginate.* Spine, 1997. **22**(24): p. 2885-93.

208. Baer, A.E., et al., *Collagen gene expression and mechanical properties of intervertebral disc cell-alginate cultures.* J Orthop Res, 2001. **19**(1): p. 2-10.

209. Le Visage, C., et al., *Small intestinal submucosa as a potential bioscaffold for intervertebral disc regeneration.* Spine, 2006. **31**(21): p. 2423-30; discussion 2431.

210. Gruber, H.E., et al., *Cell shape and gene expression in human intervertebral disc cells: in vitro tissue engineering studies.* Biotech Histochem, 2003. **78**(2): p. 109-17.

211. Nesti, L.J., et al., *Intervertebral disc tissue engineering using a novel hyaluronic acid-nanofibrous scaffold (HANFS) amalgam.* Tissue Eng Part A, 2008. **14**(9): p. 1527-37.

212. Crevensten, G., et al., *Intervertebral disc cell therapy for regeneration: mesenchymal stem cell implantation in rat intervertebral discs.* Ann Biomed Eng, 2004. **32**(3): p. 430-4.

213. Wilke, H.J., et al., *New in vivo measurements of pressures in the intervertebral disc in daily life.* Spine, 1999. **24**(8): p. 755-62.

214. Albala, D.M., *Fibrin sealants in clinical practice.* Cardiovasc Surg, 2003. **11 Suppl 1**: p. 5-11.

215. Bensaid, W., et al., *A biodegradable fibrin scaffold for mesenchymal stem cell transplantation.* Biomaterials, 2003. **24**(14): p. 2497-502.

216. Weisel, J.W., *The mechanical properties of fibrin for basic scientists and clinicians.* Biophys Chem, 2004. **112**(2-3): p. 267-76.

217. Weisel, J.W., *Structure of fibrin: impact on clot stability.* J Thromb Haemost, 2007. **5 Suppl 1**: p. 116-24.

218. Rousseau, M.A., et al., *Stab incision for inducing intervertebral disc degeneration in the rat.* Spine, 2007. **32**(1): p. 17-24.

219. Haschtmann, D., et al., *Vertebral endplate trauma induces disc cell apoptosis and promotes organ degeneration in vitro.* Eur Spine J, 2008. **17**(2): p. 289-99.

220. Zheng, H., et al., *Impact of aging on rat bone marrow-derived stem cell chondrogenesis.* J Gerontol A Biol Sci Med Sci, 2007. **62**(2): p. 136-48.

221. Yoshimura, H., et al., *Comparison of rat mesenchymal stem cells derived from bone marrow, synovium, periosteum, adipose tissue, and muscle.* Cell Tissue Res, 2007. **327**(3): p. 449-62.

Publishing Agreement

It is the policy of the University to encourage the distribution of all theses, dissertations, and manuscripts. Copies of all UCSF theses, dissertations, and manuscripts will be routed to the library via the Graduate Division. The library will make all theses, dissertations, and manuscripts accessible to the public and will preserve these to the best of their abilities, in perpetuity.

Please sign the following statement:

I hereby grant permission to the Graduate Division of the University of California, San Francisco to release copies of my thesis, dissertation, or manuscript to the Campus Library to provide access and preservation, in whole or in part, in perpetuity.

Author Signature

June 12, 2009

Date